Q.
547
IL6s1
2000/2001:
1
cop.2

ORGANIC CHEMISTRY
SEMINAR ABSTRACTS
2000-2001 Semester I

University of Illinois at Urbana-Champaign
Department of Chemistry
600 South Mathews Avenue
271 Roger Adams Laboratory
Urbana, IL 61801

January 2001

Digitized by the Internet Archive
in 2012 with funding from
University of Illinois Urbana-Champaign

http://archive.org/details/organicsemi00011univ

Q. 547
Il6s1
2000/2001:1
cop. 2

Organic Chemistry Seminar Abstracts
2000-2001 Semester I

PAGE

DEVELOPMENT AND APPLICATIONS OF DNA MICROARRAYS 1
MOUSHUMI PAUL

BIOMOLECULAR ARCHITECTURE: SYNTHESIS AND APPLICATIONS OF DNA AND PEPTIDE TOPOLOGICAL MOTIFS 9
ERIN CRISWELL

THE KHARASCH ADDITION REACTION 17
DENNIS COMPTON

COVALENT ELECTRO- AND PHOTO-CHROMIC MOLECULAR SWITCHES 25
AMY BALIJA

TOTAL SYNTHESIS OF MANZAMINE A 33
TYSON MILLER

SCOPE AND DEVELOPMENT OF THE KULINKOVICH REACTION 41
MICHAEL OBER

CHIRAL POISONING AND CHIRAL DRUGGING 49
MATTHEW CHRISTY

RECENT DEVELOPMENTS TOWARD SYNTHETIC MUSCLES BASED ON ORGANIC MOLECULES AND POLYMERIC MATERIALS 57
DAHUI ZHAO

NICKEL-CATALYZED SEQUENTIAL CARBON-CARBON BOND FORMATIONS 65
SHINJI FUJIMORI

CONTROLLED RELEASE OF NITRIC OXIDE: THE DIAZENIUMDIOLATE GROUP 73
MARGARET COLLINS

VIRTUAL COMBINATORIAL LIBRARIES AND THEIR APPLICATIONS 81
KEUNCHAN OH

DEVELOPMENT AND APPLICATIONS OF DNA MICROARRAYS

Reported by Moushumi Paul September 7, 2000

INTRODUCTION

In the past ten years, various groups have undertaken the challenge to sequence the entire human genome. Completion of this extraordinary feat is expected by 2001. The yeast genome was sequenced in 1996 while, to date, the sequences of more than fifty bacterial genomes have been partially or fully determined.[1] Access to the information encoded in the genomes of these organisms has provided a vast resource for progress towards determining the causes of human diseases as well as the development of therapeutic agents. This advancement has been achieved with the advent and development of genomic and proteomic tools for DNA sequencing. In addition, researchers have developed combinatorial techniques to analyze these sequences quickly and efficiently.

DNA microarrays are one of the tools used for sequencing and analysis of genome sequences. The methodology behind DNA microarrays is based upon a technique known as sequencing by hybridization.[2] For this technique, synthetic oligonucleotides of known sequence are bound to a support and probed with an unknown radiolabeled sequence. The patterns formed by complementary hybrids are analyzed, and the sequence of the unknown DNA strand is determined.[3] In the early sequencing techniques, polyacrylamide gels typically functioned as the support and sequence determination was limited to small oligonucleotides (smaller than 200 bases). The elucidation of the unknown sequence, however, was sometimes ambiguous because of the resolution of bands on these gels.[4] To alleviate these problems, it was necessary to find a less expensive yet durable support, and a less time-consuming approach to sequencing.[5] Microchips that are commonly used today allow for high throughput analysis using inexpensive methods. These tools are not limited to sequencing alone, but are useful in mutational analysis and gene expression monitoring, as well.[6]

This review will illustrate the evolution of DNA sequencing from early methods to those used today, focusing on the development and utilization of microarrays.

FUNCTIONAL GENOMICS

With the development of analytical tools such as DNA microchips, fully sequenced genomes are now available. These sequences allow researchers to investigate questions concerning genes encoded in

Copyright © 2000 by Moushumi Paul

DNA and their relationship to cellular function.[7] Genes are short segments of DNA that serve as templates for the building of proteins within a cell. DNA is transcribed into RNA, which, in turn, is translated into proteins. These proteins may be involved in a biosynthetic pathway of interest, or may be a suitable target for the treatment of a disease. All of the genes within any given cell, however, are not active simultaneously. Expression of genes can change in response to external stimuli or can be affected by functions within the cell, such as cell division and DNA replication. Functional genomics seeks to probe the questions of when, where and the degree to which genes are expressed at any given moment in a cell's cycle.[8] The answers to these questions may help to elucidate the therapeutic potential of various gene products as well as to identify novel drug targets against disease.[9] By comparing the expression patterns of diseased cells to those of healthy ones, potential pharmaceutical targets can be obtained. In order to access information concerning protein expression, it is first necessary to sequence the genome that encodes it.

BACKGROUND

Early DNA Sequencing

The various DNA sequencing technologies are based upon the methods developed by several research groups in the late 1970s. Maxam and Gilbert reported a technique that employs chemical reagents which preferentially cleave DNA at each of the four bases.[10] Dimethyl sulfate is used as the purine-specific reagent (adenine and guanine), while hydrazine acts upon pyrimidines (cytosine or thymine). The products of these four reactions are resolved by size using gel electrophoresis and the sequence of the oligonucleotide is determined from a pattern of bands on a polyacrylamide gel.

Simultaneously, Sanger and coworkers implemented another innovative method of DNA sequencing which involves the use of chain-terminators (dideoxyribonucleotides) and DNA Polymerase I.[11] DNA Polymerase I extends the complimentary strand of the unknown sequence, which cannot elongate once a chain-terminator is introduced, resulting in shortened DNA fragments. These oligomers are size separated by polyacrylamide gel electrophoresis (PAGE) and the sequence determined in a manner analogous to the Maxam-Gilbert method.

The Sanger method was actively being used for DNA sequencing until the late 1980s. The primary disadvantage of the method, however, is that sequencing is limited to between 300 and 400 bases. The automation of this method has decreased the time necessary for the sequencing of DNA. A non-gel based method which could access the sequences of fragments larger than 400 bases was sought after as a more efficient, less expensive alternative to those techniques established by Sanger and Maxam.[12] A miniaturized system would allow for access to greater numbers of sequences in a shorter amount of time. Mirzabekov and coworkers developed a novel method coined "Sequencing by Hybridization" (SBH).[13] This advance in DNA sequencing exploited the inherent characteristics of DNA duplexes, i.e. the hybridization of complimentary strands of nucleic acids (Figure 1). In these arrays, a probe with known sequence is covalently linked to each spatially defined area (wells) on a solid support. For example, a 3 x 3 array would contain nine different probes. The unknown DNA sequence is then applied to each individual well on the array. Those sequences that form complementary duplexes (sequences with perfectly matched base pairs), are visualized. These arrays are the building blocks for the automated sequencing systems used today.

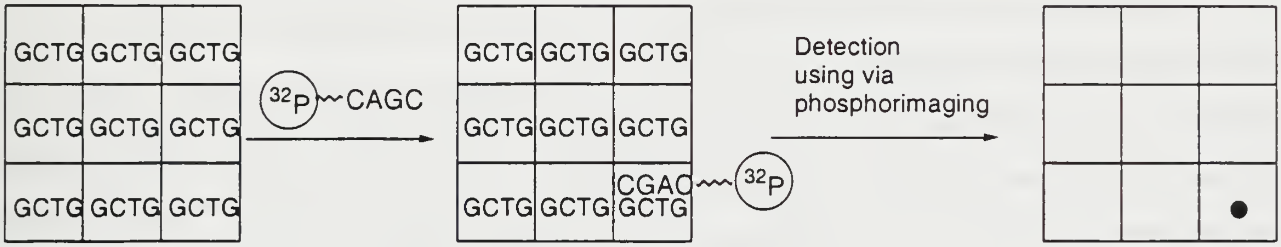

Figure 1. General Principles of Sequence by Hybridization

Early Microarrays

DNA microarrays are a technological advancement of early molecular biology tools for sequencing. The Southern Blot, a method used for DNA sequencing, can be thought of as the first DNA array.[14] This method involves the transferring (or blotting) of DNA oligomers from agarose gels onto cellulose nitrate filters.[15] The DNA fragments are first subjected to electrophoresis. Slices of the gel containing the desired oligonucleotides are subsequently placed on dry pieces of the filter. The gel is then washed with a buffer containing sodium chloride and sodium citrate, which pulls the fragments of DNA from the gel and embeds them in the filter. The fragments are then probed with radiolabeled mRNA of known sequence and the complimentary duplexes are detected by visualization on X-ray film. Drmanac and coworkers developed this method further, utilizing nylon-filters as a less expensive replacement for cellulose nitrate filters, and automated means were employed to deposit short pieces of genomic DNA onto the support.[16] In this method, the unknown fragment is immobilized on the solid support and radio-labeled (generally ^{32}P) octamers and nonamers of known sequence are used as probes to determine sequence information. Those probes whose sequences perfectly complement the unknown sequence remain bound to the support, while probes containing base pair mismatches are removed through succesive washings. The probes that remain are visualized using phosphorimaging and through their sequences, the sequence of the unknown DNA fragment can be elucidated.

The Drmanac method of microarray production has further evolved into the two types of production methods commonly used in DNA sequencing today, the Southern method and the combinatorial photolithographic process. Both of these techniques capitalize on the same basic principles as those stated above, but differ in the method of chemical synthesis of the DNA oligomers and the numbers of sequences that can be analyzed at once.

MODERN MICROCHIP PRODUCTION

The Southern Method

Southern and coworkers developed a variation on microarrays, using the same SBH methodology. SBH methodology exploits the fact that, through hydrogen bonding, adenine binds to thymine and guanine binds to cytosine in perfectly matched DNA. DNA segments containing mismatched base pairs are thermodynamically less stable relative to complimentary duplexes. For this reason, the probes used in microarray sequencing are generally octamers or nonamers. With probes this size, one mismatched base pair will affect the hybridization of the DNA strands and will be removed easily. Probes of longer sequences with one mismatch are sufficiently stabilized by the other base pairs and will not be removed through washings. The Southern method utilizes short, synthetic oligonucleotides of known sequence as probes that are bound to the solid support, while the unknown sequence is radio-labeled and deposited onto the probes.[18] This allows for binding between the matched probes and surface oligomer that is sequence-specific. The solid support used in this technique is a glass plate, rather than a nylon filter.

Scheme 1. Synthesis of Probes

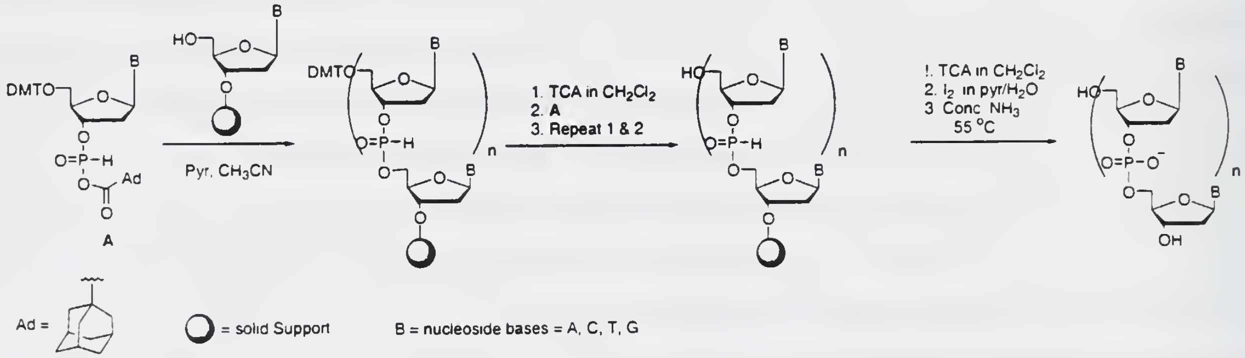

The various oligomer probes of known sequence are synthesized using routine solid-phase oligonucleotide synthetic methods developed by Andrus and coworkers (Scheme 1).[20] Using this synthetic route, a 5'-hydroxyl-protected deoxynucleoside is first activated with 1-adamantanecarbonyl chloride allowing for coupling with the free 5'-hydroxyl group of a deoxynucleoside bound to a solid support, forming an internucleoside hydrogen-phosphonate diester. This process is repeated sequentially with the desired nucleotide until the oligomer of required length and sequence is complete. These probes generally consist of a series of heptamer and octamers containing all four bases in every possible combination.

The nucleotide fragments are then immobilized through covalent attachment to glass supports using an aliphatic polyether linker with a primary hydroxyl (Figure 2).[21] The hydroxyl group can be activated with trace amounts of acid and coupled to the free 3'-end of the known sequences. Once the synthetic probes are immobilized on the glass plate, the identical ^{32}P-labeled unknown sequence is added to every probe on the support. Mismatched duplexes are eliminated through successive washings. Once the hybridizations are complete, the pattern of the array is recorded using phosporimaging via computer programs. The arrays are two-dimensional and do not rely on gel electrophoresis, and therefore lend themselves to automation.[22]

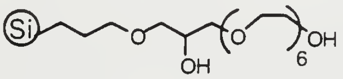

Figure 2. Linker Used for Covalent Nucleotide Attachment

The result of the Southern method of DNA sequencing is a set of wells containing probes bound to the radio-labeled unknown sequence. Wells that are not radioactive indicate the absence of those sequences in the unknown DNA fragment. The automation of this method allows for large quantities of probes to be used to sequence a DNA fragment at once, simultaneously decreasing the amount of time required for sequencing large sets of DNA.

The Combinatorial Photolithographic Process

In addition to the Southern method, the combinatorial photolithographic process has been developed using the same sequencing-by-hybridization principles. Previously in the Southern method, synthetic oligonucleotides are manually deposited on a glass surface. Fodor and coworkers have developed a novel light-mediated method of synthesizing DNA fragments of known sequence on solid supports directly.

Fodor and coworkers developed the light directed oligonucleotide synthetic method in which a photolithographic mask is implemented to selectively photodeprotect the 5'-hydroxyl group of the nucleotides bound to the glass support.[24] This synthetic route utilizes phosphoramidite chemistry, with a synthetic route similar to that of the Southern method. The photolithographic masks, however, direct chemistry to take place at specific wells on the plate, and allow for the next coupling of nucleotides occur at selected sites (Scheme 2).[25] This improvement has allowed for increased automation of DNA sequencing by combining the synthesis and deposition steps.

Scheme 2. Light Directed Oligonucleotide Synthesis

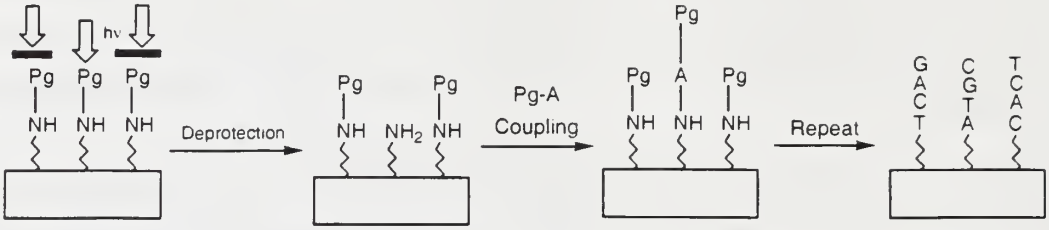

Pg = Photolabile Protecting Group

Using an amine linker with a photolabile protecting group to bind the nucleotides to the solid support, the synthesis of each oligonucleotide can be directed using this mask. The mask is moved from one place to another on the plate during each photodeprotection step, allowing for specific protecting groups to be removed. Following deprotection, the next deoxynucleoside, protected with another photolabile group, is coupled to the free amine. This process is repeated until syntheses of the full oligomers are completed.[26] Once the oligomers of known sequence are synthesized onto the solid support, the unknown sequence which is radiolabeled is added, and the matched duplexes are analyzed to determine the sequence of the unknown DNA strand.

Pirrung and coworkers are developing protecting groups that are more amenable to this type of photochemistry. The photolabile groups that are used for light-directed oligonucleotide synthesis must be removed at a wavelength of light that will not destroy the DNA fragment. Novel 3', 5'-dimethoxybenzoinyloxycarbonyl groups (**1**) for oligonucleotide synthesis have been developed and tested on the solid support (Figure 3).[27] Unfortunately, the yields of these deprotection reactions vary from near quantitative for the protected thymidine and cytidine residues to much lower for the purines bases. More recently, Pirrung and coworkers have further searched for suitable protecting groups for photolithographic-mediated solid-phase synthesis. Their efforts have resulted in the discovery of pentadienylnitrobenzyl and pentadienylnitropiperonyl groups (**2** and **3**, respectively) that are more easily removable in high yields, which may prove to increase the productivity of DNA sequencing using microarrays (Figure 3).[28]

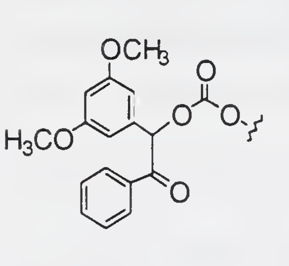
1

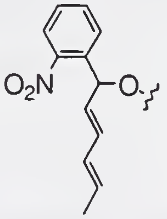
2

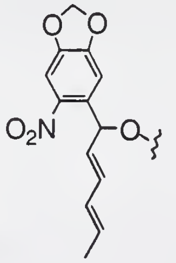
3

Figure 3. Photolabile Protecting Groups

FURTHER APPLICATION OF MICROARRAYS

Microarray technology is not limited in its utility to DNA sequencing. The newest application of microarrays is in the realm of gene expression. Determining which proteins in a cell are involved in biosynthetic pathways of interest or which can be targeted for drug therapy has become the new focus of genomics. Since gene sequences are postulated to have a direct correlation to the expression of specific proteins within a cell, the monitoring of gene expression can offer information about the relative abundances of selected proteins as well as their responses to external perturbation, such as the introduction of a potential drug.

Brown and coworkers have used microarrays to quantify the relative abundance of specific gene sequences in cells.[6] Probes containing known sequences corresponding to particular genes are immobilized on a microarray. The DNA or RNA from two different cells are isolated and fluorescently labeled with two different colored dyes. The samples are then mixed and added to the sequences on the array. After hybridization, fluorescence for each dye is measured separately using a microscope. These measurements are used to determine a ratio, thereby obtaining relative abundance of the sequence of each individual gene in the mRNA or DNA samples that were used.

The abundance of specific gene sequences in certain types of cells can then be correlated to which genes are turned off or turned on within a cell at a specific time, offering possible information about the functional role of the protein which that sequence may encode. These types of expression profiling experiments can also isolate gene sequences that are specific to certain types of cells. For example, through the examination of the expression profiles of healthy versus diseased cells, gene sequences that are overexpressed only in the diseased cells can be identified and possibly targeted as a potential treatment for that disease.

CONCLUSION

DNA microarrays have a number of potential uses in the field of genomics and have simplified the task of DNA sequencing tremendously. In this way, DNA microarrays have played a large role in the complete sequencing of the genomes from over 30 organisms to date.[7] Many methods are being developed to lower the cost of microarray production and increase the efficiency of DNA sequencing. These developments include the covalent attachment of oligomers to solid supports using Bubble Jet technologies as well as the elimination of masks in light-directed parallel synthesis of oligonucleotides by the use of micromirror arrays.[8, 30] Researchers have also extended the use of microarrays to gene expression monitoring. These experiments will potentially offer new information concerning the causes of human disease and will aid in deciphering the human genome once it is fully sequenced. With the technological advances that are being made every day, microarrays will continue to be a factor in the study of biological function at both the genome and proteome levels.

REFERENCES

1) Fields, S.; Kohara, Y.; Lockhart, D. J. *Proc. Natl. Acad. Sci. USA* **1999**, *96*, 8825-8826.
2) Hoheisel, J. D. *Trends Biotechnol.* **1997**, *15*, 465-469.
3) Sanders, G. H. W.; Manz, A. *Trends in Anal. Chem.* **2000**, *19*, 364-378.
4) Sterky, F.; Lundeberg, J. *J. Biotech.* **2000**, *76*, 1-31.
5) Debouck, C.; Goodfellow, P. N. *Nat. Genet.* **1999**, *21*, 48-50.
6) Brown, P. O.; Botstein, D. *Nat. Genet.* **1999**, *21*, 33-37.
7) Lockhart, D. J.; Winzeler, E. A. *Nature* **2000**, *405*, 827-836.
8) Okamoto, T.; Suzuki, T.; Yamamoto, N. *Nature Biotechnology* **2000**, *18*, 438-441.
9) Schena, M.; Shalon, D.; Davis, R. W.; Brown, P. O. *Science* **1995**, *270*, 467-470.
10) Maxam, A. M.; Gilbert, W. *Proc. Natl. Acad. Sci. USA* **1977**, *74*, 560-564.
11) Sanger, F.; Nicklen, S.; Coulson, A. R. *Proc. Natl. Acad. Sci. USA* **1977**, *74*, 5463-5467.
12) Khrapko, K. R.; Lysov, Y. P.; Khorlyn, A. A.; Shick, V. V.; Florentiev, V. L.; Mirzabekov, A. D. *FEBS Lett.* **1989**, *256*, 118-122.
13) Yershov, G.; Barsky, V.; Belgovskiy, A.; Kirillov, E.; Kreindlin, E.; Ivanov, I.; Parinov, I.; Guschin, D.; Drobishev, A.; Dubiley, S.; Mirzabekov, A. *Proc. Natl. Acad. Sci. USA* **1996**, *93*, 4913-4918.
14) Niemeyer, C. M.; Blohm, D. *Angew. Chem., Int. Ed. Engl.* **1999**, *38*, 2865-2869.
15) Southern, E. M. *J. Mol. Biol.* **1975**, *98*, 503-517.
16) Drmanac, R.; Labat, I.; Brukner, I.; Crkvenjakov, R. *Genomics* **1989**, *4*, 114.
17) Strezoska, Z.; Paunesku, T.; Radosavljevic, D.; Labat, I.; Drmanac, R.; Crkvenjakov, R. *Proc. Natl. Acad. Sci. USA* **1991**, *88*, 10089-10093.
18) Southern, E. M.; Maskos, U.; Elder, J. K. *Genomics* **1992**, *13*, 1008-1017.
19) Cheung, V. G.; Morley, M.; Aguilar, F.; Massimi, A.; Kucherlapati, R.; Childs, G. *Nat. Genet.* **1999**, *21*, 15-19.
20) Andrus, A.; Efcavitch, J. W.; McBride, L. J.; Giusti, B. *Tetrahedron Lett.* **1988**, *29*, 861-864.
21) Maskos, U.; Southern, E. M. *Nucleic Acids Res.* **1992**, *20*, 1679-1684.
22) Southern, E. M.; Maskos, U. *J. Biotech.* **1994**, *35*, 217-227.
23) Ramsay, G. *Nature Biotechnology* **1998**, *16*, 40-44.
24) Fodor, S. P. A. *Science* **1997**, *277*, 393-395.
25) Jacobs, J. W.; Fodor, S. P. A. *Trends Biotech.* **1994**, *12*, 19-26.
26) Fodor, S. P. A.; Read, J. L.; Pirrung, M. C.; Stryer, L.; Lu, A. T.; Solas, D. *Science* **1991**, *251*, 767-773.
27) Pirrung, M. C.; Fallon, L.; McGall, G. *J. Org. Chem.* **1998**, *63*, 241-246.
28) Pirrung, M. C.; Lee, Y. R.; Park, K.; Springer, J. B. *J. Org. Chem.* **1999**, *64*, 5042-5047.
29) Liu, Y.; Patricelli, M. P.; Cravatt, B. F. *Proc. Natl. Acad. Sci. USA* **1999**, *96*, 14694-14699.
30) Singh-Gasson, S.; Green, R. D.; Yue, Y.; Nelson, C.; Blattner, F.; Sussman, M. R.; Cerrina, F. *Nature Biotechnology* **1999**, *17*, 974-978.

BIOMOLECULAR ARCHITECTURE: SYNTHESIS AND APPLICATIONS OF DNA AND PEPTIDE TOPOLOGICAL MOTIFS

Reported by Erin S. Criswell

September 21, 2000

INTRODUCTION

The construction of three-dimensionally complex molecules has long been of interest to organic chemists. Research in biomolecular topology has recently seen advances in the syntheses of geometrically complex structures of both natural and synthetic origin. The applications of topologically complex biomolecules also warrant attention since they show promise as nanoscale devices and pharmaceutical agents. For all their complexity, however, these structures find their bases in three fundamental structural motifs, the rotaxane **1**, the catenane **2**, and the trefoil knot **3** (Figure 1).

Both rotaxanes **1** and catenanes **2** are well-known in the literature.[1,2] Molecular knots, such as trefoil knots **3**, present a synthetic challenge because they are molecular chains which cross themselves at three or more points, called nodes. Nodes can be either topologically positive or topologically negative, hence knots exhibit topological chirality as shown in Figure 1. Sauvage, Stoddart, and, more recently, Vögtle, have reported significant advances in the synthesis of knotted structures.[3-5] While this progress is notable, the use of biopolymers to form topologically interesting molecules is often overlooked. Both synthetically assembled and naturally occurring nucleic acids and peptides can exhibit three-dimensional motifs that resemble rotaxanes, catenanes, and knots.

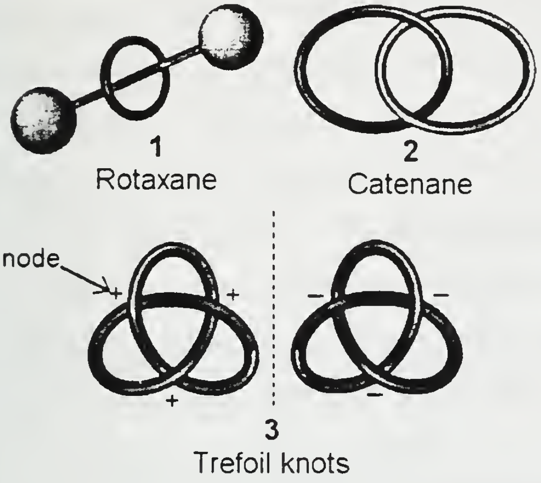

Figure 1. Basic Topological Motifs.

DNA NANOSTRUCTURES

Topological properties of DNA

Because DNA has several useful properties, it has been used to assemble molecules of complex topology. First, in relatively short 1-3 helix-turn lengths, DNA is mechanically inflexible and can be

Copyright © 2000 by Erin S. Criswell

used to synthesize rigid geometrical structures.[6] Second, solid phase synthesis of oligonucleotides is a well known process, which simplifies the production of necessary building blocks. Third, a wide variety of enzymes exist that can efficiently perform synthetic and topological modifications on DNA strands. The inherent tendency of DNA to adopt a double-helical conformation eliminates the synthetic difficulty of assembling molecular chains into the nodal configuration necessary in knotted structures. Because double-stranded DNA forms a right-handed helix under normal biological conditions, the nodes in single-stranded DNA knots are topologically negative. By taking advantage of the ability of DNA to switch from this native form, called B-DNA, into a left-handed helical form, called Z-DNA, topologically positive nodes can be synthesized.[10,12] Another useful feature of DNA is its capacity to form complementary, or "sticky" ends by the action of restriction endonucleases. DNA fragments with sticky ends hydrogen bond to segments containing their base-pair complements, and can then be covalently linked to yield new strands using DNA ligase, which catalyzes the formation of phosphodiester bonds in the DNA backbone. The sticky end formation/ligation sequence can be used to link small structural elements together to form larger topological motifs.

Although DNA can be used for efficient topological assembly and manipulation, it is limited by its unbranched helical axis. The lack of stable branch points confines the use of normal DNA to the construction of simple knots and catenanes. In order to form more complex three-dimensional motifs, a means of extending DNA helices in multiple directions from a single branch point is required. This problem was first overcome by Kallenbach,[7] who synthesized the first immobile nucleic acid branch junction from four single DNA strands designed to hybridize at right angles to each other. These branch junctions are suitable as vertices of two- and three-dimensional DNA shapes. In addition to four-armed junctions, three-, five-, and six-armed junctions have been successfully constructed, allowing for the assembly of higher-order three-dimensional shapes.[6]

These unique topological properties of DNA have been useful in the assembly of numerous biomolecular constructs. Among the simpler two-dimensional structures that have been synthesized are parallelograms[8] and triangles.[6] Some of the successfully assembled three-dimensional structures are simple trefoil knots of both right- and left-handedness,[9-12] and four-noded amphichiral knots commonly called figure-eight knots.[10,12] Since the preparation of single-stranded oligonucleotides is a relatively simple matter, the synthesis of single-stranded topological structures such as catenanes and knots is more a matter of intelligent base-pair sequencing than synthetic ingenuity.

Synthetic Methods

Solution phase synthetic strategy. The first geometric DNA objects synthesized were a simple two-dimensional quadrilateral[8] and a three-dimensional molecule with the connectivity of a cube.[13] Both were synthesized using a solution phase selective phosphorylation/ligation strategy (Scheme 1).

Scheme 1. Solution Phase Synthesis of a DNA Cube.

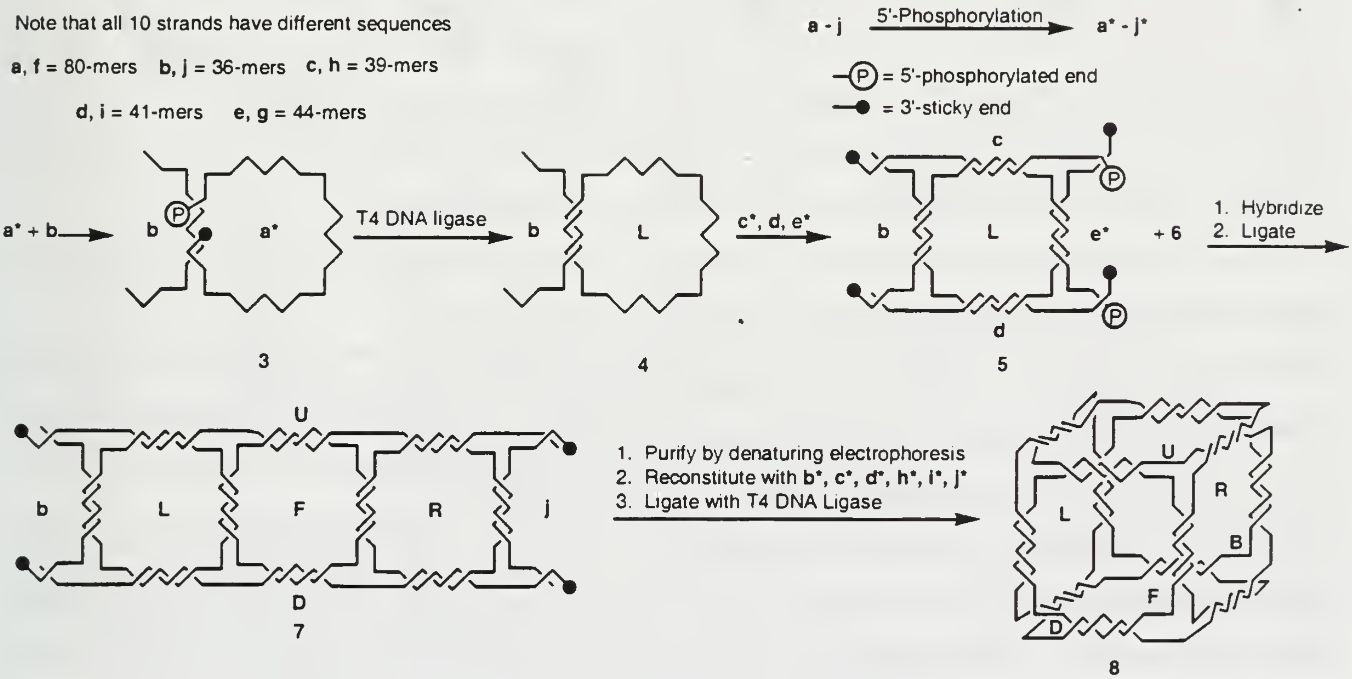
Note that all 10 strands have different sequences
a, f = 80-mers b, j = 36-mers c, h = 39-mers
d, i = 41-mers e, g = 44-mers
a - j
5'-Phosphorylation
a* - j*
P = 5'-phosphorylated end
= 3'-sticky end
a* + b
b
P
a*
T4 DNA ligase
b
L
c*, d, e*
c
b
L
e*
d
P
P
+ 6
1. Hybridize
2. Ligate
3
4
5
U
b
L
F
R
j
D
7
1. Purify by denaturing electrophoresis
2. Reconstitute with b*, c*, d*, h*, i*, j*
3. Ligate with T4 DNA Ligase
U
R
L
B
F
D
8

In the solution phase method, long 5'-phosphorylated strand **a*** is hybridized with short template strand **b** to generate non-covalently bound pseudo-cyclic structure **3**. T4 DNA ligase then seals the nick between the ends of **a***, forming hybridized DNA circle **4**. The circle can then be combined with strands **c***, **d**, and **e***, its three other linear single-stranded complements, to form the double-stranded, sticky-ended left face **5** of cube **8**. Note that the T-shaped branch junctions form double helices just as the straight edges do, but the helical twists are shown only on the edges for clarity. A similarly shaped but chemically distinct square **6** is constructed from strands **f***, **g***, **h***, **i**, and **j**. The two squares **5** and **6** are then hybridized and ligated to form tricatenane belt **7**. Due to the formation of intermolecular ligation products, it is necessary to purify **7** by denaturing gel electrophoresis, which dissociates it from strands U, D, **b**, and **j**. Reconstitution of the single-stranded tricatenane core with 5'-phosphorylated strands **b***, **c***, **d***, **h***, **i***, and **j*** regenerates **7**, and all nicks are sealed to form hexacatenated cube **8**. While an intelligent synthetic strategy, the solution phase synthetic method presents inherent complications and requires extra steps that detract from the yield of the overall process. In order to circumvent these additional steps, an alternate synthetic strategy was developed.

Solid phase synthetic strategy. The synthetic sequence demonstrated in Scheme 2 begins with a linker sequence synthesized on a Teflon-based solid support. Treatment of the double-stranded linker with 4,5',8-trimethylpsoralen followed by exposure to ultraviolet light generates a stable, cross-linked, sticky-ended duplex that helps make the growing shape impervious to denaturing and exonucleolytic purification conditions.[14] Attachment of a branch junction to the linker yields the starting material **9**, where the psoralen-crosslinked portion is shown as closely spaced horizontal lines. Hairpin structures A and B are DNA protecting groups for sticky ends and can be selectively removed by restriction endonucleases. Restriction sites are destroyed when the edges of the molecule are elongated, thus rendering finished edges immune to further cycles of restriction and ligation. Restriction of site A yields sticky-ended structure **10** that hybridizes with branch junction **11** and is ligated to give **12**. After purification, the synthesis continues in like manner. The remaining hairpins in structure **13** are removed, and ligation gives parallelogram **14**. The solid phase technique has several advantages over the solution phase method. The yield of this DNA quadrilateral increased from 15% to 60% by carrying out the synthesis on solid phase. The use of a solid support also immobilizes and isolates growing nanostructures from each other. This simplifies the purification process and reduces the occurrence of intermolecular ligations. Also, the solid phase method allows for increased control over the intermediate products of the reaction, since each edge of a structure is synthesized individually. Such control was demonstrated in the solid phase synthesis of a truncated octahedron, the most complex shape to date.[15]

Scheme 2. Solid Phase Synthesis of a DNA Parallelogram.

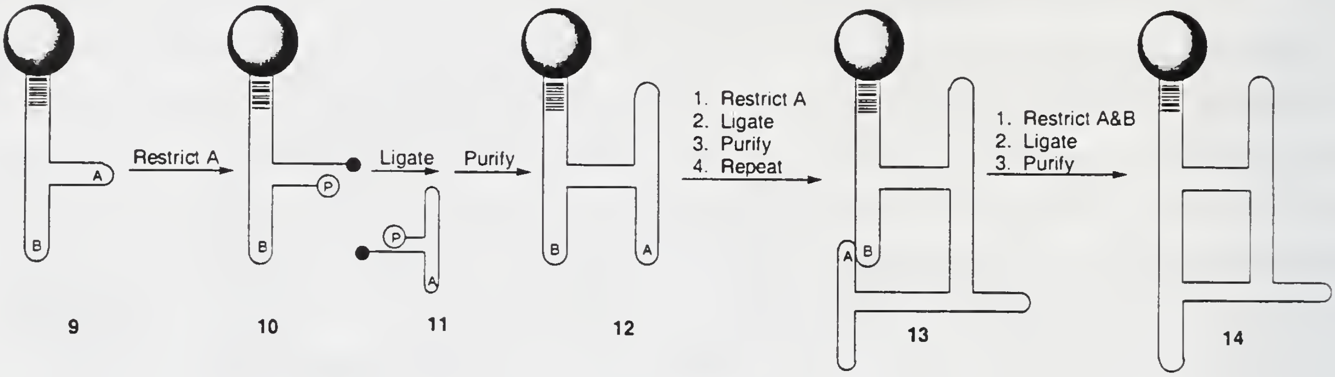

Three-dimensional shapes such as the cube and truncated octahedron were not synthesized simply as curiosities. The initial intent was to use repeating lattices of such objects as crystallization scaffolds for other biomolecules that are difficult to crystallize. Such lattices could be used to orient guest molecules so that crystal structure analysis would be feasible.[6,16] This is an unrealized goal of DNA nanostructure research, primarily because it was discovered that DNA branch junctions are flexible and unsuitable for crystallography.[6] In light of this development, a more inflexible structural component was sought and eventually found.

Scheme 3. Naturally Occurring and Synthetic DX Motifs.

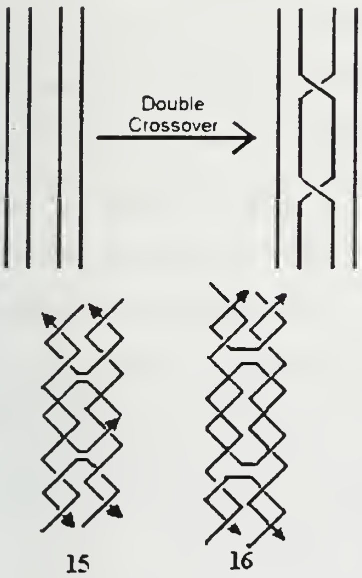

Synthesis by self-assembly. The conformational flexibility of DNA branch junctions makes them unsuitable for the assembly of well-behaved periodic structures.[16] The latest advances in DNA topological research involve rigid anti-parallel double-crossover (DX) molecules.[17] and their ability to self-assemble into periodic arrays.[18] DX molecules are observed in nature, as part of the genetic recombination pathway in cells. They consist of two double-stranded helices that overlap each other at two points. The schematic representation of the formation of a natural DX motif, Scheme 3, top, shows the double helices untwisted, as though the single strands of the backbone are parallel to one another for clarity. The natural versions of this motif are unstable, but the synthetic molecules that mimic their structure are specifically designed to overcome this difficulty. DX molecules **15** and **16** are stable and can be used as structural elements for nanoconstruction.[17] DX molecules can be synthesized as sticky-ended tiles which will self-assemble into periodic, two dimensional arrays held together solely by the hydrogen bonding of their component base pairs.[18] These arrays are visible by atomic force microscopy, and they can be surface-modified after assembly.[19] This development is particularly exciting in that it represents a very significant achievement in the control of nanoscale construction. The applications of DX molecules are not limited to self-assembling arrays, but include the recent construction of a simple nanomechanical DNA machine composed of two sets of interlinked DX tiles connected by a short double-stranded segment. This segment can be easily switched from a right-handed helix to a left-handed helix by inducing a B-DNA/Z-DNA transition. The tiles change their relative orientations, thus allowing the nanomachine to function as a switch or lever.[20]

CYSTINE KNOT POLYPEPTIDES

In addition to the structures produced by DNA nanotechnology research, there are topological motifs such as the cyclic cystine knot that are found in naturally occurring peptides. The cyclic cystine knot comprises six cysteine residues in the interior of a polypeptide backbone.[21-23] These six cysteines are interlinked such that two disulfide bonds and their connecting peptide sequences form a ring. The third disulfide bond passes through the ring to form a structure that is very similar to a rotaxane. This motif is found in a wide variety of proteins, including protease inhibitors, peptide hormones, and insect venom. The interesting properties of knotted peptides and the challenges associated with their topological construction make them worthy synthetic targets.

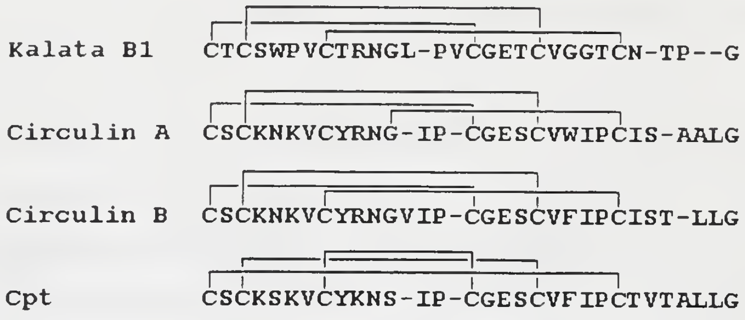
Kalata B1 CTCSWPVCTRNGL-PVCGETCVGGTCN-TP--G
Circulin A CSCKNKVCYRNG-IP-CGESCVWIPCIS-AALG
Circulin B CSCKNKVCYRNGVIP-CGESCVFIPCIST-LLG
Cpt CSCKSKVCYKNS-IP-CGESCVFIPCTVTALLG

Figure 2. Sequences of kalata, CirA, CirB, and Cpt.

One of the most interesting classes of cystine knot proteins discovered in recent years is a group of four peptides isolated from plant sources.[22,23] While several such cyclotides have been found, kalata B1, circulin A (CirA), circulin B (CirB), and cyclopsychotride (Cpt), Figure 2, have attracted considerable attention because they exhibit useful pharmaceutical properties.[22,23] They are unusually large for cyclic peptides and are about 30 residues in length.[22] They are resistant to proteolysis because of their unique cystine knot structure.[23] This property makes them very promising drug candidates, as the increased stability would allow for lower drug doses. They show approximately 45% sequence homology and have similar three-dimensional structures, so a single synthetic protocol can be applied to all four peptides.

Synthetic Studies on Cystine Knot Cyclotides

The linear peptide precursors are synthesized using standard solid phase Boc chemistry. The solid support used is Boc-Gly-SCH_2CH_2CO-4-methylbenzhydrylamine resin.[23] Although the linear peptides are not difficult to synthesize, the cyclic backbone and interlinked disulfide bonds present a more complicated problem. Traditional synthetic methods would dictate the use of a multiply orthogonal protecting group scheme. To expedite the synthesis and eliminate the intermediate steps which would significantly reduce the yields of the final product, Tam and coworkers have developed a synthetic methodology based on intramolecular orthogonal ligation.[24] The reactions use semi-protected peptide precursors in order to form the desired disulfide bonds and a unique rearrangement to form the cyclic backbone. Control over disulfide bond formation is derived from the choice of cysteine protecting groups. Four cysteine resides are protected with the 4-methylbenzyl protecting group (4-MeBn). The remaining two are protected with the acetamidomethyl protecting group (Acm).[23,24] After backbone synthesis, the finished linear peptide is cleaved from the solid support using 9:1 (v/v) HF/anisole, a step that also removes the 4-methylbenzyl protecting groups.[22,23]

The peptides are cyclized by way of the thia zip reaction, a reaction that involves a series of cyclizations assisted by free thiols, shown in Scheme 4. The cysteine residues have been assigned Roman numerals for clarity.[24] In order for this reaction to proceed, there must be an N-terminal cysteine

Scheme 4. The Thia Zip Reaction and Two-Tiered Oxidation.

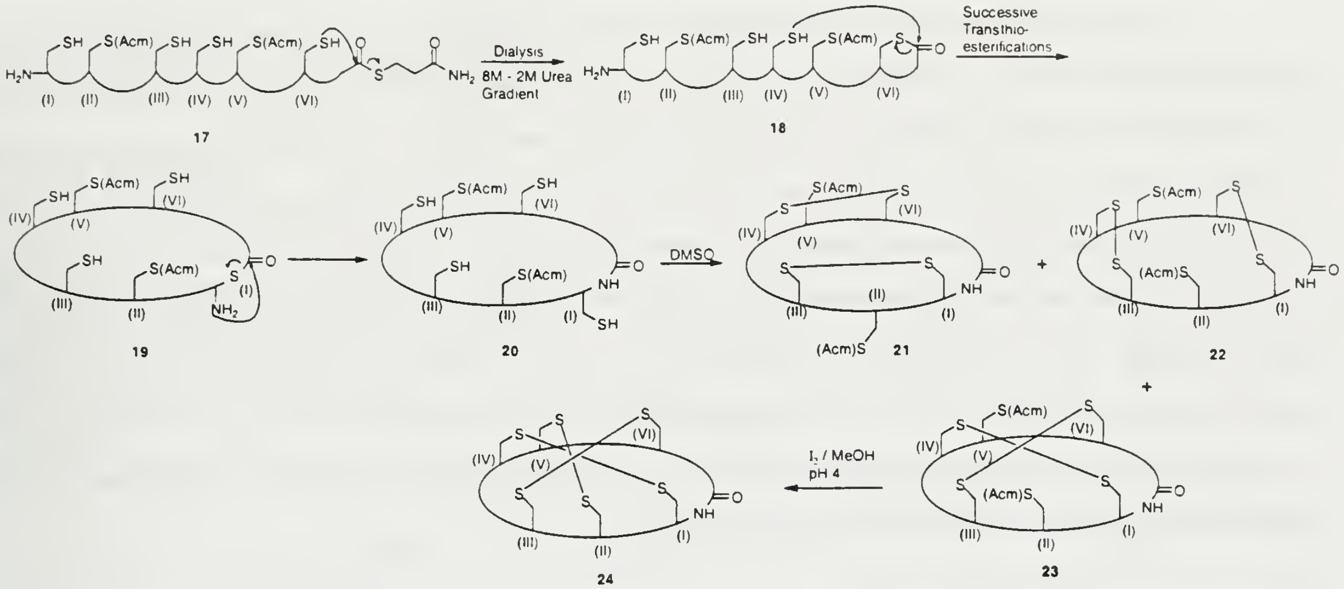

residue, a C-terminal thioester, and at least one internal thiol present in the polypeptide. In an entropically driven step, transthioesterification of linear peptide **17** dissociates the peptide from the resin linker and generates a C-terminal thiolactone **18**. Subsequent transthioesterifications enlarge the ring until the largest possible thiolactone **19** is generated. This aminothiolactone undergoes a spontaneous ring contraction via an S,N-acyl migration, thus generating unknotted cyclic peptide **20**. Two of the necessary disulfide bonds, CysI/CysIV and CysIII/CysVI, are formed by dimethylsulfoxide oxidation of cyclized peptide **20**. Three disulfide structural isomers **21**, **22**, and **23** are formed in this step, each synthesized in about 30% yield.[23,24] These three isomers are separated by HPLC, and the synthesis is continued with disulfide isomer **23**.[24] The Acm protecting groups are removed and the remaining disulfide bond, CysII/CysV, is formed concomitantly in an I_2-mediated deprotection/oxidation, thus completing the construction of the final product in its knotted topology. This may appear to be an inefficient strategy given the loss of two-thirds of the original starting peptide, but without the orthogonal protecting scheme, nine to fifteen disulfide isomers can be formed, dramatically reducing product yield. Using the two-tiered oxidation method, only three isomers are synthesized, and the desired peptides can be obtained in about 15-30% yield, a marked improvement over the 2-5% yield using more traditional methods.[22,23]

These four peptides exhibit various pharmaceutical activities. Kalata B1 has been used as a uterotonic agent.[22] CirA and CirB were discovered during an anti-HIV drug screening and show very promising anti-viral activity. Cpt inhibits neurotensin binding in humans, a property which may be useful in the treatment of pancreatic cancer. All four cyclotides have also exhibited antimicrobial and antifungal activity, thus making them promising pharmaceutical agents.[23]

CONCLUSION

In recent years, research in biomolecular topology has yielded significant progress in the field of molecular architecture. The physical and chemical properties of DNA make it uniquely suited to the purposes of topological assembly, and these properties have been used in the construction of numerous complex motifs. Solution phase, solid phase, and self-assembly synthetic methodologies have been developed to construct and manipulate DNA topological motifs. The wide variety of structures that can be synthesized have applications that are under investigation, including the construction of rigid DNA crystals and in DNA-based computing.[25] Cyclic cystine knot peptides present a synthetic challenge that has been met by the development of the thia zip reaction and two-tiered disulfide oxidation strategy. Plant cyclotides kalata B1, CirA, CirB, and Cpt have been synthesized using this method and are promising peptide pharmaceuticals.

REFERENCES

(1) Schill, G. *Catenanes, Rotaxanes, and Knots;* Boeckman, J., Translator; Academic: NY, **1971.** (2) Sauvage, J. P.; Dietrich-Buchecker, C. (Eds.) *Molecular Catenanes, Rotaxanes and Knots, A Journey Through the World of Molecular Topology* Wiley-VCH, **1999**.

(3) Dietrich-Buchecker, C. O.; Sauvage, J. P. *Angew. Chem. Int. Ed. Engl.* **1989,** *28,* 189-192.

(4) Ashton, P. R.; Matthews, O. A.; Menzer, S.; Raymo, F. M.; Spencer, N.; Stoddart, J. F.; Williams, D. J. *Leibigs Ann. Rec.* **1997,** 2485-2494.

(5) Safarowsky, O.; Neiger, M.; Frohlich, R.; Vogtle, F. *Angew. Chem. Int. Ed. Engl.* **2000,** *39,* 1616-1618.

(6) Seeman, N. C. *Annu. Rev. Biophys. Biomol. Struct.* **1998,** *27,* 25-48. and references therein.

(7) Kallenbach, N. R.; Ma, R. I.; Seeman, N. C. *Nature* **1983,** *305,* 829-831.

(8) Chen, J. H.; Kallenbach, N. R.; Seeman, N. C. *J. Am. Chem. Soc.* **1989,** *111,* 6402–7,

(9) Chen, J.; Seeman, N. C. *Nature* **1991,** *350,* 631–33.

(10) Du, S. M.; Seeman, N. C. *J. Am. Chem. Soc.* **1992,** *114,* 9652–55.

(11) Du, S. M.; Seeman, N. C. *Biopolymers* **1994,** *34,* 31–37.

(12) Du, S. M.; Stollar, B. D.; Seeman, N. C. *J. Am. Chem. Soc.* **1995,** *117,* 1194–1200.

(13) Mueller, J. E.; Du, S. M.; Seeman, N. C. *J. Am. Chem. Soc.* **1991,** *113,* 6306–8.

(14) Zhang, Y.; Seeman, N. C. *J. Am. Chem. Soc.* **1992,** *114,* 2656–63.

(15) Zhang, Y.; Seeman, N. C. *J. Am. Chem. Soc.* **1994,** *116,* 1661-1669.

(16) Li, X. J.; Yang, X. P.; Qi, J.; Seeman, N. C. *J. Am. Chem. Soc.* **1996,** *118,* 6131-6140.

(17) Fu, T. J.; Seeman, N. C. *Biochemistry* **1993,** *32,* 3211-3220.

(18) Winfree, E.; Liu, F.; Wenzler, L. A.; Seeman, N. C. *Nature* **1998,** *394,* 539-544.

(19) Liu, F.; Sha, R.; Seeman, N. C. *J. Am. Chem. Soc.* **1999,** *121,* 917-922.

(20) Mao, C.; Sun, W.; Shen, Z.; Seeman, N. C. *Nature* **1999,** *397,* 144-146.

(21) Christmann, A.; Walter, K.; Wentzel, A.; Kratzner, R; Kolmar, H. *Prot. Eng.* **1999,** *12,* 797-806.

(22) Craik, D. J.; Daly, N. L.; Bond, T.; Waine, C. *J. Mol. Biol.* **1999,** *294,* 1327-1336.

(23) Tam, J. P.; Lu, Y. A.; Yang, J. L.; Chiu, K. W. *Proc. Natl. Acad. Sci. USA.* **1999,** *96,* 8913-8918. (and references therein)

(24) Tam, J. P.; Lu, Y. A., *Protein Sci.* **1998,** *7,* 1583-1592.

(25) Winfree, E. *DNA Based Computers: DIMACS Workshop, April 4, 1995.* R. J. Lipton and E. B. Baum, Eds. American Mathematical Society, **1996.**

THE KHARASCH ADDITION REACTION

Reported by Dennis R. Compton October 16, 2000

INTRODUCTION

In 1945 M.S. Kharasch and co-workers[1] first reported the addition of carbon tetrachloride across an olefin (**Scheme 1**). This addition took place in an anti-Markovnikov fashion and was initiated by peroxide, which led Kharasch to propose a free-radical mechanism[1] (**Scheme 2**). The mechanism begins with peroxide, **4**, first undergoing homolytic cleavage of the O-O bond followed by radical decarboxylation producing 2 equivalents of CO_2 and 2 equivalents of a methyl radical (**5**). The methyl radical abstracts a halogen from **2** to form the radical species **7**. Compound **7** abstracts an electron from olefin **1** producing the more stable secondary radical, **8**. Compound **8** then abstracts a halogen from **2** yielding the Kharasch product **3** and the radical intermediate **7**, which further propagates the reaction sequence. Further evidence for the free-radical mechanism was found in the side products. The reaction mixture was found to contain high molecular weight polymers that Kharasch left unidentified. The amount of polymerization that occurred led to a wide range of yields, 5 – 85 %. This procedure was later extended to chloroform, bromoform, carbon tetrabromide, as well as di- and tri-chloromethylesters (Scheme 1).[1] Since its introduction, the Kharasch reaction has been employed for the addition of halomethanes, polyhaloalkanes, and chloromethylesters to olefins. The ability to add

Scheme 1 Kharasch Addition Reaction

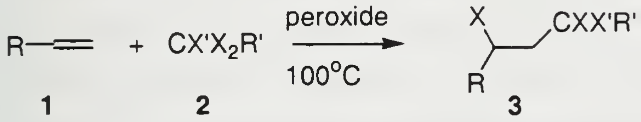

2a) X' = X = R' = Cl
b) X' = H, X = R' = Cl
c) X' = X = R' = Br
d) X' = H, X = R' = Br
e) X' = X = Cl, R' = CO_2CH_3
f) X' = H, X = Cl, R' = COCl

Peroxide = $(CH_3CO_2)_2$
$(PhCO_2)_2$

Scheme 2 Free Radical Mechanism

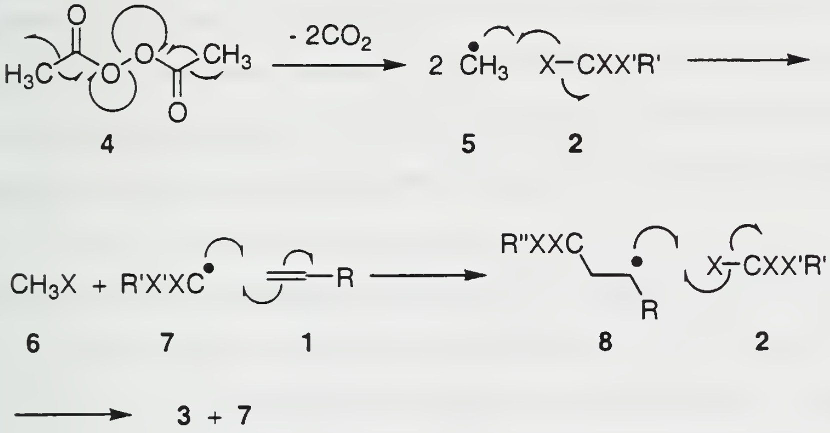

© 2000 By Dennis R. Compton

polyhaloalkanes across an olefin allows for further transformation of the product and makes the Kharasch product a versatile intermediate in organic synthesis. However, to maintain synthetically useful yields, it is best to use terminal olefins. Even with its limitations the Kharasch reaction has been applied to a variety of synthetic problems.[14-21]

TRANSITION METALS

Since the introduction of the Kharasch reaction, it has been found that transition metals catalyze the reaction more efficiently than peroxide initiators. The use of transition metals allows for greater control of the radical intermediates that are generated in the reaction. The ability to control the radical reduces the amount of polymerization that can occur, leading to improved yields. The general catalytic cycle proposed by Davis and co-workers[2] is found in **Scheme 3**. The cycle was elucidated through a study of various molybdenum complexes ($[Mo_2(CO)_4(\eta^5\text{-}C_5H_5)_2]$, $[Mo_2(CO)_4(\eta^5\text{-}C_5Me_5)_2]$, $[Mo_2(CO)_6(\eta^5\text{-}C_5H_5)_2]$, $[\{Mo(CO)_3(\eta^5\text{-}C_5H_4)_2\}_2CH_2]$) and was found to be applicable for any transition metal. Ruthenium complexes are the exception to the catalytic cycle. It has been found that Ru complexes which contain phosphine ligands are inhibited by excess triphenyphosphine (PPh_3).[3a] Davis and co-workers proposed that the catalytic cycle for Ru begins with dissociation of a phosphine ligand, Ru then proceeds through the catalytic cycle shown in scheme 3. When $RuCl_2(PPh_3)_3$ (**12**) and **1** were observed by IR and NMR, without CCl_4, there was no indication that **1** interacted with **12**.[3] A similar experiment was not performed with the molybdenum catalysts leaving it unknown if there is interaction between 1 and the molybdenum catalyst.

Scheme 3 Catalytic Cycle

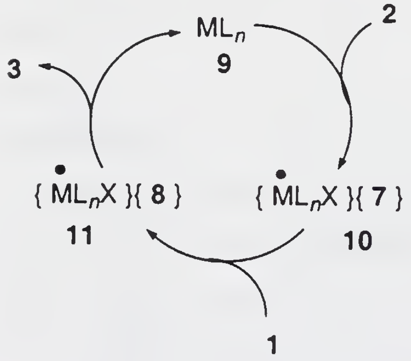

M = Mo(II)^2, Ru(II)^3, Cu(I)^{4,7}, Fe(0)^5, Pd(0)^6, Ni(II)^8,Fe(II)^{14}

When the transition metal systems are examined (**Table 1**) it is noted that the yields can vary significantly depending on the system chosen. The $RuCl_2(PPh_3)_3$ (entry 1) has been the most widely used catalyst for the Kharasch reaction. It consistently produces good yields at lower temperatures than other transition metals.[3c] Still milder conditions can be utilized with the use of Wilkinson's catalyst and pinacolborane (PBH)[12], entry 2, while maintaining high yields. When entries 3 and 4 are compared, it is noticed that the same molybdenum catalyst produces poor yields at 60°C, but increasing the temperature to 120°C produces moderate yields. Cuprous chloride, entry 5, can be used without ligands, but high temperatures are required. As can be seen from table 1, not only is there extensive variety at the metal center there is also a large variety in the types of ligands that are used.

Table 1 Catalyst Systems & Yields

Entry	Catalyst	Halide	Olefin	Conditions	Yield	Ref.
1	$RuCl_2(PPh_3)_3$	CCl_4	Styrene	80 °C, 4h	92	3c
2	$RhCl(PPh_3)_3$/PBH	CCl_4	Styrene	25 °C, 3h	100	12
3	$Mo_2(CO)_6(\eta\text{-}C_5H_5)_2$	CCl_4	1-octene	60 °C, 18h	8	2a
4	$Mo_2(CO)_6(\eta\text{-}C_5H_5)_2$	CCl_4	1-octene	120 °C, 18h	56	2a
5	CuCl	Cl_3CCN	1-octene	130 °C, 18h	79	4

Mechanism

Several experimental studies have been performed that provide support for a radical mechanism when transition metals are present. The radical is not a free radical, rather it is contained within the coordination sphere of the transition metal. This type of radical is referred to as a caged radical. The use of radical inhibitors such as galvinoxyl or butylated hydroxy toluene (BHT) have been found to inhibit the Kharasch reaction. Another experiments that can offer support for a radical mechanism is the crossover experiment (**Scheme 4**). If the only products obtained from the crossover experiment were **13** and **14** then a radical mechanism would likely not be operating; however, if products **13** – **16** were obtained then a radical would likely be present. Compounds **15** and **16** could only be produced if there was a radical process at work. When Davis and co-workers[3] performed the experiment using **1**, CCl_4, and CBr_4 in the presence of catalyst **12** the ratio of compounds **13:14:15:16** was determined to be 14:1:5:2. The formation of all 4 products supports a radical mechanism. When the same experiment was performed with $Mo_2(CO)_6(\eta\text{-}C_5H_5)_2$ all 4 products were obtained, this indicated that the radical process was not limited to just ruthenium. When the side products of the reaction mixtures were investigated there was additional support for a radical process. Transition metals helped prevent polymerization, but in some cases there were trace amounts of low molecular weight polymers.[3b] It was also found that the reaction mixtures contained trace amounts of C_2Cl_6[3a,b] which could only arise by the coupling of two trichloromethyl radicals. Unfortunately Davis was unable to obtain direct evidence of a radical when he performed EPR studies on Mo and Ru complexes. Though the EPR did not indicate the presence of a radical, strong support can still be found from the aforementioned experiments.

Scheme 4 Crossover Experiment

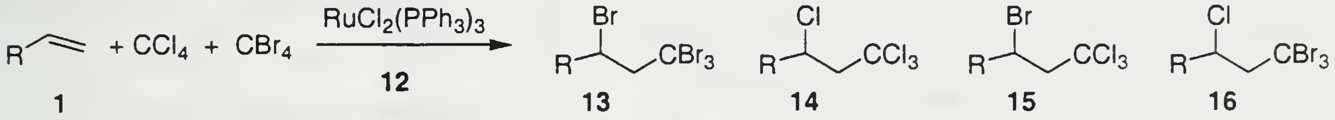

This same type of one electron transfer radical mechanism is believed to be operating in other transition metals used in the Kharasch reaction, such as iron,[5] copper,[7] and nickel.[8] In the case of copper, Nondek and co-workers[7] were able to obtain EPR evidence for the generation of Cu(II) in solution when Cu(I) was the initial oxidation state of the catalyst. Gossage and co-workers[8] also obtained EPR evidence for Ni(III) when a Ni(II) catalyst was initially used. With the EPR spectra of copper and nickel indicating the one electron transfer to the metal center, additional support for a radical process is provided.

Asymmetric Induction

The Kharasch reaction generates a chiral center at the internal carbon of the olefin, and the examples discussed previously were obtained as racemates. There have been two significant studies that have examined asymmetric induction with the Kharasch reaction. Murai and co-workers[9] studied the products obtained when [(-)-diop]RhCl (**17**) was reacted with styrene (**Scheme 5**); Kameyama and co-workers[11] studied Ru_2Cl_4[(-)-diop] (**18**) and Ru_2Cl_4[(+)-diop] (**19**) with a variety of substituted aromatic olefins (**Scheme 6**). Murai[9] reacted **20** with **21** to obtain the Kharasch product **22**, since the enatiomeric excess (ee) of **22** could not be measured directly, **22** was converted to **23**. This conversion involved inversion of the stereocenter with azide followed by reduction with lithium aluminum hydride. The absolute configuration and % ee of **23** was measured by comparison of optical rotation of pure **23** and the optical rotation of **23** generated from the Kharasch reaction. It has been reported by Hiron and co-workers[10] that 30% racemization can occur when azide is used to displace a halogen at the benzylic position in 4:1 ethanol:water. Kameyama[11] studied asymmetric induction with catalyst **18** or **19**, CCl_4 and a variety

Scheme 5 Asymmetric Induction, Murai

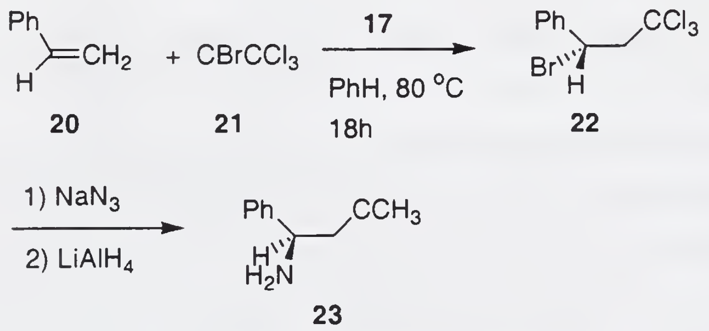

Scheme 6 Asymmetric Induction, Kameyama

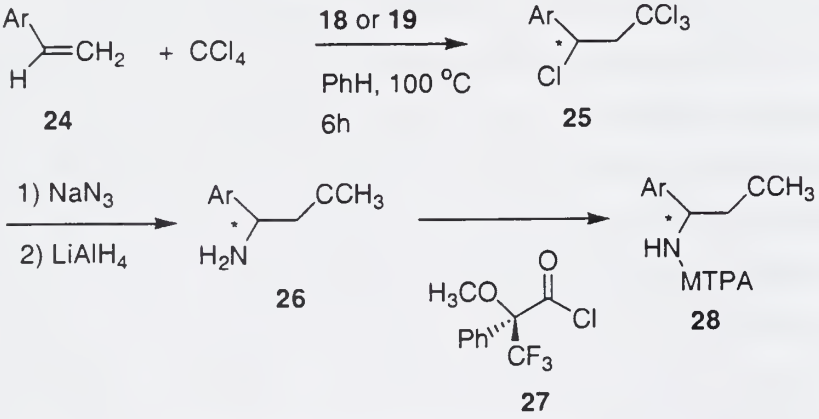

of aromatic olefins **24** to yield **25**. Kameyama inverted the stereocenter of **25** with azide, and reduced the azide to form **26**. Instead of comparing optical rotations to determine % ee Kameyama converted the enatiomers of **26** to diastereomers **28** using the chiral auxiliary **27**. The authors then measured the ee by separating the diastereomers on an HPLC column and measuring the ratio of the peaks. The absolute configuration of **26** was determined by comparison of the optical rotation of **26** with a pure known sample of **26**. The data obtained is summarized in **Table 2**, showing only the results for the (-) – diop. When entries 3 and 5 are examined in Table 2 it is noticed that there was optical rotation before inversion of the stereocenter, but after inversion and reduction no ee was obtained. This indicates that racemization occurred in at least two cases and it is likely there was some racemization in all cases. To measure the actual ee of the Kharasch products a chiral HPLC column can be used, since it is known what the absolute configuration of the product will be when **18** or **19** is used. The larger peak can be attributed to the *R* enatiomer when **18** is the catalyst and the *S* enatiomer when **19** is the catalyst allowing for direct measurement of the ee of the Kharasch product.

Table 2 Results for (-) - diop

Entry	Ar	$[\alpha]_D$ **22, 25**	% ee **23, 28**	Yield	Absolute Configuration
1	Ph	-22.5	32	26	S
2	Ph	+12	13	68	R
3	p-$CH_3C_6H_4$	+10	--	80	R
4	p-ClC_6H_4	+5.2	10	68	R
5	m-NO_2C_6H4	+5.2	--	57	R

Figure 1 Structure of (-) - diop (*R*,*R*)

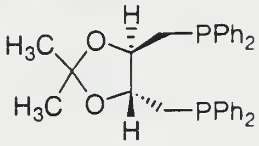

29

Efficient Low Temperature Reactions

The conditions for the Kharasch reaction involve the use of higher temperatures and long reaction times (Table 1). The ability to obtain the Kharasch products with mild conditions would enable it to be used regularly in the laboratory. Wilkinson's catalyst[12] (**Scheme 7**) and Grubbs' ruthenium

Scheme 7 Wilkinson's Catalyst

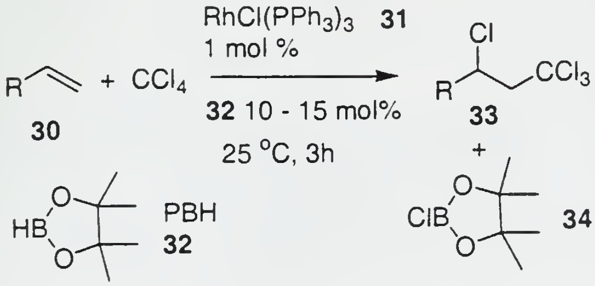

Scheme 8 Grubbs' Ruthenium Catalyst

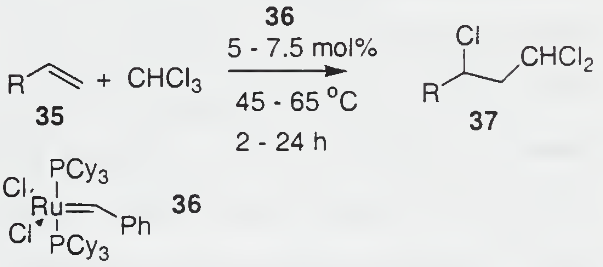

catalyst[13] (**Scheme 8**) are two well-known catalysts that have provided the Kharasch products in high yields at lower temperatures.

Pereira and Srebnik[12] were investigating hydroboration of olefins with pinacolborane (PBH) **32** using a variety of solvents and conditions. The use of CCl_4 as the solvent produced the Kharasch product instead of the hydroboration product. When the authors looked at the starting materials it was discovered that **32** was converted to B-chloropinacolboranate **34**. To determine if **34** was the active species it was added with **31** instead of **32**, which resulted in no product formation. It was also found that the use of galvinoxyl or BHT did not inhibit the reaction. No further studies were performed to elucidate the mechanism of the reaction.

Tallarico and co-workers[13] studied the reaction of **35** with 10 equivalents of chloroform in the presence of **36**. The authors found that no olefin metathesis occurred, but the Kharasch products were obtained in moderate to high yields. Moderate heating of the reaction was required, since $CHCl_3$ reacts slower due to the less stable $CHCl_2$ radical. Even with moderate heating the use of **36** is an improvement over previous conditions utilizing chloroform. The reaction was inhibited by galvinoxyl and BHT indicating that the Kharasch reaction followed the same radical mechanism as other transition metals. The radical inhibitors did not affect olefin metathesis with **36**. The authors wanted to show that **36** could be used for the Kharasch reaction and that when $CHCl_3$ is used as the solvent for olefin metathesis the undesired Kharasch reaction may also occur.

SYNTHESIS OF RING SYSTEMS

Since its introduction the Kharasch reaction has been utilized to synthesize small organic molecules. Recently, De Campo and co-workers[14] used trichloromethyl esters to perform intramolecular cyclizations with terminal olefins (**Scheme 9**). They obtained good yields of lactones **37** and **38** in 99% and 70% yield respectively. The procedure was also extended to polyether lactones with 15 atoms, **39**, and 18 atoms, **40**, giving a 70% yield for **39** and **40**. The intramolecular ring closure was catalyzed by CuCl and amine **41** or **42** as the ligand. The yields varied depending on the catalyst system, but the ring

Scheme 9 Lactones and Polyether Lactones

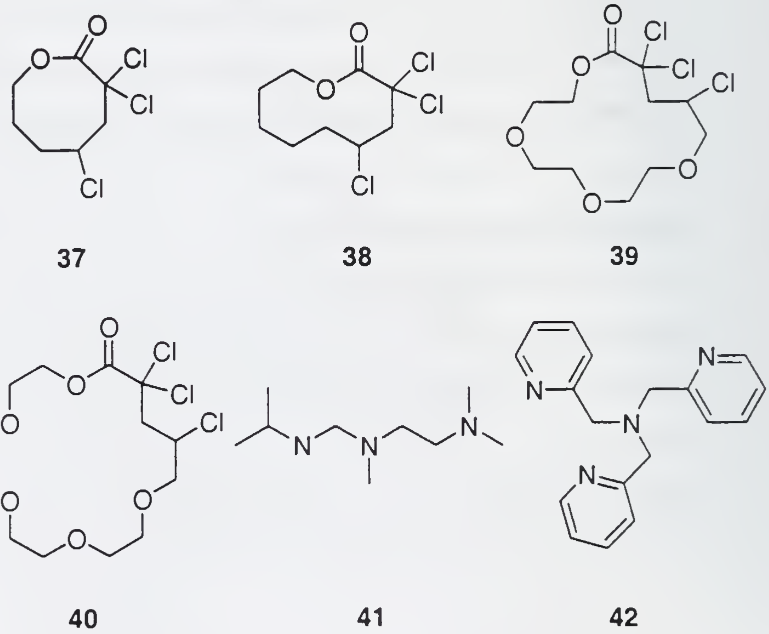

37 38 39

40 41 42

closures still proceeded cleanly. The use of amine **42** proceeded with higher yields than **41** in most cases. The catalytic system was generated *in situ* by adding equimolar amounts of CuCl and the desired ligand. The reactions were found to proceed with higher yields when 10 mol % Fe(0) was added to act as a radical scavenger. To confirm the formation of **38**, it was reduced by 3 equivalents of tributyltin hydride. The spectroscopic characteristics of **38** after reduction was identical to that of a pure sample of 1-oxacyclodecan-2-one. This method for forming lactone rings is complimentary to the process of intramolecular transesterification.

Martin and co-workers[16] have used the Kharasch products as intermediates in the formation of pyrone **48** (**Scheme 10**). The synthetic utility of the pyrone system is that it can be used in [4+2] cycloaddition reactions to generate either fused ring systems or aromatic systems after decarboxylation (**Scheme 11**). The authors used the Kharasch reaction in the first step when **43** was reacted with **44** in the presence of CuCl as the catalyst to form the Kharasch product **45**. Refluxing **45** in toluene in the presence of triethylamine gave butadienes **46** and **47** by elimination of HCl. Compounds **46** and **47** were obtained in a 83:17 mixture, respectively. The mixture of **46** and **47** was refluxed in mesitylene to give the pyrone **48**. The pyrone was then used in various [4+2] cycloadditions to generate compounds **49** – **51**. Scheme 10 illustrates that the Kharasch product can be utilized as an intermediate, instead of the final product. Along with lactones[14,15] and pyrones[16] the Kharasch products have been utilized as in the synthesis of pyridines,[17] lactams,[17,18] epoxides,[19] cyclopropyl,[20] cyclobutyl,[20] and fused[21] ring systems.

Scheme 10 Synthesis of Pyrone

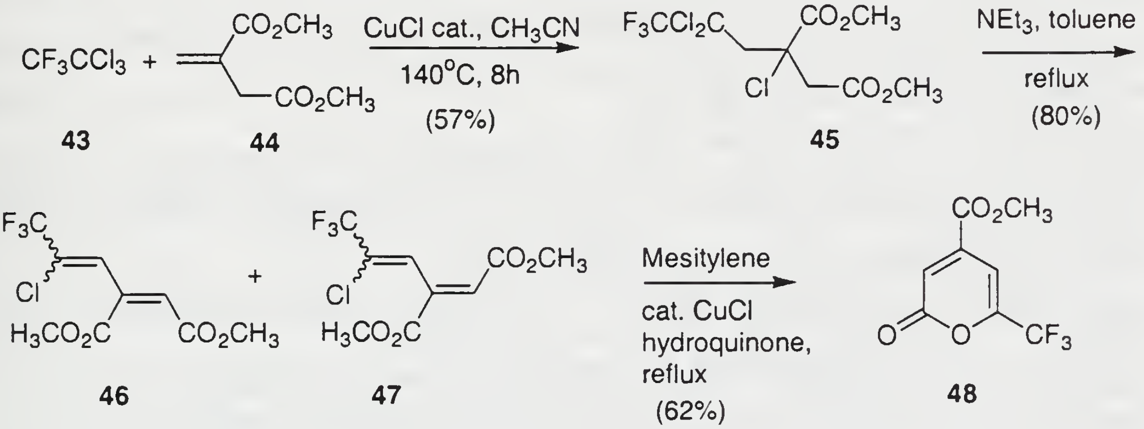

Scheme 11 Products of [4+2] Cycloadditions

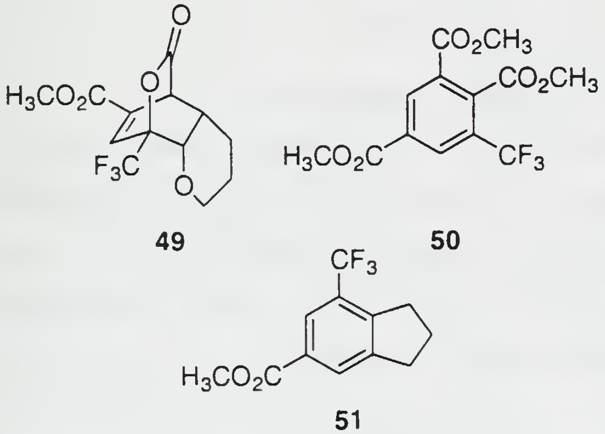

CONCLUSION

The Kharasch addition reaction has proven to be a valuable tool to the synthetic organic chemist. The use of transition metals to catalyze and control the radical has reduced the amount of polymerization that occurs in the reaction. Wilkinson's catalyst and Grubbs' catalyst have reduced the temperatures required for the reaction while maintaining good yields. The ability to form a new carbon-carbon bond in a molecule is a useful reaction, especially when the new bond has additional functionalization that can be used for further transformations. Introduction of a new stereocenter also occurs with the Kharasch reaction. Further investigations involving new transition metals and ligands may produce better results than those obtained by Murai and Kameyama. If this can be fully realized, the Kharasch reaction will find many new applications in the years to come.

REFERENCES

(1) Kharasch, M.S.; Jensen, E.V.; Urry W.H. (a) *Science,* **1945**, *102,* 128. (b) *J. Am. Chem. Soc.,* **1945**, *67,* 128. (c) *J. Am. Chem. Soc.,* **1946**, *68,* 154 d) *J. Am. Chem. Soc.,* **1946**, *69,* 1100, 1105

(2) (a) Davis, R.; Khazal, N.M.S., *J. Organomet. Chem.,* **1990**, *397,* 51. (b) Davis, R.; Groves, I.F., *J. Chem. Soc. Dalton Trans.,* **1982**, 2281

(3) (a) Bland, W.J., Davis, R.; Durrant, J.L.A., *J. Organomet. Chem.,* **1985**, *280,* 397. (b) Davis, R.; Furze, J.D., *J. Organomet. Chem.,* **1992**, *440,* 191 c) Matsumoto, H.; Nakano, T.; Nagai, Y., *Tetrahedron Lett.,* **1973**, *14,* 5147

(4) Murai, S.; Tsutsumi, S., *J. Org. Chem.,* **1966**, *31,* 3000

(5) Forti, L.; Ghelfi, F.; Libertini, E.; Pagnoni, U.M.; Soragni, E, *Tetrahedron,* **1997**, *53,* 17761

(6) Tsuji, J.; Sato, K., Nagashima, H., *Chem. Lett.,* **1981**, 1169

(7) Nondek, L.; Hun, L.G.; Wichterlová, B.; Krupicka, Š, *J. Mol. Cat.,* **1987**, 51

(8) Gossage, R.A.; Van De Kuil, L.A.; Van Koten, G., *Acc. Chem. Res.,* **1998**, *31,* 423

(9) Murai, S.; Sugise, R.; Sonoda, N., *Angew. Chem. Int. Ed.,* **1981**, *20,* 475

(10) Hiron, F.; Hughes, E.D., *J. Chem. Soc.,* **1960**, 795

(11) Kameyama, M.; Kamigata, N., *Bull. Chem. Soc. Jpn.,* **1987**, *60,* 3687

(12) Pereira, S.; Srebnik, M., *J. Am. Chem. Soc.,* **1996**, *118,* 909

(13) Tallarico, J.A.; Malnick, L.M.; Snapper, M.L., *J. Org. Chem.,* **1999**, *64,* 344

(14) De Campo, F.; Lastécouères, D.; Verlhac, J.B., *J. Chem. Soc. Perkin Trans. 1,* **2000**, 575-580

(15) Nagashima, H.; Wakamatsu, H.; Itoh, K.; Tomo, Y.; Tsuji, J., *Tetrahedron Lett.,* **1983**, *24,* 2395

(16) Martin, P.; Streith, J.; Rihs, G.; Winlker, T.; Belluš, D., *Tetrahedron Lett.,* **1985**, *26,* 3947

(17) Martin, P.; Steiner, E. ; Streith, J.; Winkler, T.; Belluš, D., *Tetrahedron,* **1985**, *41,* 4057

(18) Clark, A.J.; Duncalf, D.J.; Filik, R.P.; Haddelton, D.M.; Thomas, G.H.; Wongtap, H., *Tetrahedron Lett.,* **1999**, *40,* 3807

(19) Klemmensen, P.D.; Kolind-Anderson, H.; Madsen, B.H.; Svendsen A., *J. Org. Chem.,* **1979**,*44*,416

(20) Belluš, D., *Pure and Appl. Chem.,* **1985**, *57,* 1827

(21) Hayes, T.K.; Freyer, A.J.; Parvez, M.; Weinreb, S.M., *J. Org. Chem.,* **1986**, *51,* 5503

COVALENT ELECTRO AND PHOTOCHROMIC MOLECULAR SWITCHES

Reported by Amy M. Balija October 23, 2000

INTRODUCTION

The drive to miniaturize electrical and mechanical components has lead scientists to develop devices on a molecular scale. Such devices include brakes, gears, turnstiles, ratchets, and switches.[1] Combining molecular devices can result in the development of systems that can perform tasks on a subnano- to nanoscopic scale. The digital revolution has created a special need for molecular systems capable of data storage. The molecular switch is likely to be one of the main components in such data storage devices.

Molecular switches are compounds that undergo an electrical, ionic, structural or magnetic change when exposed to an external stimulus.[2,3] Currently, approaches have used photons, ions, protons and electrons as external stimuli. These stimuli alter the molecular switch's conformation, complexation or redox form. A molecular switch can exist in two forms, e.g., **1** and **2** (Figure 1). Introduction of external stimuli S_1 or S_2 causes a shift in the equilibrium toward a specific form. Switching between forms **1** and **2** may be induced by a single stimulus (i.e.: $S_1 = S_2 =$ light) or two different stimuli (i.e.: $S_1 =$ light, $S_2 =$ heat). The reaction is reversible if conversion between **1** and **2** is possible.[3] A single mode molecular switch exists in two forms as shown in Figure 1.

Figure 1

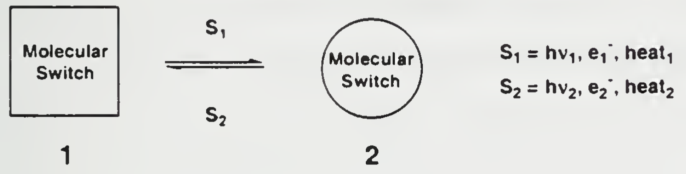

Several reports on molecular switches that use light as the external stimulus have appeared recently.[4,5] These photomolecular switches are thermally irreversible, a large thermal energy barrier between **1** and **2** is present. Furthermore, the equilibrium between **1** and **2** is resistant to fatigue with little decomposition of the molecular switch present after multiple stimulations. Encouraged by the results obtained using light, scientists began to search for other reversible systems that could be exploited in a molecular switch. Electrochemistry is advantageous because detectable structural changes in a compound may occur with a change in redox state. Electrochemical switches show promise in future applications in data storage devices.

Copyright © 2000 by Amy M. Balija

ELECTROCHROMIC AND PHOTOCHROMIC MOLECULAR SWITCHES

For a compound to be considered a molecular switch, it must meet several criteria[4]: (1) the switch must be bistable (i.e., both **1** and **2** must be stable); (2) the conversion between forms **1** and **2** must be efficient, (3) a complete shift in the equilibrium must be attained after stimulation by S_1 or S_2; (4) **1** and **2** must be highly sensitive to the specific stimuli; and (5) **1** and **2** must be distinguishable from each other. An electrochemical switch that has a shift in its UV/Vis absorption spectra after being exposed to an external stimulus is considered an electrochromic molecular switch. A photochemical switch that shifts its UV/Vis absorption spectra after exposure to light is a photochromic molecular switch. In principal, any compound that undergoes a reversible reaction could be considered a molecular switch. However, for only a few such compounds have all the criteria been tested. This report will cover some of the advances in the development of electrochromic and photochromic molecular switches and their use in the development of dual-mode electro-photochromic switches.

SINGLE MODE MOLECULAR SWITCHES

5,5'Azinobis(1,3-diphenyltetrazole)

In 1999, Araki and coworkers reported an electrochromic molecular switch based on 5,5'-azinobis(1,3-diphenyltetrazole) **3** which could convert between redox forms **4** and **5**[6] (Scheme 1).

Scheme 1

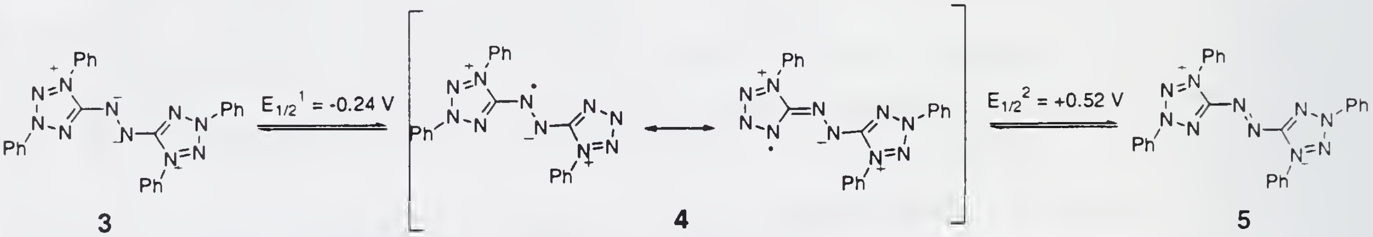

Electrochemical oxidation of **3** in methylene chloride resulted in the formation of the resonance stabilized radical cation **4** and dication **5** in two sequential one-electron oxidation steps. Two distinct reversible potentials were recorded at –0.24 and +0.52 V, respectively. The stability of the switch was evidenced by the fact that all three states **3-5** formed single crystals. However, the authors noted a gradual conversion from **5** to **4** in ethanol and acetonitrile over 24 hours, indicating the instability of **5** in solution. Furthermore, oxidation from **4** to **5** was irreversible when performed in pyridine. Araki and coworkers hypothesized that after the formation of **5**, pyridine acted to nucleophilically cleave **5**.

The system in Scheme 1 showed favorable electrochromic properties; upon stepwise oxidation, a shift in UV/Vis spectra was observed (**3**→**4**→**5**, λ_{max} 542→625→446 nm). Araki and coworkers further verified the electrochemical formation of **4** and **5** by comparing the NMR, cyclic voltammetry (CV), and melting point to the chemically oxidized forms. Synthetically, **3** was oxidized to **4** by lead tetra-acetate. Addition of concentrated nitric acid subsequently oxidized **4** to **5** completely. However, oxidation of **5** to **3** with zinc powder was incomplete. Thus, conversion between **3-5** was more efficient electrochemically than chemically. The degree of fatigue in this system was not reported.

1,2-Bis(2-Methylbenzo[b]thiophen-e-yl)perflurorcycloalkene

In 1992, Irie and coworkers developed a perfluorocycloalkene **6** that underwent cyclization after exposure to light[7] (Scheme 2).

A sample of the uncyclized perfluorocycloalkene **6** in hexane formed **7** in a 45 : 55 photostationary ratio when irradiated at 313 nm showing incomplete conversion. UV/Vis spectroscopy was used to detect the shift in absorption maximums (6→7, 258→517 nm). Conversion from **7** back to **6** occurred after irradiation at wavelengths over 500 nm.

Scheme 2

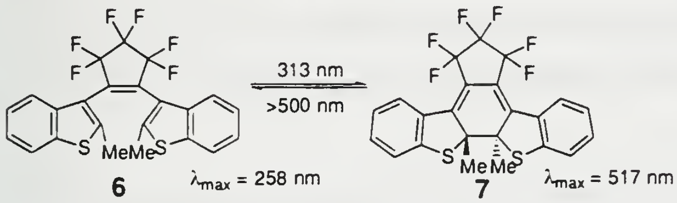

The thermal stability of the switch was studied by heating a sample of **6** in toluene at 80°C for six months. No change in the sample composition was detected by UV/Vis spectroscopy. In addition, the ability to photochemically interconvert between **6** and **7** without decomposition was investigated. The photostationary ratio was 90 % maintained after 14,000 cycles, verifying the stability of **6**. Recently, several reports have appeared using derivatives of the photochromic switch **6**, indicating the versatility of the perfluoroalkene as a photo-active molecular switch.[8]

DUAL-MODE ELECTRO-PHOTOCHROMIC MOLECULAR SWITCHES

Uses of molecular switches include the incorporation into molecular circuits for controlling the movement of electrons through molecular wires and the application to data storage systems.[2,3] Switching between two bistable forms **1** and **2** can be considered a write/read/erase data system. Excitation of **1** by S_1 causes a shift in the equilibrium to **2**. Data is stored. The information is retained unless the molecular switch is affected by S_2. Photochromic molecular switches allow for the storage and UV/Vis detection of saved information. However, detection of saved information could easily affect the molecular switch, erasing the data being stored. To solve this dilemma, chemists have developed dual-mode molecular switches that consist of two covalently linked switches (Figure 2).

Figure 2

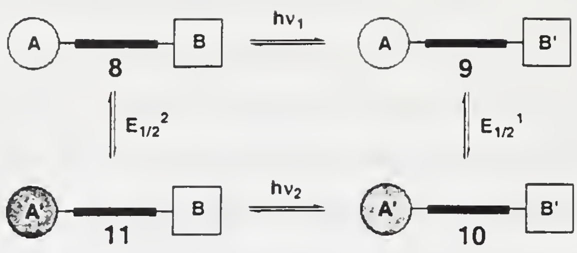

A dual-mode molecular switch **8** contains two functional groups **A** and **B** that are sensitive to different stimuli. These groups are connected through a conjugated linker to ensure a pathway for electron transfer between **A** and **B**. The functional groups **A** and **B** regulate each other's ability to change conformations under specific stimuli. Structure **8** is exposed to the stimulus **$h\nu_1$** to induce a change in functional group **B** to form **9**. Since the linker allows electron transfer between functional groups, the electronic properties of **A** have also changed. Structure **9** is then exposed to the potential **$E_{1/2}^{1}$**, inducing a conformation change in **A** and, in turn, an electric change in **B'**. Irradiating with **$h\nu_2$** causes the reversal from **B'** to **B** without affecting **A'** (Structure **11**). Because of different electron densities between **8** and **10**, the intensities of **$h\nu_1$** and **$h\nu_2$** are different (i.e.: **$h\nu_1$** = 500 nm, **$h\nu_2$** = 400 nm). Similarly, the conversion from **11** to **8** is stimulated by **$E_{1/2}^{2}$** with a different potential than $E_{1/2}^{2}$. All conversions are reversible.

For data storage, information is retained in the molecular switch when the stimulant **$h\nu_1$** induces the conversion of **8** to **9**. Structure **9** is then exposed to **$E_{1/2}^{1}$**, locking the information. Detection of this saved information by light can be performed without the chance for accidental erasure. To write over data that has been stored, **A** and **B** must be excited sequentially. The ideal molecular switch for use in data storage would be unable to convert to **11**.

2-(4'-Methoxyphenylazo)anthraquinone

One of the first electro-photochromic molecular switches, developed by Shimidzu and coworkers, was the azo-anthraquinone **12**.[9] This compound is comprised of the photo-active azo group (**12** to **13**) and the electro-active anthraquinone (**12** to **15**) as illustrated in Scheme 3.

Irradiating **12** at 380 nm in chloroform resulted in the formation of **13**, as observed by the decreased λ_{max} values for **12** and increasing λ_{max} value for **13**. The formation of two isosbestic points at 316 and 416 nm indicated no by-products formed. Conversion back to **12** was induced by irradiation of **13** at 500 nm. Irradiation of **14** at 350 nm caused the disappearance of the λ_{max} value at 354 nm (**14**) and the emergence of a λ_{max} value at 445 nm, corresponding to **15**. Irradiation of **15** at 500 nm resulted in obtaining **14**. Two reversible monoelectric oxidations to **13** via a semiquinone radical were noted by CV when an electropotential was applied to a saturated solution of **14** in DMF at –0.50 and –1.20 V, respectively. Similar potentials were obtained for the redox reaction between **12** and **15**. UV/Vis

Scheme 3

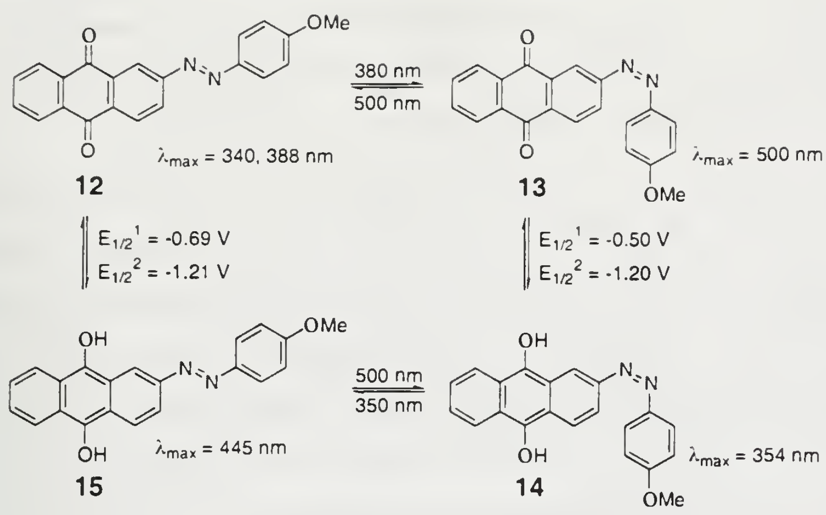

absorption maximums shifted when the structures were exposed to a potential (**12**→**15**, **13**→**14** with λ_{max} 340→445 nm and 500→354 nm, respectively).

Detection of stored information in computers requires the use of semiconductor lasers. To apply the molecular switching of **12** toward use in computer data storage devices, Shimidzu and coworkers synthesized derivatives **16a-c** whose absorption values lie closer to the near-infrared region of the electromagnetic spectra (Figure 3). Compounds **16a-c** exhibited similar reversible electrochromic and photochromic data as **12**.

Figure 3

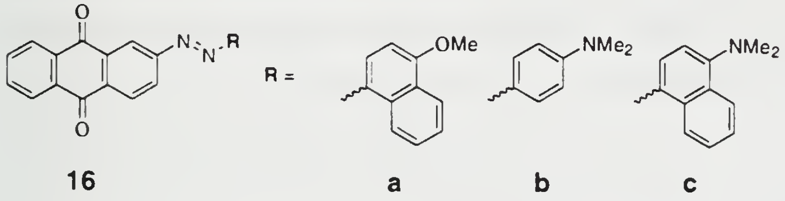

Although all four species, **12-15**, could be detected spectrochemically, the compounds exhibited limited thermal stability. Warming a solution of **13** in chloroform at 30 °C resulted in complete transformation to **12** in 100 minutes as detected by UV/Vis spectroscopy. Similar results were obtained for the *cis/trans* isomerization of **14** to **15** where total conversion was achieved in 3000 minutes. The redox systems **12** to **15** and **13** to **14** were only reversible under aprotic conditions. Upon addition sulfuric acid, a quasi-reversible bielectric redox system developed. Furthermore, the azo group could be easily reduced at –0.98 V, giving rise to an irreversible side product. The thermal and electronic instability of the azo group does not fulfill the criteria of a molecular switch. In addition, the compound converts between four different states, **12-15**, not ideal for data storage.

5,6,7-Tri-*tert*-butyl-1,4-Anthraquinone

Miki and coworkers synthesized anthraquinone **17** that incorporated moieties for both a photoisomerization reaction (**17** to **18**) and the electrochemical reaction (**17** to **20**)[10] (Scheme 4).

Irradiating **17** at 460 nm in hexane induced a cyclization to **18** as monitored by the shift in λ_{max} values (**17**→**18**, 333→398 nm). Isosbestic points at 355 and 402 nm indicated the absence of by-products. Conversion back to **17** by irradiating at 402 nm resulted in a photostationary state of **17** : **18** in

Scheme 4

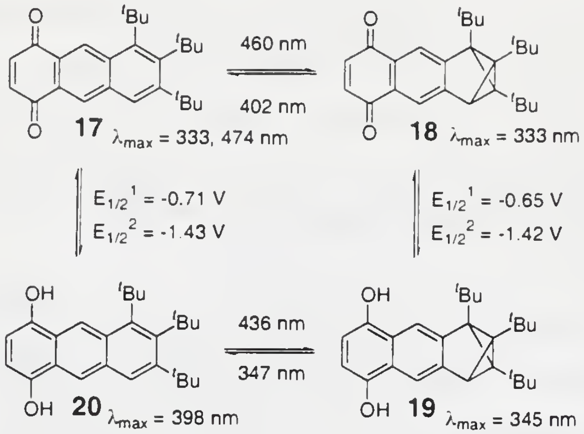

a 7.2 : 1 ratio. Furthermore, photoisomerization of **19** at 436 nm in ethyl ether showed complete conversion to **20** as noted by the UV/Vis absorption shifts. Similar results were recorded for the conversion of **20** to **19**.

The redox reaction from **17** to **20** was performed in dry DMF and acetic acid with two reversible reduction waves as observed by CV. A different potential (+0.20V) was obtained for the oxidation of **20** to **17** due to the oxygens being protonated. Similar results were obtained in the redox reaction between **18** and **19**. A change in the UV/Vis absorption wavelengths as a potential was applied to the redox couples (**17→20**, **18→19** with λ_{max} = 474→398 nm, λ_{max} = 333→345 nm, respectively) were reported.

Miki and coworkers indicated that the four states, **17-20**, were thermally stable; however, experiments supporting this claim were not conducted. Each conversion was performed in a different solvent. For use in a computer data storage device, this molecular switch would need to be responsive to the stimuli in one solvent. Miki and coworkers' preliminary work is the groundwork for further development of **17** as a dual-mode molecular switch.

Bisphenolic Diethienylethene

Lehn and coworkers developed a bisphenolic diarylethene **21** that incorporated the photocyclization reaction of **21** to **22** and the redox conversion of **22** to **23**[11] (Scheme 5).

Irradiation of **21** in deuterated acetonitrile at 312 nm resulted in the light-induced electrocyclization of **21** to **22** in over 98 % yield. A red shift in the UV/Vis absorption from **21** to **22** was detected. Furthermore, an isosbestic point at 318 nm was observed, indicating no by-products. Re-opening of **22** to **21** was achieved with a 98 % conversion by irradiating a solution of **22** in red light with wavelengths greater than 600 nm. The reversible oxidation/reduction of **22** in acetonitrile occurred through a bielectronic transfer at +0.72 V as verified by a red UV/Vis absorption shift. The existence of **23** as a protonated source resulted in different reduction/oxidation potentials.

Lehn and coworkers studied the stability of **21-23** many different ways. A sample of **23**, either as a solid or dissolved in acetonitrile, remained unchanged after one year at 25°C. When **23** was heated at 60°C in acetonitrile, irreversible decomposition occurred with a half life of 13 hours. Continuous shifting of the equilibrium between **21** to **22**, showed a 1% decomposition after ten cycles demonstrating photochemical stability of the molecular switch. Structure **23** did not exhibit appreciable photochemical

Scheme 5

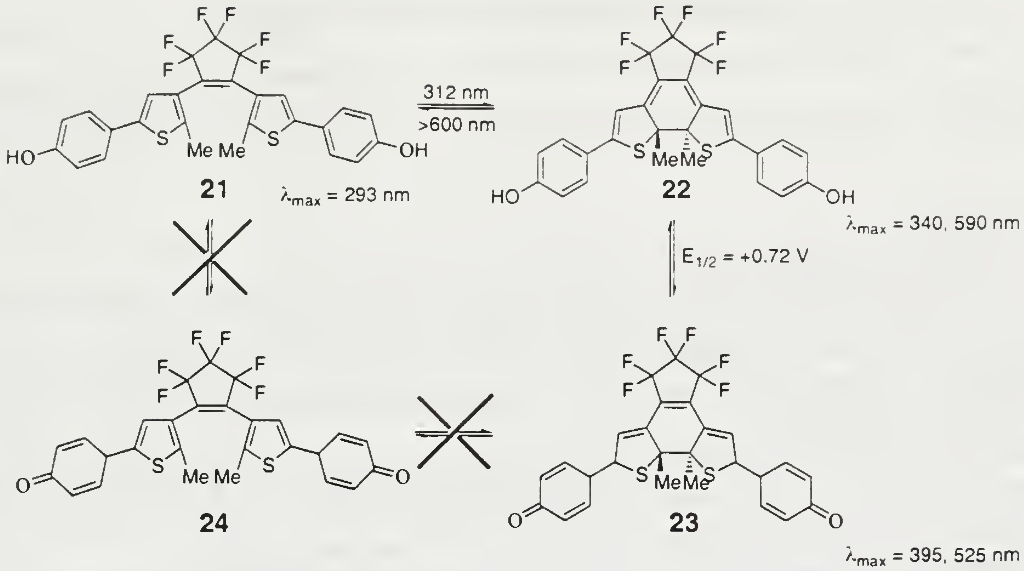

affects after exposure to red light for 8 hours. Therefore, **21** was photochemically inert. Studies done with CV indicated that **21** was electrochemically inert between the range –1.4 to +1.0 V. This demonstrates that **24** can not be obtained through either photo or electrical means.

The development of **21** by Lehn and coworkers illustrates the most advanced dual-mode molecular switch to date. Structure **24** can not be formed under the stimuli conditions for **21-23**, creating a write/store/lock molecular switch. However, the use of **21** as a switch for data storage is impractical because its inability to bind with other molecular devices. Lehn performed experiments on derivatized hydroquinones showing that substituents on **21** resulted in the undesired ability to electrochemically affect both the cyclized and uncyclized structures. Thus, the molecular switch would not be able to save information.

CONCLUSION

The development of the electrochromic molecular switch was in response to the need to investigate other stimuli that effect reversible reactions. An electro or photochromic molecular switch has the ability to change a compound's conformations by electron or photon transfer, respectively. Combining an electro- and photo-chromic molecular switch (i.e. **6**) can form a dual-mode switch. Unlike a single mode switch in which information can be erased, a dual-mode switch allows information to be stored and locked, minimizing accidental erasure. Structures **17** and **21** have potential toward the development of data storage devices although further research must be conducted. Additional dual-mode molecular switches must be synthesized that can be used in the development of data storage devices. These molecular devices can be combined with other molecular devices to develop a nanoscale computer, capable of performing the same basic operations as their counterparts on the molecular scale.

Recently, preliminary reports have shown that catenanes can repetitively switch between two states on a solid support, useful in the development of nanoscale computers.[12] However, additional research must be conducted to further develop dual-mode molecular switches that can be used as data storage devices.

REFERENCES:

(1) (a) Kelly, T. R.; Bowyer, M. C.; Bhaskar, K. V.; Bebbington, D.; Garcia, A.; Lang, F.; Kim, M.H.; Jette, M. P. *J. Am. Chem. Soc.* **1994**, *116*, 3657-3658. (b) Clayden, J.; Pink, J. H. *Angew. Chem., Int. Ed. Engl.* **1998**, *37*, 1937-1939. (c) Beddard, T. C.; Moore, J. S. *J. Am. Chem. Soc.* **1995**, *117*, 10663-10671. (d) Kelly, T. R.; Tellita, I.; Sestelo, J. P. *Angew. Chem. Int. Ed. Eng.* **1997**, *36*, 1866-1868.

(2) (a) Bergonzi, R.; Fabbrizzi, L.; Licchelli, M.; Mangano, C. *Coord. Chem. Rev.* **1998**, *170*, 31-46. (b) Goulle, V.; Harriman, A.; Lehn, J.-M. *J. Chem. Soc., Chem. Commun.* **1993**, 1034-1036.

(3) Lehn, J.-M. *Supramolecular Chemistry*. VCH: Weinheim, 1995.

(4) Feringa, B. L.; Jager, W. F.; de Lange, B. *Tetrahedron* **1993**, *49*, 8267-8310.

(5) (a) Balzani, V.; Gomez-Lopez, M.; Stoddart, J. F. *Acc. Chem. Rev.* **1998**, *31*, 405-414. (b) Irie, M.; *Chem. Rev.* **2000**, 1685-1716. (c) Yokoyama, F. *Chem. Rev.* **2000**, 1717-1716. (d) Feringa, B. L. *Chem. Rev.* **2000**, 1789-1816.

(6) Araki, S.; Yamamoto, K.; Inoue, T.; Yamamura, H.; Kawai, M.; Butsugan, Y.; Zhou, J.; Eichhorn, E.; Ricker, A.; Huber, M. *J. Chem. Soc., Perkin Trans. 2* **1999**, 985-995.

(7) Hanazawa, M.; Sumiya, R.; Horikawa, Y.; Irie, M. *J. Chem. Soc., Chem. Commun.* **1992**, 206-207.

(8) (a) Saika, T.; Irie, M.; Shimidzu, T. *J. Chem. Soc., Chem. Commun.* **1994**, 2123-2124. (b) Mrozek, T.; Gorner, H.; Daub, J. *Chem. Comm.* **1999**, 1487-1488.

(9) (a) Iyoda, T.; Saika, T.; Honda, K.; Shimidzu, T. *Tetrahedron Lett.* **1989**, *30*, 5429-5432. (b) Saika, T.; Iyoda, T.; Honda, K.; Shimidzu, T. *J. Chem. Soc., Chem Commun.* **1993**, 1181-1187.

(10) Miki, S.; Noda, R.; Fukunishi, K. *Chem. Comm.* **1997**, 925-926.

(11) (a) Kawai, S. H.; Gilat, S. L.; Ponsinet, R.; Lehn, J.-M. *Chem. Eur. J.* **1995**, *1*, 285-293. (b) Gilat, S. L.; Kawai, S. H.; Lehn, J.-M. *J. Chem. Soc., Chem. Commun.* **1993**, 1439-1442. (c) Kawai, S. H.; Gilat, S. L.; Lehn, J.-M. *J. Chem. Soc., Chem. Commun.* **1994**, 1011-1013.

(12) Collier, C. P.; Mattersteig, G.; Wong, E.; Lou, Y.; Beverly, K.; Sampaio, J.; Raymo, F. M.; Stoddart, J. F.; Heath, J.R. *Science* **2000, *289***, 1172-1175.

TOTAL SYNTHESIS OF MANZAMINE A

Reported by Tyson A. Miller October 26, 2000

INTRODUCTION

Sponges are an excellent source of biologically and chemically interesting molecules.[1] Nitrogenous marine alkaloids make up roughly 25% of all reported marine natural products, and of these, 54% are alkaloids that are extracted from sponges.[2] β-Carboline containing manzamine alkaloids are one such class of compounds that have received attention due to their reported antitumor activities.[1-3] The goal of this review is to provide a brief introduction of manzamine alkaloids and to present the various synthetic avenues developed toward the total synthesis of manzamine A, **1**.[4]

ISOLATION AND STRUCTURE DETERMINATION

Chart 1. Ring labeling of 1.[3]

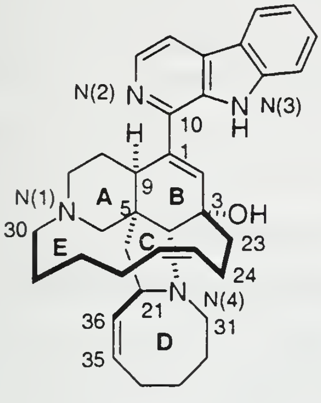

Manzamine A, **1**

Higa and co-workers harvested the sponge *Haliclona sp.* from the shores of Okinawa, Japan in 1985.[3] An isolated extract from the sponge afforded manzamine A, **1**, which inhibited the growth of P388 mouse leukemia cells with an IC_{50} of 0.07 μg/mL.[3] Structural features of **1**, highlighted in Chart 1, included a β-carboline moiety, a hydroisoquinoline core (AB) with fused pyrrolidine (C) and azocine (D) rings as well as a *cis*-cycloazatridecene ring (E).

The relative configuration of the hydrochloride salt of **1** was deduced by NMR and the absolute configuration was established by X-ray crystallography.[3] Alkaloid **1** features one tri- and two disubstituted olefins in the main ABCDE skeletal core, as well as the β-carboline moiety and 5 stereogenic centers (Chart 1). Piperidine ring A and cyclohexane ring B assume chair and boat conformations, respectively, while the pyrrolidinium ring C (HCl salt of X-ray) is an envelope. Azocine ring D adopts an envelope-boat conformation[5] while the 13-membered macrocycle E is rigid, unlike most odd-membered macrocycles.[6]

RETROANALYSIS AND STRATEGIC DISCONNECTIONS

Several syntheses of **1** have revolved around cycloaddition strategies. An intermolecular Diels-Alder approach[7-12] to simplify the AB ring core (Chart 2) can leave dihydropyridinone and activated diene[7,8,10-12] or modified naphthyridine retrons.[8] An intramolecular Diels-Alder strategy to reduce the ABC ring core can create tethered and highly functionalized pyrrolidine ring C precursors[13-18] that can eventually establish the configuration of up to three of the five stereogenic centers simultaneously.

Copyright © 2000 by
Tyson A. Miller

Chart 2. Strategic Disconnections of 1.

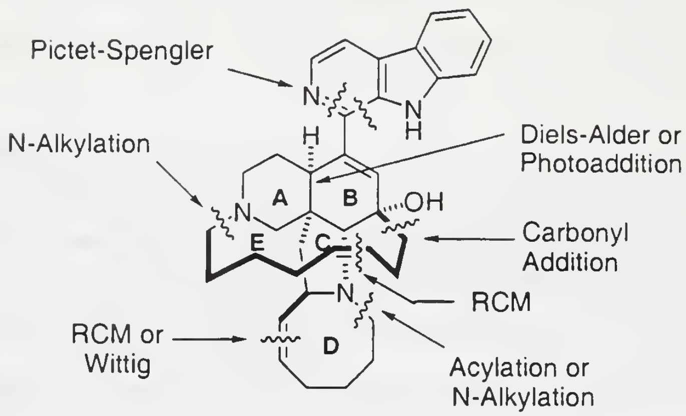

Non-cycloaddition strategies have also been utilized to disconnect the ring cores of **1**. Disconnections of strategic carbon-carbon bonds within the ABC ring core (Chart 2) can afford retrons susceptible to radical processes.[19] to photoaddition,[20] to Michael addition,[21] and to Mannich closure.[22]

The azocine D-ring and the cycloazatridecene E-ring both possess an olefin and a nitrogen atom. Olefinic disconnections can lead to ring closing metathesis (RCM),[9,18,19] Wittig,[20] or carbene precursors.[23] Detachment at the isoquinoline N-1 and pyrrolidine N-4 nitrogens reduce the D and E rings to alkyl chains with good leaving groups that N-alkylate[9,16,20,24-26] or carboxylic acid derivatives that N-acylate.[16,18]

Finally, the alcohol can be derived from a carbonyl group and an organometallic species.[16,18] One could also envision detachment of the β-carboline moiety at C-10 to yield an aldehyde and tryptamine. A Pictet-Spengler reaction with oxidation could successfully reattach these moieties.[18,20,27,28]

SYNTHESIS OF RING CORE

Multiple approaches have been developed for the synthesis of the pentacyclic ring core system. Most of them focus on either the AB or ABC rings. Only three groups have reported a successful synthesis of the ABCDE core[18,20,28] and only two of those[18,20] have completed total syntheses of **1**. A biosynthetic hypothesis[29] has been devised by Baldwin, with some success of proof of principle.[30] The most interesting highlights from the numerous other synthetic efforts toward the synthesis of the Manzamine A ring core will be discussed here.

Intermolecular Diels-Alder

The intermolecular Diels-Alder strategy has not been commonly used except for the synthesis of partially developed hydroisoquinoline AB ring cores.[7-9] However, during the synthesis of the ABCD ring core, Nakagawa and co-workers used an α,β-unsaturated lactam **2** and Danishefsky's diene **3** to afford a diastereomeric mixture of hydroisoquinoline AB ring core **4** in 93% yield (Scheme 1).[10] The cycloaddition reaction created two new stereocenters at C-5 and C-9 that are similar to the natural product **1**. Related stereochemical studies by Nakagawa have show that endo-selectivity is dictated by secondary orbital overlap which lowers the energy of the endo reaction path.[11,12]

Scheme 1. Nakagawa's Use of Intermolecular Diels-Alder.[10]

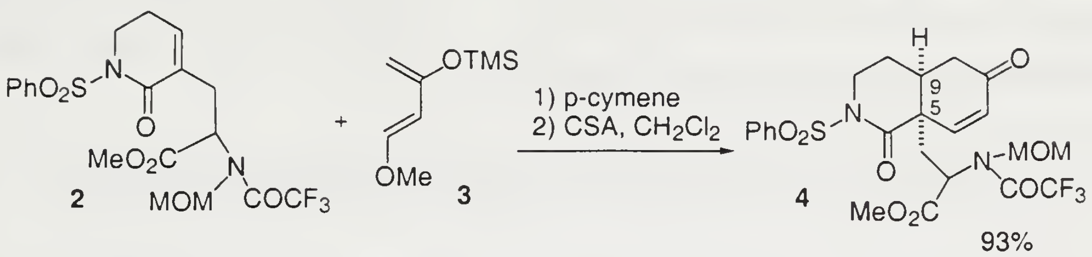

Intramolecular Diels-Alder

Intramolecular Diels-Alder strategies have been more prominent in the synthesis of manzamine A ring cores, due to ease of installation of multiple stereocenters with moderate success. Leonard and co-workers developed a tandem sulfolene extrusion/Diels-Alder sequence.[14] This strategy (Scheme 2) features a sulfolene **5** as a masked diene with ester or amide functionality that is later incorporated into the β-carboline moiety of **1**. Upon heating, sulfur dioxide was removed chelotropically to give an *in-situ* s-*cis* diene **6** that undergoes an intramolecular Diels-Alder closure upon the dihydropyrrole olefin.[14] Unfortunately, despite calculations and encouraging model studies,[15] the product was not the expected cis-decalin, endo-adduct 7. The trans-decalin, exo-adduct (with respect to the tether) **8** was isolated exclusively in 82% yield, with the undesired stereochemical configuration at C-9.[14]

Scheme 2. Exo Stereoselection in Tandem Sulfolene Extrusion/ Intra Diels-Alder.[11]

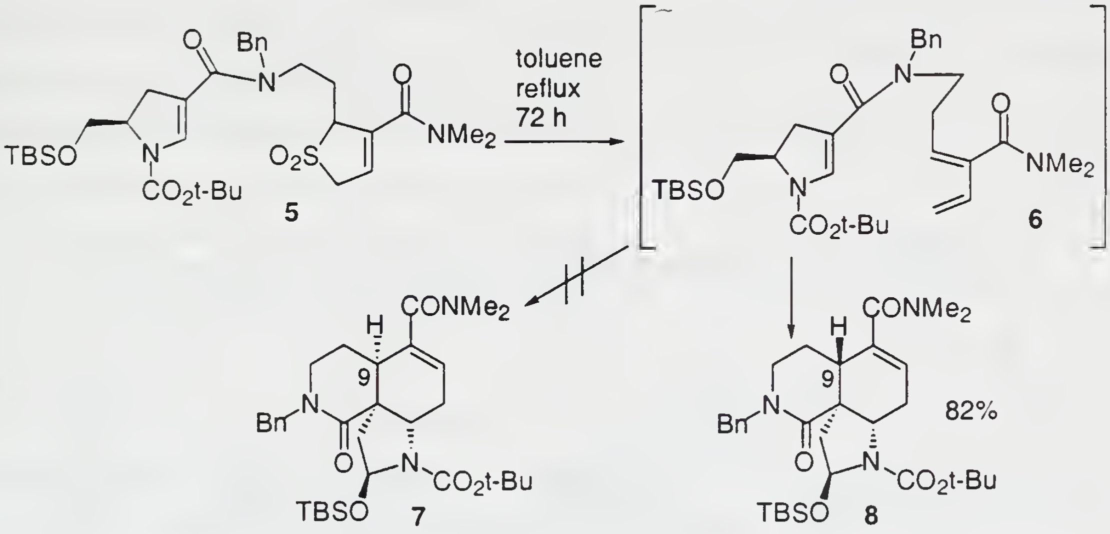

Pandit and coworkers successfully synthesized the first ABCDE core structure **9** (Scheme 3). The necessary diene **10** was prepared in 11 steps from L-serine **11**. Pyrrolidine **10** was then subjected to refluxing xylenes for 4 hours to afford a 90% yield of **12** in a mixture of diastereomers at C-9.[17] The desired diastereomer was carried forward 6 steps to **13** which underwent RCM to yield **14**. Subsequent steps included 1) alcohol deprotection and oxidation, 2) olefination of an aldehyde, 3) hydrolysis of the carbamate, and 4) acylation of the pyrrolidine nitrogen. These steps afforded a second diolefinic precursor which was subjected to RCM to afford the ABCDE core **9**.[16]

Scheme 3. ABCDE Ring Core Using Intramolecular Diels-Alder.[16]

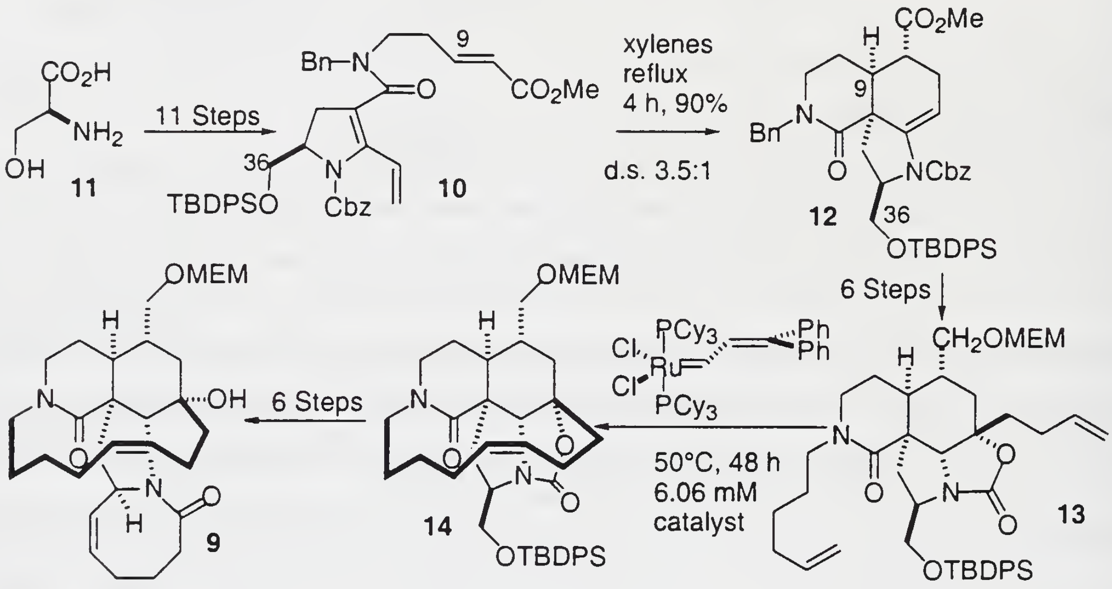

Non-Cycloaddition Strategies

There were multiple approaches by several groups[19,21-23,25,31] that yielded various permutations of 2, 3, or 4 rings of the manzamine A **1** pentacyclic structure. The most interesting of these was by Brands and coworkers[21] where complete stereocontrol was contained within the lone stereocenter of pyroglutamic acid **15** (Scheme 4).

Scheme 4. Construction of Ring A with Complete Stereocontrol.[21]

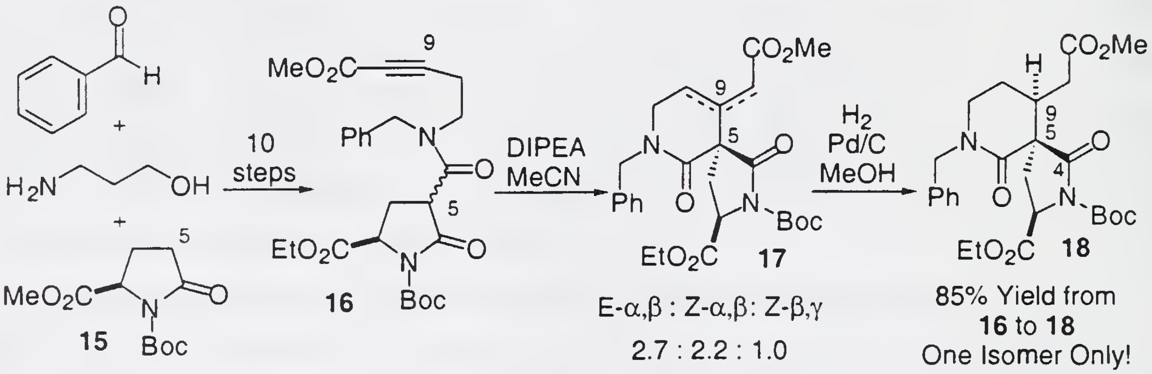

The cyclization precursor **16** was generated in 10 steps from **15**, benzaldehyde, and 3-amino-1-propanol. Pyroglutamate derivative **16** was then subjected to Hünig's base in acetonitrile which abstracted the C-5 proton on **16** to generate an enolate ion that added to the Michael acceptor alkyne at C-9 to yield a mixture of α,β and β,γ unsaturated esters **17**. Selective hydrogenation from the bottom face of **17** due to steric hindrance of the oxygen atom on the C-4 pyrrolidine carbonyl afforded only one enantiomeric product **18** with both of the desired C-5 and C-9 configurations in 85% yield. Spirocycle **18** was carried forward to an ABC ring core structure in 5 steps.

TOTAL SYNTHESIS OF MANZAMINE A

The leader in synthetic efforts towards the total synthesis of **1** for much of the 1990's was U.K. Pandit, due to the fact that he had attached a β-carboline moiety to an ABCD ring core by 1994,[28] and in 1996, was the first to synthesize a viable analog of the ABCDE ring core.[16] However, it was Winkler and co-workers in 1998 who first published the successful total synthesis of **1**[20] using a tandem photoaddition/retro-Mannich/Mannich closure methodology that was developed within his laboratories.[32] Martin and co-workers published a more efficient total synthesis in 1999.[18] These are the only two total syntheses reported to date. The key step for each total synthesis is highlighted here.

Winkler Total Synthesis

Winkler's key strategies and steps to his total synthesis included the following: 1) installation of the C-21 stereocenter using pseudoephedrine[32] which afforded stereocontrol throughout the synthesis,[26] 2) early construction of the azocine D-ring via nucleophilic substitution and tethered attachment to a modified A ring; 3) utilization of a tandem photoaddition/retro-Mannich/Mannich closure methodology on the AD ring precursor **19** to construct rings B and C (Scheme 5); 4) macrocyclization of the E-ring via N-alkylation; and 5) installation of the β-carboline moiety.[27]

Photoaddition precursor **19** was afforded from 3-pyridinylmethanol in 21 steps using a pseudoephedrine mediated alkylation developed by Myers[32] to install the C-21 stereocenter (Scheme 5). A 450W mercury pressure lamp activates **19** to undergo a [2+2] photoaddition and retro-Mannich fragmentation with O-closure of a ketoiminium intermediate to afford aminal **20**. When **20** is subjected to pyridinium acetate, Mannich closure leads to **21** as a single isomer in 20% overall yield from **19**. The absolute configurations at C-4, C-5, and C-9 were set with this sequence. As shown in Scheme 6, protection of the C-30 hydroxyl group with TBS-Cl, installation of a C-10 ester moiety at C-1 with lithium hexamethyldisilazane and methyl cyanoformate, reduction of the C-2 ketone with sodium borohydride, activation of the C-2 alcohol with mesyl chloride, followed by mesylate elimination to form a 2:1 (α,β- : β,γ) mixture of unsaturated esters. The β,γ-unsaturated ester **22** was transformed to ircinal A **23** in the following steps: 1) selective epoxidation of the C-2/C-3 olefin from the bottom face with *meta*-chloroperbenzoic acid; 2) deprotection of the C-30 alcohol with tetrabutylammonium fluoride;

Scheme 5. Tandem Vinylogous Amide / Retro-Mannich / Mannich Cyclization.[20]

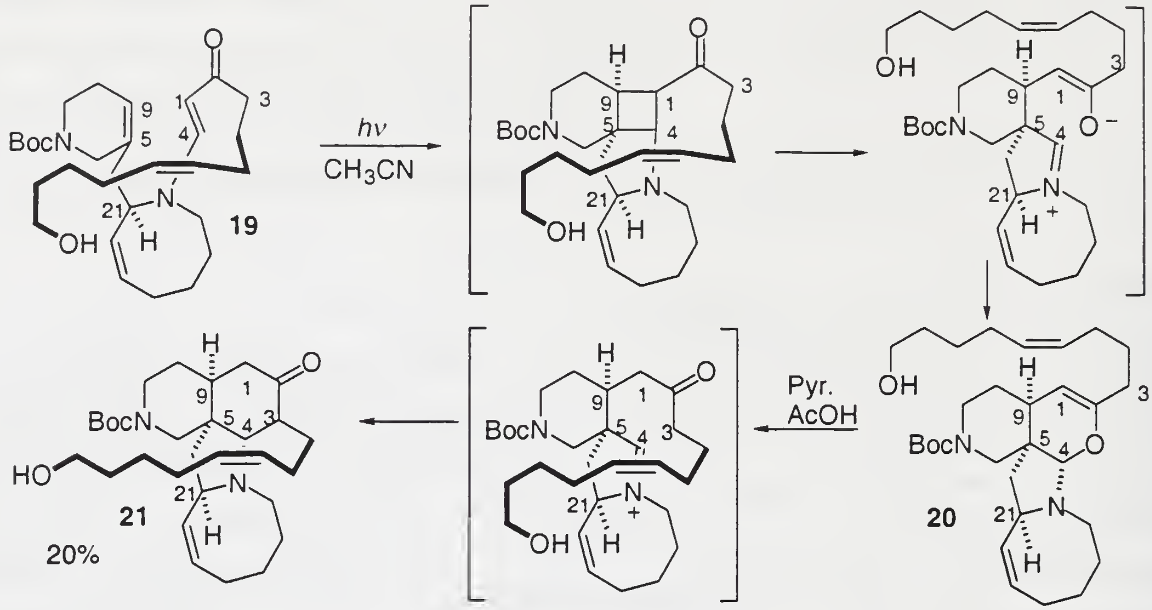

3) activation of the C-30 alcohol as a leaving group with tosyl chloride; 4) deprotection of N-1 with trifluoroacetic acid (TFA); 5) deprotonation of N-1 with Hünig's base which closes the E-ring via N-alkylation; 6) reduction of the C-10 ester to an alcohol with DIBALH; 7) oxidation of the aldehyde with Dess-Martin periodinane to afford ircinal A **23**. Finally, using Kobayashi's procedure,[27] Winkler and coworkers installed the β-carboline moiety by reacting **23** with tryptamine and TFA in a Pictet-Spengler reaction, followed by DDQ oxidation of the intermediate to afford the natural product **1**.

Scheme 6. Completion of Winkler's Total Synthesis of Manzamine A 1.[20]

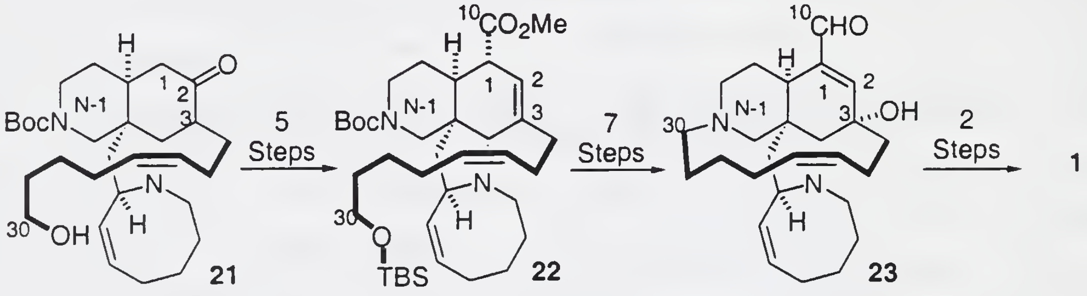

Martin Total Synthesis

Martin's total synthesis[18] of manzamine A **1** relies on a domino Stille/intramolecular Diels-Alder reaction of a pyroglutamate derivative ring C to construct the A and B rings, followed by two subsequent RCM reactions to close the D and E rings using Grubbs' catalyst. The key steps are featured in Scheme 7.

Scheme 7. Intramolecular Diels-Alder / Ring Closing Metathesis.[18]

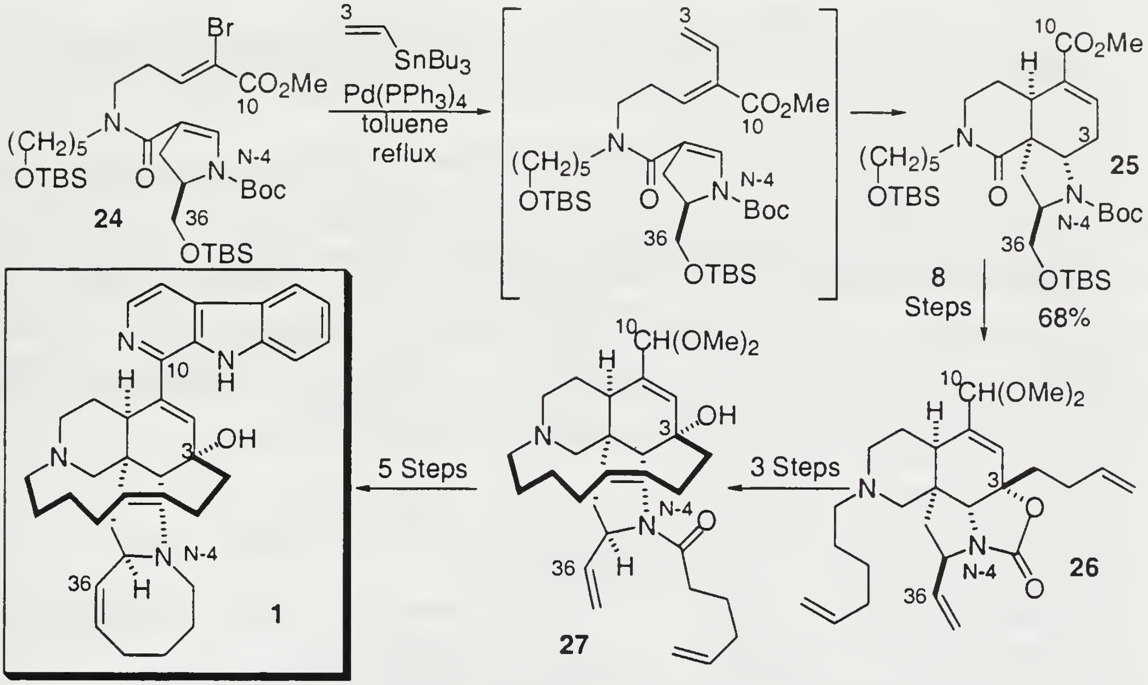

Vinylogous amide **24** was synthesized from methyl pyro-D-glutamate in 14 steps (Scheme 7). Addition of tributylallylstannane to pyroglutamic acid derivative **24** created an in-situ deactivated diene that cyclized spontaneously and stereoselectively to a single isomer Diels-Alder adduct **25** in 68% yield.[18] The lone stereocenter on **23** defined the absolute and relative configurations of the remaining ABC ring core stereocenters. Conversion of **25** to triolefinated product **26** occurred through the following steps: 1) allylic oxidation of the C-3 carbon to the α,β-unsaturated ketone; 2) deprotection of the C-36 alcohol with HCl; 3) oxidation of the alcohol to an aldehyde using Swern oxidation conditions; 4) olefination of the aldehyde using methylene triphenylphosphine; 5) reduction of the C-10 ester to the alcohol with excess DIBALH; 6) oxidation of the alcohol to the aldehyde with Dess-Martin periodinane; 7) conversion of the aldehyde to the protected dimethoxy acetal with trimethyl orthoformate; 8) organometallic addition to the C-3 carbonyl from the top face which forms an oxyanion that undergoes nucleophilic attack of the Boc carbonyl to afford **26**. Ring closing metathesis of **26** to selectively close the E ring, hydrolysis of the carbamate with KOH, and acylation of the pyrrolidine nitrogen N-4 afforded **27**. Finally, **27** was transformed to the natural product **1** through the following steps: 1) ring closing metathesis to form the azocine D-ring followed by acid workup to remove the dimethyl acetal protecting group on the C-10 aldehyde; 2) reduction of the ring D lactam (and C-10 aldehyde) with DIBALH; 3) oxidation of the C-10 primary alcohol back to the aldehyde with Dess-Martin periodinane; 4) installation of the β-carboline moiety by addition of tryptamine to the aldehyde with TFA,[27] 5) oxidation of the Pictet-Spengler product with DDQ[27] to afford manzamine A **1**.[18]

REFERENCES

(1) a) Scheuer, P.J. Ed. Marine Natural Products, Chemical and Biological Perspectives. Academic Press: New York, 1978-1983. Vol. I-V. b) Faulkner, D.J. *Nat. Prod. Rep.* **1984,** 551-598. Uemura, D.; Takahashi, K.; Yamamoto, T.; Katayama, C.; Tanaka, J.; Okumura, Y.; Hirata, Y. *J. Am. Chem. Soc.* **1985,** *107,* 4796.

(2) a) Baker, B.J. β-Carboline and Isoquinoline Alkaloids from Marine Organisms, in Alkaloids and Biological Perspectives. Pelletier, S.W., Ed. Elsevier: Oxford, 1996. Vol. 10 Chap. 4 358-407 and references therein. b) Andersen, R.J.; Van Soest, R.W.M.; Kong, F. 3-Alkylpiperidine Alkaloids Isolated from Marine Sponges in the Order of Haplosclerida, in Alkaloids: Chemical and Biological Perspectives. Pelletier, S.W., Ed. Elsevier: Oxford, 1996. Vol. 10 Chap. 3 302-355.

(3) Sakai, R.; Higa, T.; Jefford, C.W.; Bernardinelli, G. *J. Am. Chem. Soc.* **1986,** *108,* 6404.

(4) For recent reviews, see a) Magnier, E.; Langlois, Y. *Tetrahedron* **1998,** *6201.* b) Matzanke, N.; Gregg, R.J.; Weinreb, S.M. *Org. Prep. Proc. Int.* **1998,** *30,* 1. c) Pandit, U.K.; Overkleeft, H.S.; Borer, B.C.; Bieräugel, H. *Eur. J. Org. Chem.* **1999,** 959.

(5) Hendrickson, J.B. *J. Am. Chem. Soc.* **1967,** *89,* 7047.

(6) Dale, J. *J. Chem. Soc.* **1963,** 93.

(7) de Oliveira Imbroisi, D.; Simpkins, N.S. *Tet. Lett.* **1989,** *30,* 4309.

(8) de Oliveira Imbroisi, D.; Simpkins, N.S. *J. Chem. Soc., Perkin I* **1991,** 1815.

(9) Magnier, E.; Langlois, Y. *Tet. Lett.* **1998,** *39,* 837.

(10) Torisawa, Y.; Hosaka, T.; Tanaba, K.; Suzuki, N.; Motohashi, Y.; Hino, T.; Nakagawa, M. *Tetrahedron.* **1996,** *52,* 10597.

(11) Nakagawa, M.; Lai, Z.; Torisawa, Y.; Hino, T. *Heterocycles.* **1990,** *31,* 999.

(12) Torisawa, Y.; Nakagawa, M.; Takami, H.; Nagata, T.; Ali, M.A.; Hino, T. *Heterocycles.* **1994,** *39,* 277.

(13) Markó, I.E.; Southern, J.M.; Adams, H. *Tet. Lett.* **1992,** *33,* 4657.

(14) Leonard, J.; Fearnley, S.P.; Finaly, M.R.; Knight, J.A.; Wong, G. *J. Chem. Soc. Perkin I* **1994,** 2359.

(15) Leonard, J.; Fearnley, S.P.; Hickey, D.M.B. *SynLett* **1992,** 272.

(16) Pandit, U.K.; Borer, B.C.; Bieräugel, H. *Pure Appl. Chem.* **1996,** *68,* 659.

(17) Brands, K.M.J.; Meekel, A.A.A.; Pandit, U.K. *Tetrahedron* **1991,** *47,* 2005.

(18) Martin, S.F.; Humphrey, J.M.; Ali, A.; Hillier, M.C. *J. Am. Chem. Soc.* **1999,** *121,* 866.

(19) Hart, D.J.; McKinney, J.A. *Tet. Lett.* **1989,** *30,* 2611.

(20) Winkler, J.D.; Axten, J.M. *J. Am. Chem. Soc.* **1998,** *120,* 6425.

(21) Brands, K.M.J.; DiMichele, L.M. *Tet. Lett.* **1998,** *39,* 1677.

(22) Kamenecka, T.M.; Overman, L.E. *Tet. Lett.* **1994,** *35,* 4279.

(23) Clark, J.S.; Hodgson, P.B. *Tet. Lett.* **1995,** *36,* 2519.

(24) Li, S.; Kosemura, S.; Yamamura, S. *Tet. Lett.* **1994,** *35,* 8217.

(25) Campbell, J.A.; Hart, D.J. *Tet. Lett.* **1992,** *33,* 6247.

(26) Winkler, J.D.; Axten, J.; Hammach, A.H.; Kwak, Y.-S.; Lengweiler, U.; Lucero, M.J.; Houk, K.N. *Tetrahedron.* **1998,** *54,* 7045.

(27) Kondo, K.; Shigemori, H.; Kikuchi, Y.; Ishibashi, M.; Sasaki, T.; Kobayashi, J. *J. Org. Chem.* **1992,** *57,* 2480.

(28) Pandit, U.K. *J. Heterocyclic Chem.* **1994,** *31,* 615.

(29) Baldwin, J.E.; Whitehead, R.C. *Tet. Lett.* **1992,** *33,* 2059.

(30) Baldwin, J.E.; Claridge, T.D.W.; Culshaw, A.J.; Heupel, F.A.; Lee, V.; Spring, D.R.; Whitehead, R.C.; Boughtflower, R.J.; Mutton, I.M.; Upton, R.J. *Angew. Chem. Int. Ed. Eng.* **1998,** *37,* 2661.

(31) a) Li, S.; Ohba, S.; Kosemura, S.; Yamamura, S. *Tet. Lett.* **1996,** *37,* 7365. b) Li, S.; Yamamura, S. *Tet. Lett.* **1998,** *39,* 2597. c) Li, S.; Yamamura, S.; Hosomi, H.; Ohba, S. *Tet. Lett.* **1998,** *39,* 2601. d) Li, S.; Kosemura, S.; Yamamura, S. *Tetrahedron.* **1998,** *54,* 6661. e) Li, S.; Yamamura, S. *Tetrahedron.* **1998,** *54,* 8691.

(32) Myers, A.G.; Gleason, J.L.; Yoon, T. *J. Am. Chem. Soc.* **1995,** *117,* 8488.

(33) Winkler, J.D.; Muller, C.L.; Scott, R.D. *J. Am. Chem. Soc.* **1988,** *110,* 4831.

SCOPE AND DEVELOPMENT OF THE KULINKOVICH REACTION

Reported by Michael H. Ober October 30, 2000

INTRODUCTION

In 1989, the combination of ethylmagnesium bromide and titanium tetraisopropoxide was found to react with esters **1** under mild reaction conditions to form 1-substituted cyclopropanols **2** in good yields (Scheme 1).[1] The development of this reaction by Kulinkovich and co-workers is of great interest due to the importance of cyclopropanols in ring opening reactions[2] and as synthetic building blocks in the construction of cyclopropane containing natural products.[3]

Scheme 1

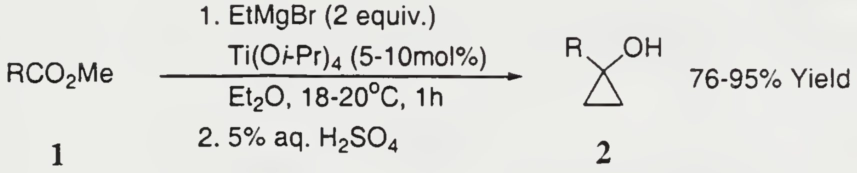

Development of this reaction has broadened its synthetic utility and has provided a better understanding of the reaction mechanism. The reaction has been extended to the synthesis of highly substituted cyclopropanols and aminocyclopropanes. Recent progress has even led to stereoselective methods of producing these functionalized compounds.

MECHANISM OF THE KULINKOVICH REACTION

The proposed catalytic cycle for the Kulinkovich reaction is initiated by the formation of an organotitanium species from the reaction of titanium tetraisopropoxide with two equivalents of a Grignard reagent (Scheme 2). The organotitanium species **3** then forms a titanacyclopropane intermediate **4** upon β-elimination, releasing ethane. This titanocycle **4** then undergoes an insertion reaction with an ester carbonyl, followed by rearrangement to produce a titanium alkoxide **6**. Metal

Copyright © 2000 by Michael H. Ober

exchange with additional Grignard reagent yields the magnesium alkoxide **7** and regenerates the active titanium species **3**.[4]

Scheme 2

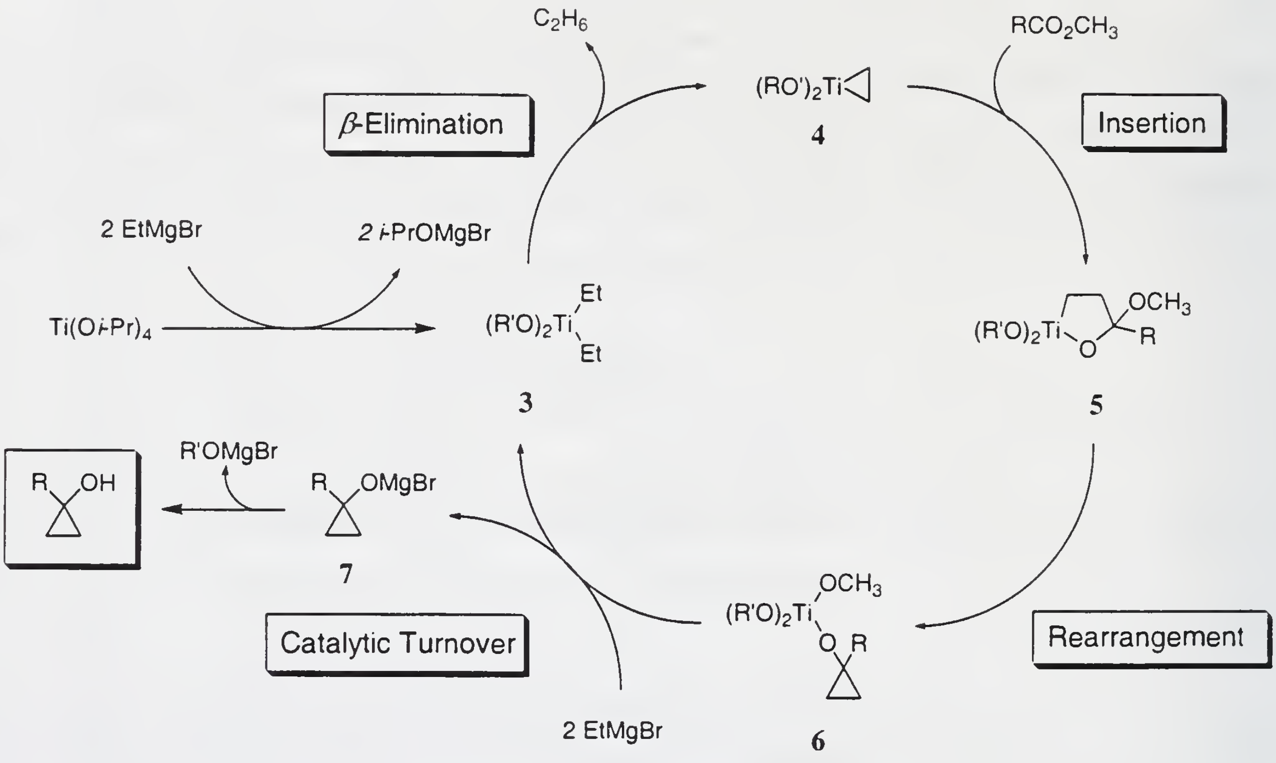

Evidence in support of this catalytic cycle has been obtained from isotopic labeling studies. The isolated cyclopropanol product **9** from the reaction of $Cl(CH_2)CO_2Et$ with $(CD_3)_2CHMgBr$ in the presence of Ti(*i*-PrO)$_4$ was found to have an isotopic substitution pattern which would arise if the reaction proceeded through the proposed β-elimination mechanism (Scheme 3).[5]

Scheme 3

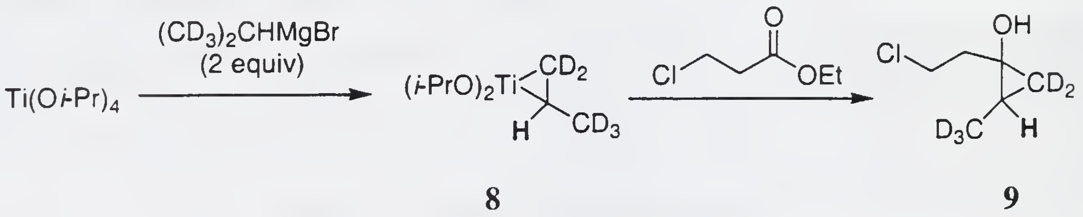

REACTION SCOPE AND LIMITATIONS

The original Kulinkovich procedure was limited to the use of titanium tetraisopropoxide and two equivalents of ethylmagnesium bromide to produce cyclopropanols in good yield. Further studies led to development of *in situ* methods for generating the Grignard reagent, simplifying the overall synthetic procedure. In addition, $ClTi(Oi\text{-}Pr)_3$ was found to be a more sterically tolerant catalyst which allowed for the use of Grignard reagents other than ethylmagnesium bromide. This expands the scope of the reaction to allow for the formation of 1,2-disubstituted cyclopropanols. In all cases formation *cis*-cyclopropane was observed, demonstrating the inherent diastereoselectivity of the reaction.[6]

Studies to better understand the nature of the organotitanium intermediates led to the realization that the initially formed titanacyclopropane intermediate **10** could undergo ligand exchange with other olefins in solution.[7] This ligand exchange mechanism allowed for the development of an intramolecular variant of the reaction where titanacyclopropane **10** is formed with an inexpensive, commercially available Grignard reagent. It can then undergo ligand exchange with a ω-vinyl carboxylic ester **11**. This titanocycle **12** can proceed to the hydroxybicyclo[3.1.0]hexane **13** in good yield (Scheme 4).[8]

Scheme 4

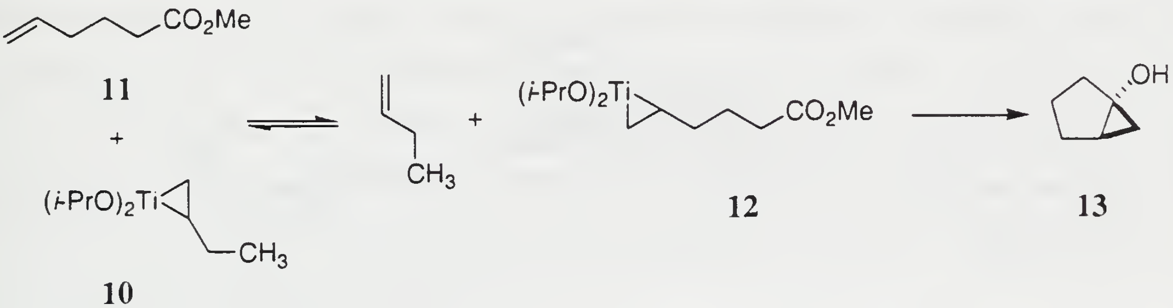

Further development of the intermolecular Kulinkovich reaction by Cha and co-workers avoids the use of an excess of a valuable Grignard reagent by utilizing cyclohexylmagnesium bromide as the initiating species (Scheme 5). In contrast to the original procedure, the equilibrium is shifted in favor of the substrate olefin **15** due to the strain release between the *cis* substituents on the cyclic olefin. The newly formed titanacyclopropane **17** then reacts to yield only the expected cyclopropanol **18**.[9]

Scheme 5

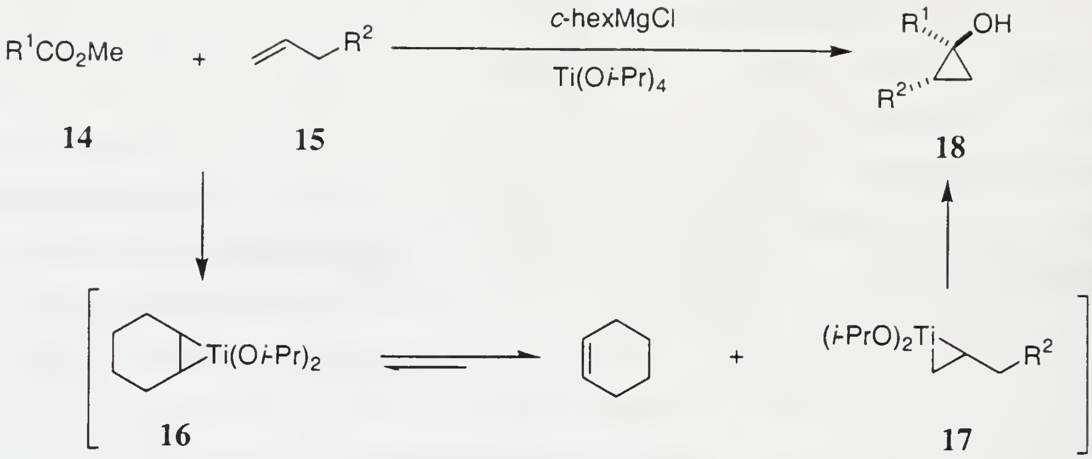

Extension of the Kulinkovich reaction to the synthesis of *trans*-disubstituted cyclopropanols has also been realized based on the ligand exchange method. Reactions involving esters of ω-buten-1-ol **19** were found to give disubstituted cyclopropanols **20** with the opposite sense of diastereoselectivity as seen with the original intermolecular reaction (Scheme 6).[10]

Scheme 6

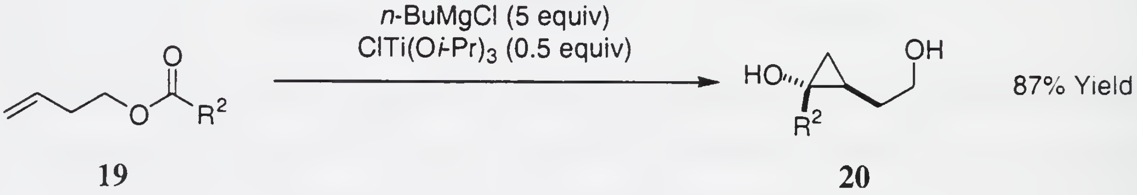

EXTENTION TO AMINOCYCLOPROPANES

The formation of aminocyclopropanes **24** was accomplished by substituting amides **21** for carboxylic esters in the presence of the titanium tetraisopropoxide / Grignard reagent combination **22** (Scheme 7). The reaction is thought to proceed by a different pathway as previously described. Due to the poor leaving group ability of the nitrogen substitutent, alkylation of the amide carbonyl followed by elimination of a titanium oxo-species is thought to occur. The mechanism is supported by the observation that a stoichiometric amount of titanium is necessary for the reaction to occur in good yield.[11] Utilization of the ligand exchange method for both the inter- and intramolecular variations of this reaction has been reported.[12]

Scheme 7

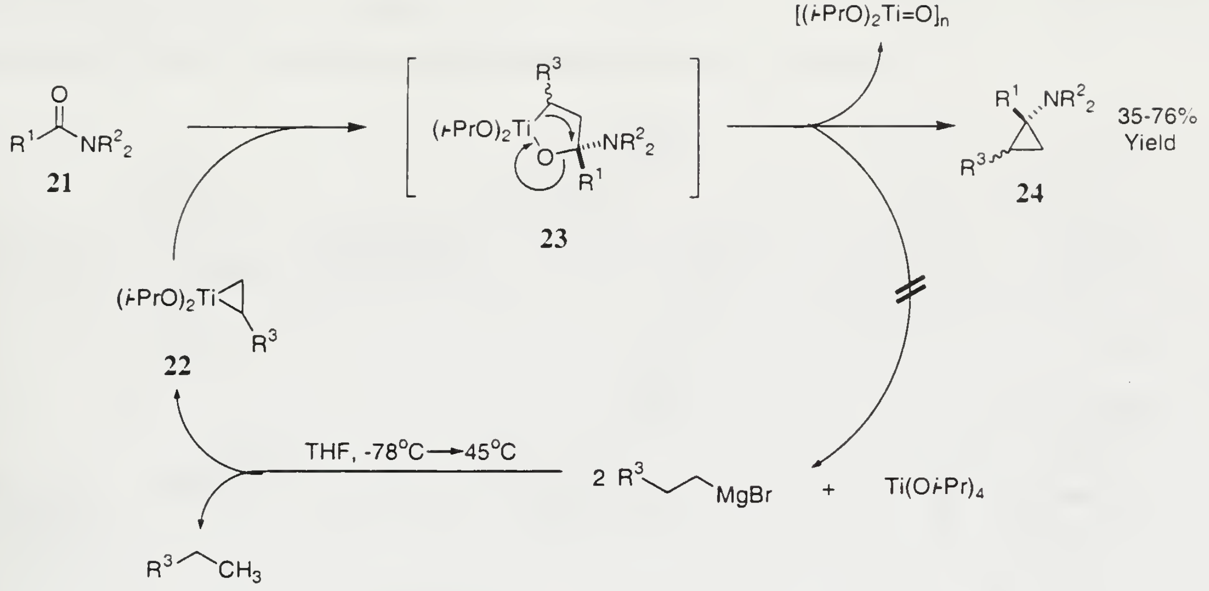

CHEMOSELECTIVITY AND STEREOSELECTIVITY

The chemoselectivity of the Kulinkovich reaction was studied via examination of the relative rates of reaction of several carbonyl species. Competition experiments between different carbonyl groups were performed and the product ratios were viewed as a reflection of their relative reaction rates. It was found that the reactivity was dependent on the steric bulk of the substrate as well as the electronic nature of the carbonyl group. The overall rates were found to be: $k_{ester} = k_{acid\ chloride} = k_{anhydride} > k_{carbonate} = k_{thioester} > k_{formamide} > k_{carboxamide}$. Therefore, intermolecular reactions with compounds such as succinic ester amides **25** resulted in a chemoselective cyclopropanation of the ester carbonyl to form the corresponding cyclopropanol **26** (Scheme 8).[13]

Scheme 8

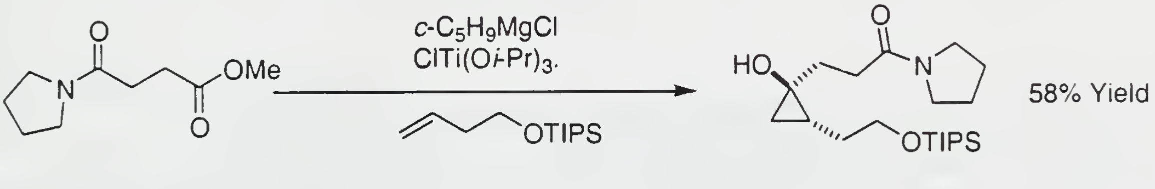

25 **26**

Asymmetric induction in the Kulinkovich reaction has been achieved through the use of chiral auxiliaries and chiral catalysis. Use of Oppolzer's camphorsultam auxiliary (**27** and **29**) was found to provide some control over the facial selectivity of the reaction. When an additional stereocenter was installed at the α-position, higher selectivity was observed, providing both high diastero- and enantioselectivity (Scheme 9).[14]

Scheme 9

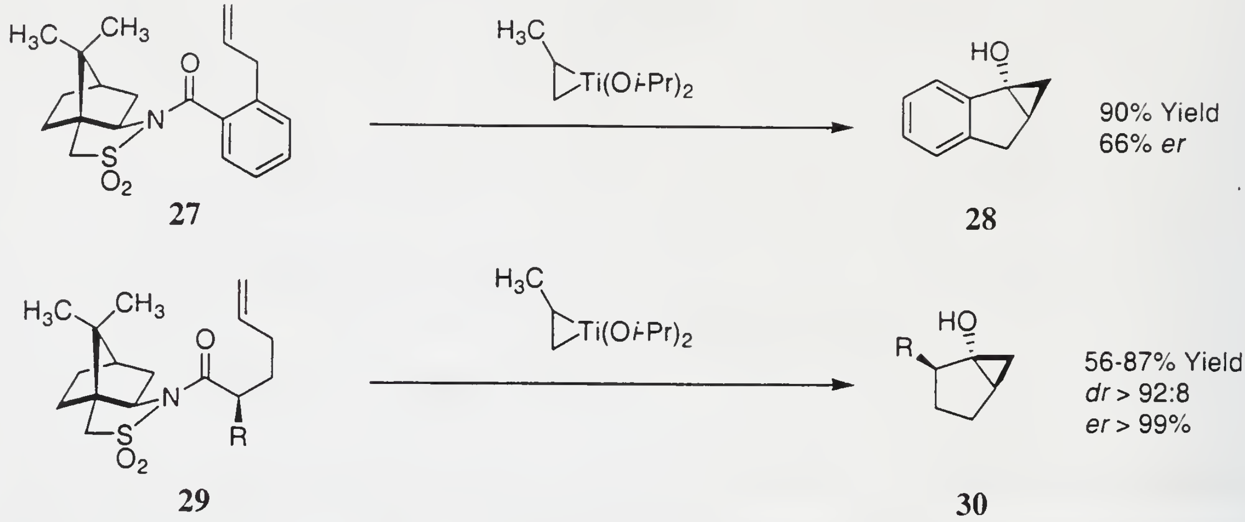

Control of enantioselectivity was also achieved by use of a TADDOL based titanium catalyst. Corey *et al* have used this catalyst to provide the corresponding cyclopropanols 32 with reasonable stereoselectivity (Scheme 10).[6]

Scheme 10

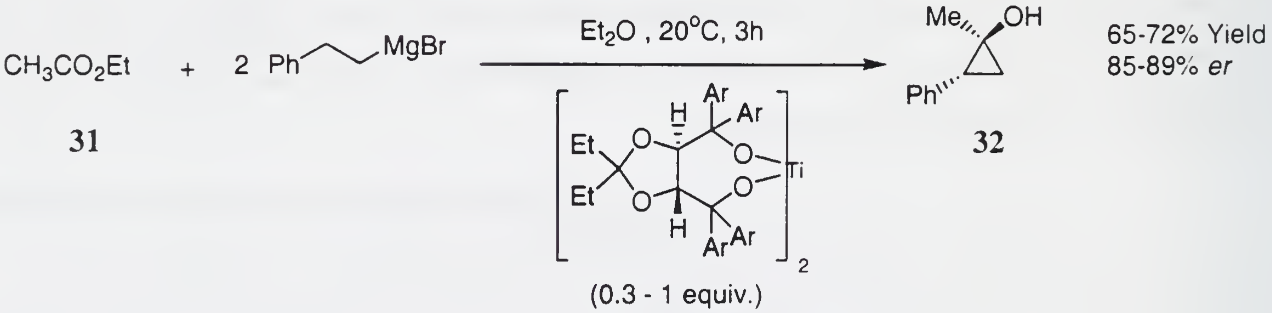

APPLICATION OF THE KULINKOVICH REACTION TO SYNTHESIS

Since the appearance of the Kulinkovich reaction, its use as an efficient method for producing cyclopropanols has been utilized in several natural product syntheses including select pheromones of the *Ips* Bark Beetles and the German Cockroach.[15] More interestingly, the cyclopropanol products formed by the Kulinkovich reaction are precursors for other useful synthetic transformations. Ring expansion reactions, such as the oxidative cleavage of a bicyclic cyclopropanol **34** with ferric chloride and sodium acetate has been found to give seven and eight membered cycloalkenones **35** in good yields (Scheme 12).[16] Similarly, α-hydroxycyclopropylcarbinols **37** have been found to yield 2-substituted cyclobutanones **38** after undergoing a pinacol-type rearrangement (Scheme 13).[17]

Scheme 12

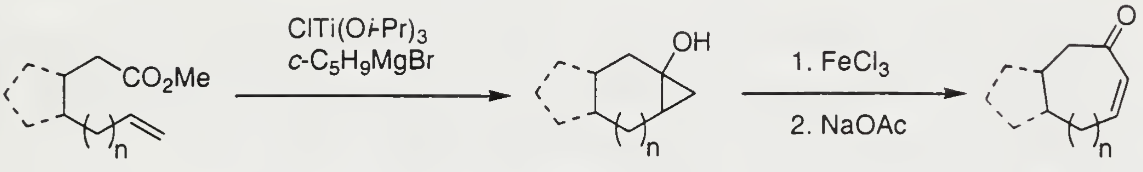

33 **34** **35**

Scheme 13

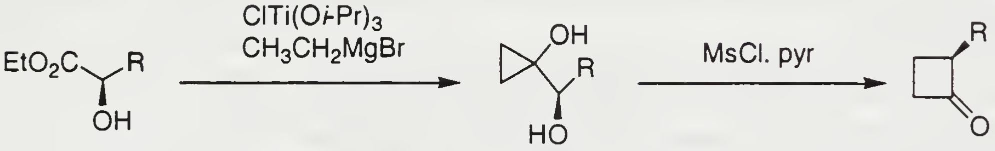

36 **37** **38**

Ring opening reactions involving cyclopropanols and cyclopropylamines have also been studied. In one example, the use of $Pd(OAc)_2$ was found to mediate ring opening with high regioselectivity (Scheme 14).[18] Other examples including radical ring openings[19] and thermal rearrangments[20] have also been explored.

Scheme 14

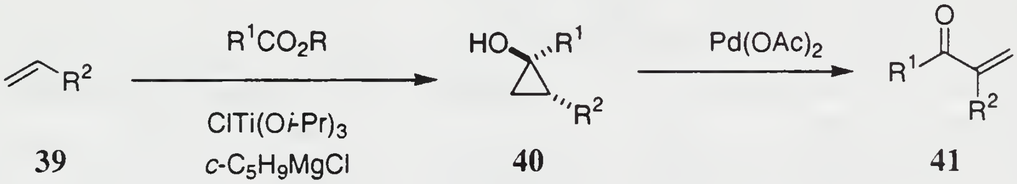

39 **40** **41**

CONCLUSIONS AND OUTLOOK

Since the first report of the Kulinkovich reaction, it has attracted a great deal of interest due to the ability to access highly substituted cyclopropanols and aminocyclopropanes. Although consider progress has been made to this methodology, there are still avenues to further improvement and novel applications. Higher selectivities in the catalytic, asymmetric process may be obtained with alternate ligands. Titanium-BINOL and titanium-sulfonamide systems have been successful in providing high enantioselectivity in catalytic carbonyl additons .[21,22] Ligand design would be aided by unambiguous identification of the rate and selectivity determining steps. Recent development of ring expansion reactions involving cyclopropanols also opens new synthetic pathways to a variety of cyclic ketone containing natural products.

REFERENCES

(1) (a) Kulinkovich, O. G.; Sviridov, S. V.; Vasilevsky, D. A.; Prityckaja, T. S. *Zh. Org. Khim.* **1989**, *25*, 2245. (b) Kulinkovich, O. G.; Sviridov, S. V.; Vasilevskii, D. A.; Savchenko, A. I.; Pritytskaya, T. S. *Zh. Org. Khim.* **1991**, *27*, 294. (c) Kulinkovich, O. G.; Vasilevskii, D. A.; Savchenko, A. I.; Sviridov, S. V. *Zh. Org. Khim.* **1991**, *27*, 1428.

(2) Depuy, C. H.; Gibson, D. H. *Chem. Rev.* **1974**, *74*, 605.

(3) Gerwick, W. H. *Chem. Rev.* **1993**, *93*, 1807.

(4) Kulinkovich, O. G.; Sviridov, S. V.; Vasilevski, D. A. *Synthesis* **1991**, 234.

(5) Kulinkovich, O. G.; Savchenko, A. I.; Epstein, O. L. *Russ. Chem. Bull.* **2000**, *49*, 378.

(6) Corey, E. J.; Rao, S. A.; Noe, M. C. *J. Am. Chem. Soc.* **1994**, *116*, 9345.

(7) (a) Kulinkovich, O. G.; Savchenko, A. I.; Sviridov, S. V.; Vasilevski, D. A. *Mendeleev. Commun.* **1993**, 230. (b) Kulinkovich, O. G.; Epstein, O. L.; Savchenko, A. I. *Tetrahedron Lett.* **1999**, *40*, 5935.

(8) Cha, J. K.; Lee, J.; Kang, C. H.; Kim, H. *J. Am. Chem. Soc.* **1996**, *118*, 291.

(9) Cha, J. K.; Lee, J.; Kim, H. K. *J. Am. Chem. Soc.* **1996**, *118*, 4198.

(10) Sato, F.; Kasatkin, A. *Tetrahedron Lett.* **1995**, *36*, 6079.

(11) (a) de Meijere, A.; Chaplinski, V. *Angew. Chem., Int. Ed. Engl.* **1996**, *35*, 413. (b) Cha, J. K.; Lee, J. *J. Org. Chem.* **1997**, *62*, 1584.

(12) (a) de Meijere, A.; Chaplinski, V.; Winsel, H.; Kordes, M. *Synlett*, **1997**, 111. (b) de Meijere, A.; Williams, C. M.; Vladimir, C.; Schreiner, P. R. *Tetrahedron Lett.* **1998**, *39*, 7695.

(13) Cha, J. K.; Cho, S. Y.; Lammi, R. K. *J. Org. Chem.* **1997**, *62*, 8235.

(14) Sato, F.; Mizojiri, R.; Urabe, H. *Angew. Chem. Int. Ed.* **1998**, *37*, 2666.

(15) (a) Kulinkovich, O. G.; Chevtchouk, T. A.; Isakov, V. E. *Tetrahedron* **1999**, *55*, 13205. (b) Kulinkovich, O. G.; Epstein, O. L. *Tetrahedron Lett.* **1998**, *39*, 1823.

(16) Cha, J. K.; Sun, J.; Lee, J. *Tetrahedron Lett.* **1997**, *38*, 5233.

(17) Cha, J. K.; Park, S.-B. *Org. Lett.* **2000**, *2*, 147.

(18) Cha, J. K.; Cho, S. Y. *Org. Lett.* **2000**, *2*, 1337.

(19) Cha, J. K.; Lee, J.; Sun, J.; Blackstock, S. C. *J. Am. Chem. Soc.* **1997**, *119*, 10241.

(20) de Meijere, A.; Williams, C. M. *J. Chem Soc., Perkin Trans. 1* **1998**, 3699.

(21) (a) Mikami, K.; Terada, M.; Nakai, T. *J. Am. Chem. Soc.* **1990**, *112*, 3949. (b) Mikami, K.; Yajima, T.; Terada, M.; Uchimaru, T. *Tetrahedron Lett.* **1993**, *34*, 7591.

(22) Yoshioka, M.; Kawakita, T.; Ohno, M. *Tetrahedron Lett.* **1989**, *30*, 1657.

CHIRAL POISONING AND CHIRAL DRUGGING

Reported by Matthew E.L. Christy November 6, 2000

INTRODUCTION

Since the initial report of an enantioselective process catalyzed by a sub-stoichiometric amount of a chiral modifying agent, there have been numerous advances in the field of catalytic, enantioselective reactions. Many catalysts have been developed to produce excellent enantioselectivities and high chemical yields. A necessity of nearly all the asymmetric methods developed to date is the need for enantiomerically pure, or at least enriched, catalysts. While an enantiopure catalyst affords the highest level of asymmetric induction, it is not necessarily mandated that the levels of induction should be linearly proportional to the enantiopurity of the catalyst. In fact remarkable deviations from linear induction have been observed under a variety of conditions. This phenomenon in asymmetric induction is known as a non-linear affect (NLE).[1]

Non-linear effects have been most notably studied by Kagan. For linear induction, the observed enantioselectivities of the products would be linearly proportional to the enantiopurity of the catalyst. Deviations from linearity are known as nonlinear affects. Situations where nonlinear induction is greater than the hypothetical linear mode are deemed positive NLE's ((+)-NLE). Conversely, decreased inductions from the linear mode are deemed negative NLE's ((-)-NLE). Three models have been proposed for the observation of NLE's, ligand effect, reservoir effect, and product inhibition. The ligand effect model assumes that multiple catalysts are present in the stereochemistry determining event as well as the rate of the single catalyst process is slower than the multiple catalyst process. NLE's are observed when there is a difference in the relative rates between the homo- and hetero-complexes. For the reservoir effect, the resting state of the catalyst is an inactive dimeric complex. In this mode, NLE's are observed when there is a difference between the rates of dissociation of the hetero- and homo-dimers to afford the catalytically active monomeric species. Product inhibition is observed when the product can bind catalyst. NLE's can be observed when the product preferentially binds one chiral antipode of the catalyst from which it was formed. A distinguishing feature of product inhibition is that stereoselectivity changes with respect to conversion.

Even in catalytic systems where (+)-NLE's permit non-enantiopure catalyst to afford high enantioselectivity, there is still an need for a partial resolution of the catalyst if it is not derived from a chiral pool. These resolutions can be costly and/or time consuming, thus giving reason to find methods that allow for the use of racemic catalysts that still result in asymmetric catalysis.

One concept that has been formulated is the use of racemic catalysts in conjuction with chiral additives to afford enantiomerically enriched products. This idea can be put forth in two different manners. In one, the chiral additive can function to bind preferentially to one enantiomer of the racemic catalyst and deactivate it (Scheme 1). The term given for this approach by Faller is "chiral poisoning."[2] For this situation the highest selectivity to be expected is that of the enantiopure catalyst.

Copyright © 2000 by Matthew E.L. Christy

Scheme 1

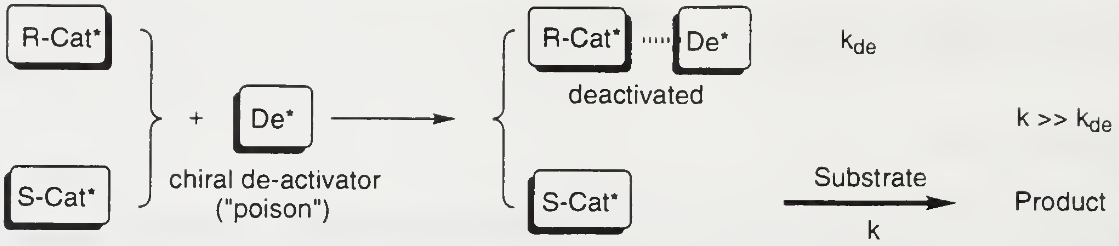

The alternative approach is to add a chiral activator. The chiral additive activates one enantiomer of the catalyst, increasing its catalytic activity ($k_{act} >> k$), enantioselectivity ($ee_{act} >> ee$), or both (Scheme 2). In this approach, termed "chiral drugging" by Mikami,[3] it is conceptually possible to achieve enantioselectivities even higher than those of the enantiopure catalyst.

Scheme 2

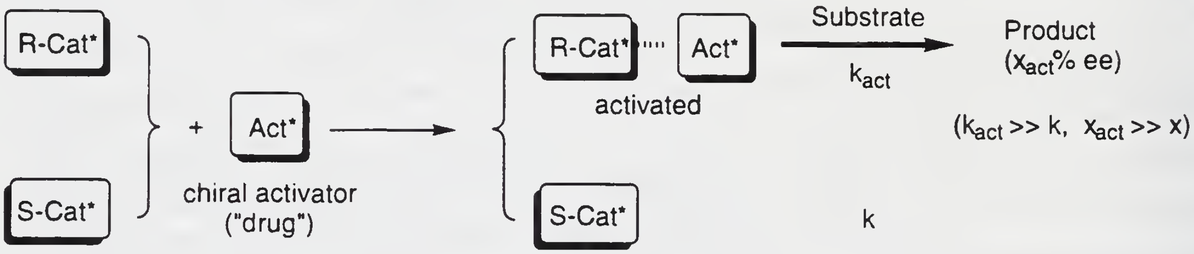

CHIRAL POISONING

Use of the concept of chiral poisoning was first reported by Brown in 1986.[4] Brown showed that one enatiomer of racemic chiraphos, (±)-**1**, could be selectively sequestered by the addition of (+)-bis(menthyl-(Z)-α-benzamidocinnamate) iridium tetrafluoroborate, (±)-**2** (Scheme 3). The selective formation of the iridium complex, **3**, with (*S,S*)-**1** leaves the remaining enantiomer, (*R,R*)-**1**, free. Upon addition of bisbicyclo[2.2.1]heptadienerhodium tetrafluoroborate $(NBD)_2RhBF_4$, **4**, and (*Z*)-α-acetamidocinnamate, **6**, under an H_2 atmosphere, the (*S*)-hydrogenation product, **7**, was obtained in 87% ee. Conversly, using (-)-**2** in a similar manner showed that (*R*)-**7** could also be obtained in a 90% ee. These results are nearly identical to the level of asymmetric induction obtained using enatiopure (*S,S*)-chiraphos, indicating nearly complete poisoning of the undesired ligand. The authors were also able to demonstrate that under similar conditions the use of (±)-*trans*-1,2-bis(diphenylphosphino)cyclohexane instead of (±)-**1** (previously not resolved) could afford (*S*)-**7** and (*R*)-**7** in 81% ee and 79% ee, respectively.

Scheme 3

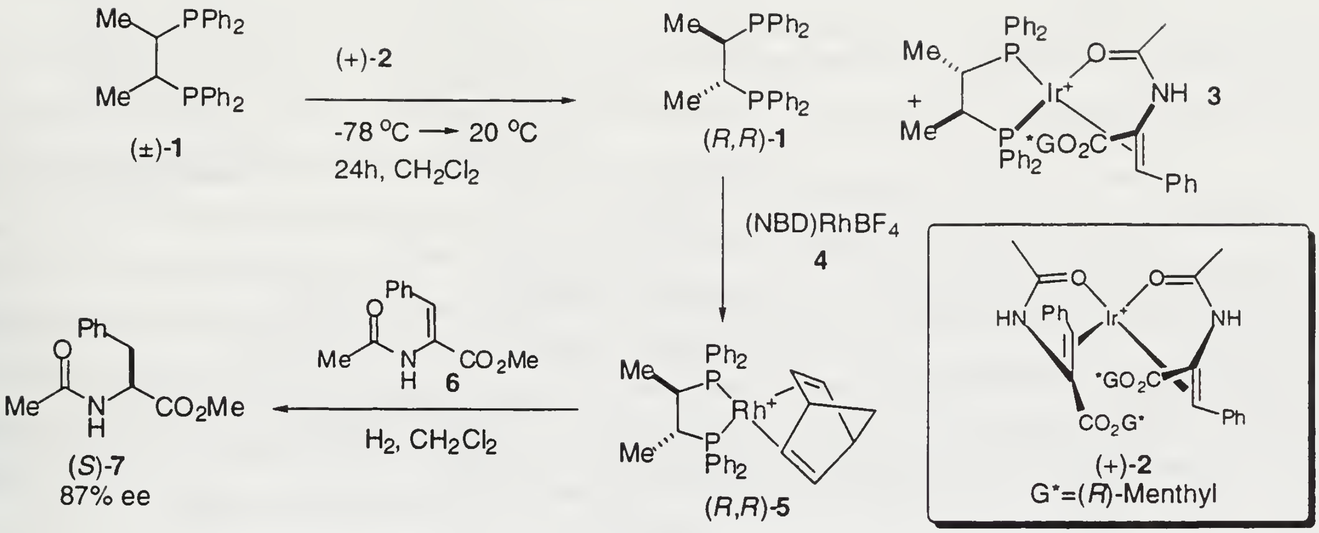

Shortly there after, Yamamoto reported that addition of an enantiopure chiral ketone, (+)-bromocamphor, **8**, to a racemic mixture of an organoaluminum reagent, (±)-**9**, formed only one of the two possible diastereomeric complexes (Scheme 4).[5] This left one enantiomer of **9** free to catalyze the hetero Diels-Alder reaction of diene **10** with benzaldehyde to yield the (*cis*)-adduct, **11**, in 82% ee and 78% yield (enantiopure (*S*)-**9** affored **11** in 95% ee).[6]

Scheme 4

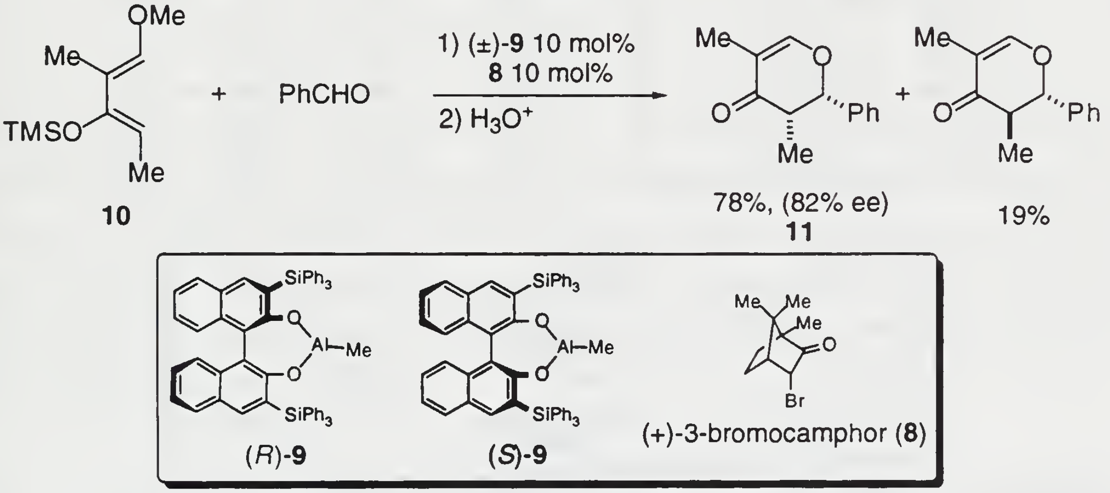

Faller was next to examine this concept and coined the term "chiral poisoning."[2] Faller demonstrated that one enantiomer of (chiraphos)Rh_2(NBD)BF_4, (±)-**5** could be poisoned with (*S*)-methophos, **12**, allowing the remaining enantiomer to catalyze the asymmetric hydrogenation of dimethylitaconate, **13,** to obtain **14** in 49% ee (Scheme 5).

To ensure that this was in fact a chiral poisoning the [(*S*)-methophos)Rh]$^+$ complex was prepared and was shown to produce **14** in less than 2% ee. Thus it can be concluded that (*S*)-methophos functions by selectively coordinating to [(*S,S*)-chiraphosRh]$^+$ and preventing its use as a hydrogenation catalyst. While this example again showed the utility of chiral poisoning, the overall results are rather disappointing considering that greater than 98% ee can be achieved when using enantiomerically pure catalyst.

Scheme 5

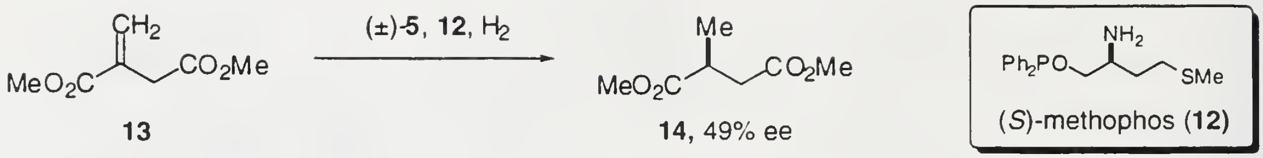

Hoping to better demonstrate the utility of chiral poisoning, Faller showed that racemic Ru(BINAP), **15**, could be selectively poisoned to effectively perform a kinetic resolution of allylic secondary alcohols.[7] Using either (+) or (-)-ephedrine, **16**, Faller could selectively poison one enantiomer of [(±)-BINAP]$RuCl_2$ and obtain 2-cyclohexenol in >95% ee. In order to maximal enantioselectivity, the poisoned reaction required a higher level of conversion, resulting in a lower recovery of the desired allylic alcohol (21% (±)-**15**/**16** verses 40% (*R*)-**15**). Thus, in this case the desire to achieve higher stereoselectivities results in a significant reduction in the yield of the desired allylic alcohol.

Scheme 6

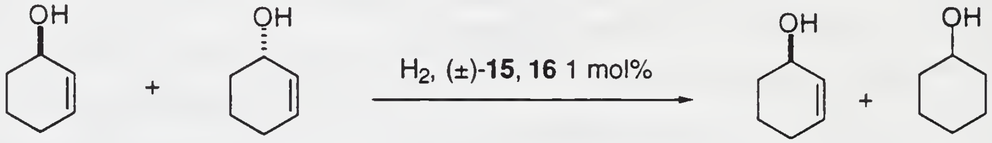

poison	catalyst (mol%)	H_2 (atm)	rxn time (min)	recovery (%)	ee %	config
none	(*R*)-**15**, 0.3	11	15	40	>95	(*S*)
none	(±)-**15**, 0.3	10	3	40	0	--
(-)-**16**	(±)-**15**, 0.3	2	720	33	53	(*R*)
(-)-**16**	(±)-**15**, 0.3	10	60	23	>95	(*R*)
(+)-**16**	(±)-**15**, 0.3	10	60	21	>95	(*S*)
(-)-**16**	(±)-**15**, 0.1	10	120	60	28	(*R*)
(-)-**16**	(±)-**15**, 0.3	100	7	43	44	(*R*)

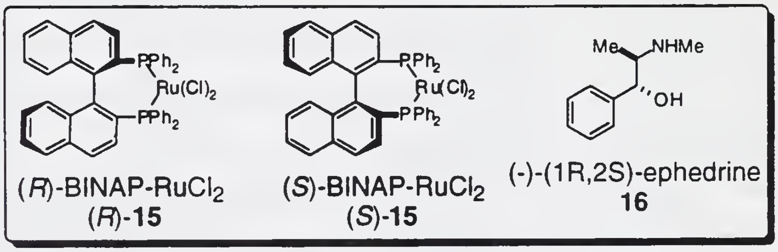

While previous examples have shown deactivation of one enantiomer of a chiral catalyst with a chiral ligand, it is also possible for a chiral organometallic complex to form inactive dimers. The organometallic complex [(+)-DIPT]$Ti(O^{i}Pr)_2$, **17**, was shown to be an effective poison of one enantiomer of [(±)-BINOL]$Ti(O^{i}Pr)_2$, **18**, allowing the remaining enantiomer to effectively catalyze an allylation reaction (Scheme 7).[8] Keck had shown that [(*R*)-BINOL]$Ti(O^{i}Pr)_2$ could promote the allylation of benzaldehyde with tributylallystanane.[9] Upon further study by Faller, it was shown that there was a (+)-NLE suggesting that the heterodimer $Ti_2(O^{i}Pr)_4$[(*S*)-BINOL][(*R*)-BINOL] is less competent than the homodimers or the monomers. One way to interpret the (+)-NLE can is that [(*R*)-BINOL]$Ti(O^{i}Pr)_2$ deactivates [(*S*)-BINOL]$Ti(O^{i}Pr)_2$ and *vice versa*. Hoping to develop an even less active dimer, Faller replaced (*S*)-**18** with (+)-**17**, and showed that the allylation product, **19,** could be obtained in 91% ee. It was also shown that (+)-**17** had no catalytic activity on its own. In addition it was shown that (*S*)-**18** could be completely inactivated by (+)-**17**, while the [(*R*)-BINOL]Ti(O^iPr)$_2$/[(+)-DIPT]Ti(O^iPr)$_2$ mixture could catalyze the reaction to afford products in >95% ee, though at a reduced yield. This demonstrated that an organometallic species could itself be an effective chiral poison.

Scheme 7

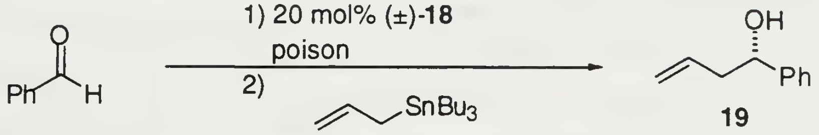

19

entry	poison (mol%) (+)-DIPT	Ti(O^iPr)$_4$	yield, %	ee, %	confuguration
1	0	0	65	0	--
2	12	10	44	19	(S)
3	15	10	40	39	(S)
4	20	10	47	81	(S)
5	30	10	63	91	(S)

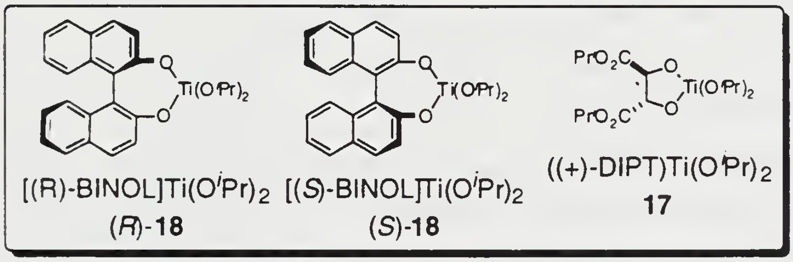

[(R)-BINOL]Ti(O^iPr)$_2$ (*R*)-**18**

[(*S*)-BINOL]Ti(O^iPr)$_2$ (*S*)-**18**

((+)-DIPT)Ti(O^iPr)$_2$ **17**

This same catalyst/poison system also was shown to be effective in the chloral-ene reaction.[10] For this reaction Faller showed that both the enantioselectivity, as well as, the regioselectivity, could be affected by the addition of a chiral deactivator. As seen in Scheme 8, entry 1, (*S*)-BINOL is both moderately regioselective for **21** and affords moderate enantioselectivity. Addition of (+)-DIPT can greatly increase the selectivity for **21**, but unfortunately cannot increase the enantioselectivity past a marginal level of 48% ee, though with a drastic reduction in yield.

Scheme 8

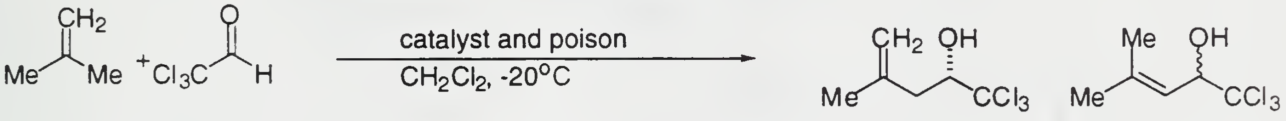

20 **21** **22**

entry	catalyst (mmol) Ti(O^iPr)$_2$Cl$_2$	BINOL	poison (mmol) Ti(O^iPr)$_2$Cl$_2$	(+)-DIPT	time	% yield	ratio (21:22)	ee (%) 21	22	config.
1	0.10	0.1(*S*)	0.00	0.00	16 h	87	67:33	24	66	*S*
2	0.20	0.2(±)	0.10	0.10	16 h	66	83:17	14	14	*S*
3	0.20	0.2(±)	0.10	0.20	16 h	53	88:12	30	20	*S*
4	0.20	0.2(±)	0.10	0.30	16 h	43	87:13	48	35	*S*
5	0.0	0.0	0.10	0.30	72 h	0				

Thus, several attempts at chiral poisoning have certainly demonstrated its utility. There have been several other attempts[11] that have demonstrated the concept but provided no advantage over the enantiopure catalyst. While use of chiral poisoning can yield enantioselectivities that are quite enhanced, the upper limit in this case would only be the enantioselective produced by the enantiopure catalyst.

CHIRAL DRUGGING

Many cases have been documented where achiral additives can activate a chiral catalyst to improve rates, yields, or enantioselectivites.[12] Not long after the development of chiral poisoning, it was conceived that by adding a chiral activator it may be possible to differentiate enantiomers in a racemic catalyst (as in chiral poisoning) at the same time the catalytic activity or enantioselectivity is enhanced. Thus the concept of chiral drugging was developed. The possible benefit of this methodology would be that the enatioselectivies of the product could be enhanced over that of the reaction catalyzed by unactivated enantiomerically pure catalyst.

The first to investigate this contrasting approach was Mikami. While the chiral poisoning of (±)-**18** with tartrate in an ene reaction met with limited sucess, Mikami found that the addition of chiral biaryl ligands could activate one enantiomer of the catalyst selectively (Scheme 9).[3,13] In this system the catalyst is ill-effective in the absence of an activator. The addition of achiral biphenol does slightly activate the catalyst but has no effect on the enantioselectivity. However the addition of (*R*)-BINOL dramatically increases the yield and enantioselectivity (52%, 90% ee). Thus the enantioselectivities achieved through chiral drugging are similar to the levels of asymmetric induction obtained using enantiopure catalyst, and demonstrates the potential utility of this process. While in this case the enantiopure chiral additive is still the same chiral ligand used in the active catalyst, the total amount of resolved BINOL required can be greatly decreased with only a minor decrease in the enantioselectivity.

Scheme 9

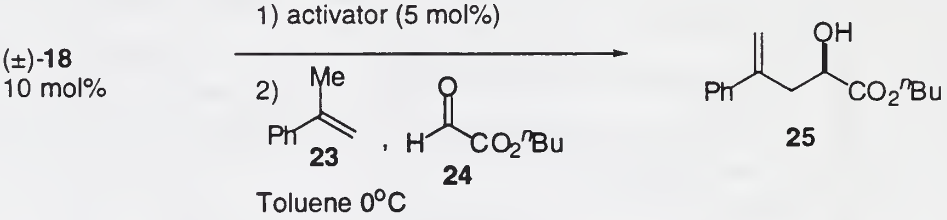

Run	Activator	Yield (%)	ee(%)
1	none	5.9	0
2	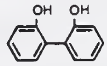	20	0
3	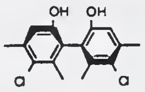	38	80.8
4	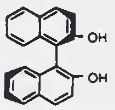	52	89.8

While in the ene reaction the chiral activator could produce enatioselectivities close to that of the enantiopure catalyst, the same Ti(BINOL)/chiral activator system can dramatically increase the enatioselectivity in the product of the Diels-Alder reaction of Danishefsky's diene, **26**, and glyoxylate, **24**.[3,13,14,15] Catalysis using enantiopure (*R*)-**18** in 10 mol % affords products in only 5% ee, where as the addition of (*R*)-BINOL in 5 mol % to (±)-**18** under the same conditions increases the level of enantioselectivity to 50% ee. While this may still not be synthetically useful it does demonstrate the ability of chiral activators to enhance the enantioselectivity of racemic catalyst past that of their enantiopure counterparts.

Scheme 10

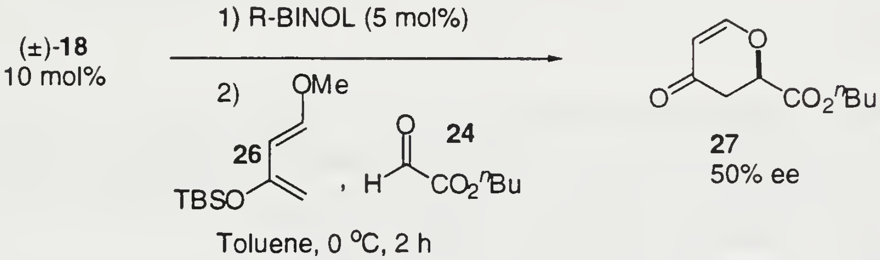

The chiral drugging strategy has also been employed in the asymmetric hydrogenation of ketones.[13,16] While $RuCl_2$(tolbinap), **28**, either racemically or in its enantiopure form, is a poor catalyst for the hydrogenation of ketones, addition of diamines has been shown to effectively activate $RuCl_2$(tolbinap).[17] When (*S,S*)-1,2-diphenylethylenediamine, (*S,S*)-DPEN, **29**, is added to (±)-**28**, (*R*)-**28** is activated and the subsequent hydrogenation of 2,4,4-trimethyl-2-cyclohexeneone, **30**, is performed, the allylic alcohol, **31**, is obtained in quantitative yield and 95% ee (Scheme 11). This is nearly identical to the enantioselectivity (96% ee) obtained using the independently prepared (*R*)-$RuCl_2$(tolbinap)/(*S,S*)-DPEN catalyst system. Thus use of enantiopure $RuCl_2$(tolbinap) is not needed to obtain very good enantioselectivity.

Scheme 11

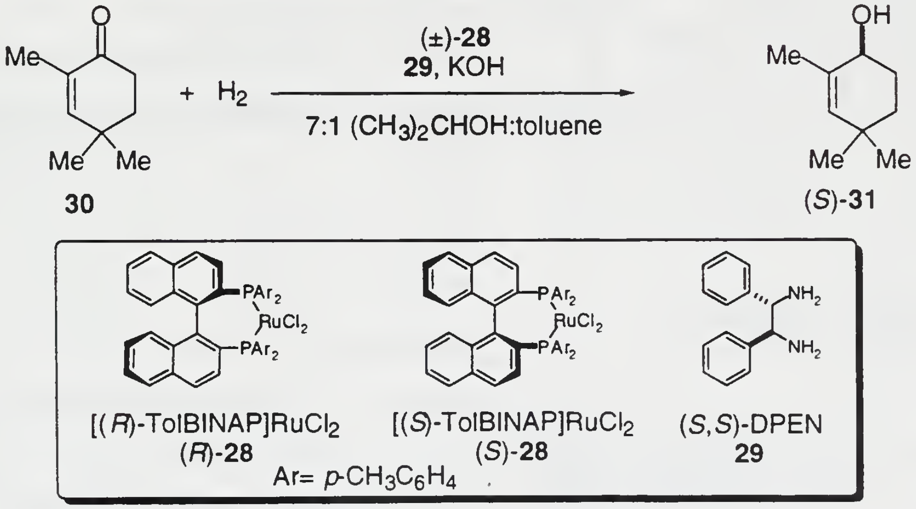

CONCLUSION

Chiral poisoning and chiral drugging have been shown to be effective methods to allow the use of racemic catalyst and still obtain enantioselectivity in the product. Examples have shown that additives such as chiral ligands and chiral organometallic complexes can be added to either a racemic ligand prior to active catalyst formation or to the active catalyst itself. These chiral additives function to selectively activate or deactivate the racemic catalyst, affording enantioselectivity in hydrogenation reactions, ene reactions, Diels-Alder reactions and allylations. In order for chiral drugging and chiral poisoning to become common place in organic chemistry, further exploration in this field needs to demonstrate that high enantioselectivities can be achieved in a wider range of reactions. Ideally the chiral additives used would be derived from chiral pool reagents, thus reducing the need for resolution of synthesized chiral ligands.

REFERENCES

(1) (a) Grirard, C.; Kagan, H.B. *Angew. Chem. Int. Ed.* **1998**. *38* 2922. (b) Guillaneux, D. Zhao, S.; Samuel, O.; Kagan, H.B. *J. Am. Chem. Soc.* **1994**, *116*, 9430. (c)Avalos, M.; Babiano, R.; Cintas, P.; Jiménez, J.L.; Palacios, J.C. *Tetrahedron: Asymetry* **1997**, *8*, 2997.
(2) Faller, J.W.; Parr, J. *J. Am. Chem. Soc.* **1993**, *115*, 804.
(3) Matsukawa, S.; Mikami, K. *Enantiomer* **1996**, *1*, 69.
(4) Alcock, N.W.; Brown, J. M.; Maddox, P.J. *J. Chem. Soc. Chem. Commun.* **1986**, 1532.
(5) Maruoka, K.; Yamamoto, H. *J. Am. Chem. Soc.* **1989**, *111*, 789.
(6) Maruoka, K.; Itoh, T.; Shirasaka, T.; Yamamoto, H. *J. Am. Chem. Soc.* **1988**, *110*, 310.
(7) (a) Faller, J.W.; Tokunaga, M. *Tetrahedron Lett.* **1993**, *34*, 7359. (b) Faller, J.W.; Mazzieri, M.R.; Nguyen, J.T. et al *Pure Appl. Chem.* **1994**, *66*, 1463.
(8) Faller, J.W.; Sams, D.W.I.; Liu, X. *J. Am. Chem. Soc.* **1996**, *118*, 1217.
(9) Keck, G.E.; Tarbet, K.H.; Geraci, C.S. *J. Am. Chem. Soc.* **1993**, *115*, 8467.
(10) Faller, J.W.; Liu, X. *Tetrahedron Lett.* **1996**, *37*, 3449.
(11) (a) de Vries, A.H.M.; Jasen, J.F.G.A.; Feringa, B.L. *Tetrahedron* **1994**, *50*, 4479. (b) Sablong, R.; Osborn, J.A.; Faller, J.W. *J. Organometallic Chem.* **1997**, *527*, 65.
(12) Vogl, E.M.; Gröger, H.; Shibasaki, M. *Angew. Chem. Int. Ed.* **1998**. *38*. 1571.
(13) (a) Mikami, K.; Korenga, T.; Matsukawa, S.; Matsumoto, Y.; Ding, K.; Isjil, A.; Volk, T; Terada. M. *J. Syn. Org. Chem Jpn.* **1998**, *56*, 975. (b)Mikami, K.; Terada, M.; Korenga, T.; Matsumoto, Y.; Matsukawa, S. *Acc. Chem. Res.* **2000**, *33*, 391.
(14) Matsukawa, S.; Mikami, K. *Nature* **1997**, *385*, 613.
(15) Matsukawa, S.; Mikami, K. *Tetrahedron: Asymetry* **1997**, *8*, 815.
(16) Ohkuma, T.; Doucet, H.; Pham, T.; Mikami, K.; Korenga, T.; Terada, M. *J. Am. Chem. Soc.* **1998**, *120*, 1086.
(17) (a) Maneney, P.; Tejero, T.; Alexakis, A.; Grosjean, F.; Normant, J.; *Synthesis*. **1988**, 255. (b) Pikul, S.; Corey, E.J.; *Org. Synth.* **1993**, *71*, 22.

RECENT DEVELOPMENTS TOWARD SYNTHETIC MUSCLES BASED ON ORGANIC MOLECULES AND POLYMERIC MATERIALS

Reported by Dahui Zhao November 9, 2000

INTRODUCTION

One of the most striking characteristics of biological entities is their capability of coordinated motion. Humans have long been trying to mimic these movements of biosystems using synthetic materials. The contraction and stretching functions of skeletal muscles, due to their ubiquitous nature and importance, have always attracted the most interest. In the past few years, significant progress has been made in reproducing the motility of muscle both at the molecular level and in the bulk properties of materials. The most recent developments in this area will be addressed herein.

MOLECULAR MUSCLES

Myosin-Actin Complex — A Linear Molecular Motor

In order to understand how the artificial systems that have been developed mimic a biosystem, a thorough understanding of the chemical structure and mechanism of the biosystem is needed. Skeletal muscle, one of the best-studied biological systems, consists of long parallel bundles of muscle fibers which may span the entire length of the muscle. Each muscle fiber is, in turn, composed of parallel bundles of even thinner fibers, termed myofibrils. These myofibrils are composed of alternating sets of thick and thin filaments whose major molecular components are myosin and actin, respectively. Each repeating unit of myofibril, called a sarcomere, contains one set of myosin filaments interdigitating with a set of actin filaments at either end. The length of the sarcomere decreases to about two thirds of its fully extended length when muscle contracts, while the lengths of thick and thin filaments remain constant. Muscle contraction occurs when the interpenetrating thick and thin filaments slide past each other, progressively shortening the length of the

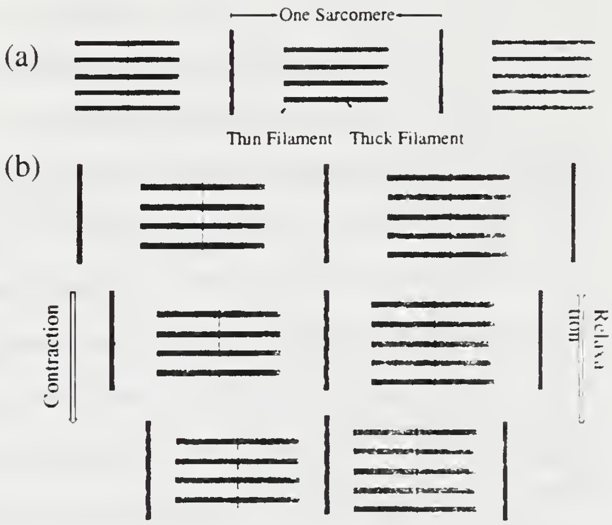

Figure 1. Schematic myofibril structure (a) and its progressively contracted states (b).

Copyright © 2000 by Dahui Zhao

sarcomeres (Figure 1).[1] This sliding process is accompanied by hydrolysis of ATP into ADP and P_i.[2] Myosin-actin complex acts as a biological "motor" by transforming the chemical energy released from ATP hydrolysis into mechanical energy.

A variety of molecular motors are commonly present in biological systems. They are classified as either linear[2, 3] or rotary motors,[4] depending on the motions they activate. The myosin-actin complex represents a typical example of a linear motor.

Synthetic Molecular Motors

The term "molecular motor" usually applies to a molecular assembly where large amplitude movement can be induced by an external stimulus,[5] while "molecular muscle" specifically refers to motors with the capacity to reproduce certain properties of natural muscles. To mimic the controllable motion of biological motors, a variety of strategies have been adopted to induce relatively large magnitudes of movement in organic or inorganic molecules.[6, 7]

One of the most elegant and promising strategies applied in constructing molecular motors involves utilizing the unique topography of catenanes and rotaxanes. Catenanes consist of two interlocked cyclic components. Rotaxanes are molecules consisting of a ring structure threaded by a linear molecule having bulky groups (stoppers) on both ends preventing dethreading. Each component of these molecules undergoes relatively independent translational and/or rotational movement without dissociating from the other component. This appealing characteristic of catenanes and rotaxanes makes them ideal candidates for constructing molecular motors. Synthesis of such threading or inter-locked molecules, once a significant synthetic challenge, has been elegantly performed by several groups using efficient templating effects such as metal-ligand coordination, π-electron donor/acceptor interactions and hydrogen-bonding.[8]

Various types of motion have been achieved based on rotaxane and catenane topography. A few examples are shown in Figure 2. One specific type of rotaxane bearing particular importance in achieving muscle-type motility is the "shuttle" (Figure 2b). The architecture of the shuttle consists of a rod fragment containing two distinct recognition sites, and a cyclic moiety with structure complementary to both recognition sites. The cyclic fragment can be translocated from one site to the other through an external stimulus. The recognition process is made

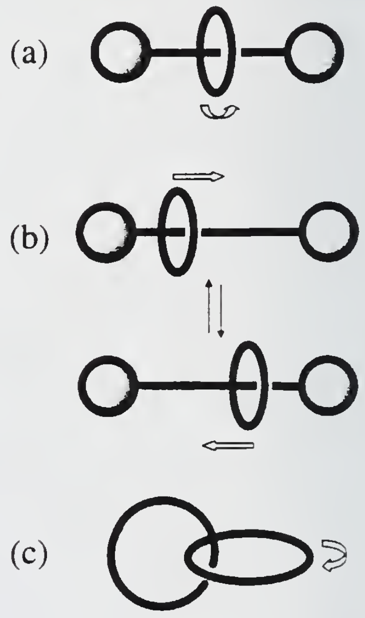

Figure 2. Schematic representations of molecular motors: (a) wheel and axle in motion; (b) shuttle; (c) rolling catenane.

possible by π-electron donor/acceptor interaction,[9] transition metal coordination,[10] or H-bonding.[11] The position of the cyclic fragment may be switched back and forth through chemical or electrochemical reaction.

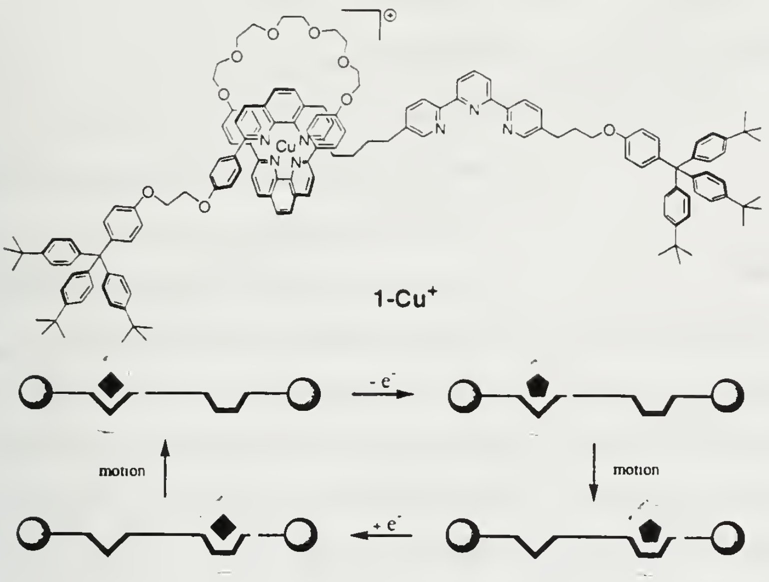

Figure 3. Copper(I)-complexed rotaxane **1** and the schematic mechanism of its motility (◆ = Cu^{I}, ⬟ = Cu^{II}).

A representative "shuttle" molecule **1**, was synthesized by Sauvage and co-workers using a coordination templating strategy.[10] The rotaxane molecule developed in this group was composed of a linear unit (string) containing both a bidentate ligand and a terdentate coordinating unit, and a ring fragment carrying another bidentate ligand. The sliding motility of this molecule relied on the different coordination numbers and geometries of Cu(I) and Cu(II). In presence of Cu(I), the bidentate ligand of the ring and the bidentate ligand of the rod coordinated to the metal ion in a tetrahedral configuration. When Cu(I) was oxidized into Cu(II), the ring moved down the chain and coordinated the metal ion with the terdentate ligand in a pentacoordinate geometry. Therefore, by electrochemically switching the oxidation state of the copper, movement of the ring and relative control of the ring position was accomplished (Figure 3).

Approaching Synthetic Muscle from the Molecular Level

As translational motion had been achieved in multicomponent rotaxane-type molecules, further efforts were made to design and synthesize molecules with motions reminiscent of biological muscle function. The strategy of dimerizing self-complementary monomers into double threading pseudorotaxanes was adopted to mimic the architectural structure of the myosin-actin complex. A doubly threaded motif was first achieved by Stoddart and coworkers in the solid state.[12] More recently, a molecule with a rotaxane topography that could undergo reversible contractile movement induced by a chemical signal was synthesized by Sauvage and coworkers.[13] This doubly threaded psuedorotaxane **2** consists of two identical monomers, each containing a linear fragment and a cyclic fragment covalently bonded to each other. The chain fragment of one molecule was threaded through the ring of its counterpart, which in turn threaded its chain through the ring of the first monomer. A bulky stopper was

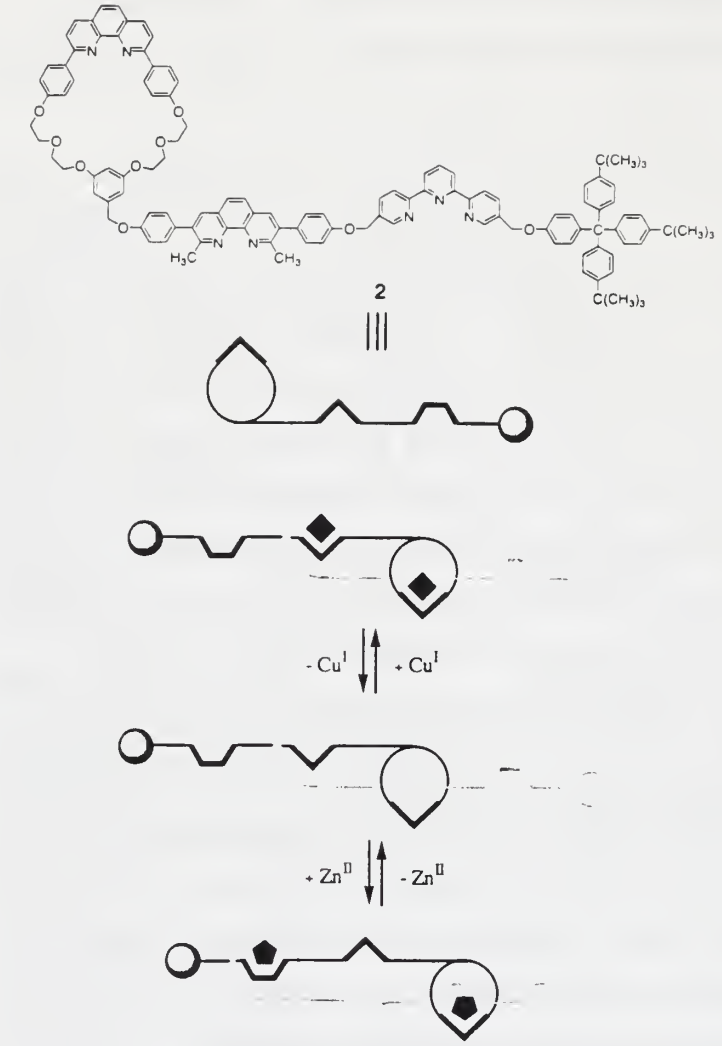

Figure 4. Schematic representation of the principle of the "molecular muscle" motion (◆ = Cu^{I}, ⬟ = Zn^{II}).

added to the end of the chain to prevent dethreading. The two components in such a molecular assembly could slide along each other, back and forth, leading to "contraction" and "relaxation", analogous to the reversible sliding motility of thick and thin filaments in biological muscles. The ring fragment had a bidentate ligand, whereas the chain portion contained two distinct coordinating sites, one bidentate, and one terdentate. The motion of the molecule is derived from the different coordination number and geometrical arrangement of ligands for different metal atoms. In the presence of a tetracoordinated metal ion, Cu(I), the molecule adopted an extended conformation with the two bidentate ligands coordinating to the copper. When the copper(I) was replaced by the pentacoordinated Zinc(II) ion, the molecule responded by sliding the two components along each other and the ion coordinated to the terdentate ligand of the chain; in other words, the molecule "contracted" (Figure 4). In this way, a molecular translation was induced by a chemical reaction in a similar fashion to the sliding of the muscle filaments. During the contraction process, according to the molecular modeling, the length of the compound changed from 83 Å to 65 Å, roughly the same relative amount as observed in natural muscles.

Polymeric Approach toward Large Amplitude Molecular Motion

For molecules with a self-complementary "ring-and-string" structure, polymeric or oligomeric complexes can be formed through a "head-to-tail" single-threading process (Figure 5).[14] If each repeating unit of the polymeric complex were to undergo "contraction" and "relaxation", a large magnitude of motion would be expected. In fact, this is how biological muscles achieve movement at a macroscopic level. Numerous contractible sarcomeres are linked up to form myofibrils which exhibit macroscopic contraction. However, for the contractible molecules developed by the Sauvage group, doubly threaded dimers proved to be the thermodynamically stable and therefore the predominant product.

Although attempts have been made,[15] coupling the movement of individual unit through polymerization to achieve a large magnitude of motion and mimic the contraction behavior of myofibrils still remains an unsolved problem.

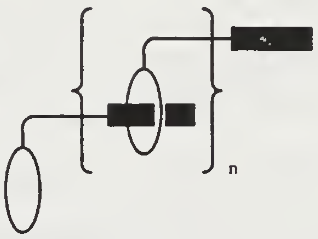

Figure 5. **Schematic representation of polymeric pseudorotaxane.**

ARTIFICIAL MUSCLES

While studies into mimicking the contracting properties of muscles have been carried out at the unimolecular level, research into the development of synthetic muscles has also been directed by addressing the bulk properties of materials. The first generation of "artificial muscles" was developed by Katchalsky and co-workers in the 1950s.[16] Significant developments have been made since then on various systems that undergo a shape change and produce a contractile force in response to environmental stimuli. Among the diversified stimuli that have been successfully applied, electrical induction is the most desirable for practical application, especially when compared to the change of pH, temperature, solution ionic strength, or solvent composition. In terms of materials, polymeric gels[17] and conducting polymers[18] have been most widely investigated for use as artificial muscles, although other materials, such as nanotube sheets, have also been attempted.[19]

A Conducting Polymer-Based Muscle-Like Device

A chemomechanical device is a system capable of transforming chemical energy into mechanical work. When a transformation is driven by an electric pulse, an electrochemomechanical device is developed. Natural muscle is an electrochemomechanical system that transforms the chemical energy liberated by ATP hydrolysis, which is triggered by a nervous (electrical) pulse, into the conformational changes of proteins (myosin and actin) resulting in muscle contractions (mechanical work).

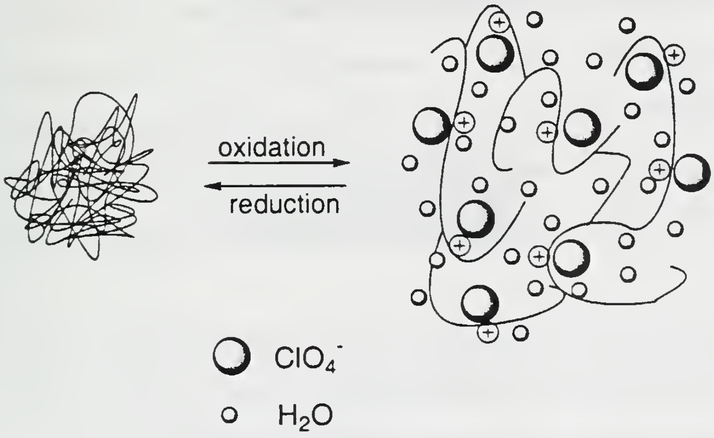

Figure 6. Conformational and volumetric changes of conducting polymer during redox process.

Recently, an electrically-driven chemomechanical device based on a conducting polymer was reported by Otero and workers.[20] Their design relied on the conformational change of the conducting polymer (polypyrrole or polythiophene) chains in response to oxidation and reduction. When a polypyrrole was oxidized, positive charges accumulated along the polymer chains. Due to electrostatic repulsion and osmotic pressure, the chains extended generating free volume. Counterions and water molecules then penetrated into the polymer from the environmental solution, balancing the charge neutrality and swelling the film. Upon reduction, electrons were injected back into the polymer establishing charge neutrality. The counterions and water molecules were then expelled back into the solution and the polymer shrank (Figure 6).

This molecular conformational change was amplified into macroscopic movement in a bilayer device. A flexible polypyrrole film, ranging in thickness from 4 to 12 μm, was attached to a flexible and non-conducting polymeric tape. The bilayer film was connected to an electrode at one end and immersed in an aqueous solution of $LiClO_4$. When the polypyrrole was oxidized, swelling of the conducting polymer film ensued, and the bilayer bent in one direction. When the current was reversed, the polypyrrole was reduced and the conducting film shrank, bending the bilayer in the other direction (Figure 7).

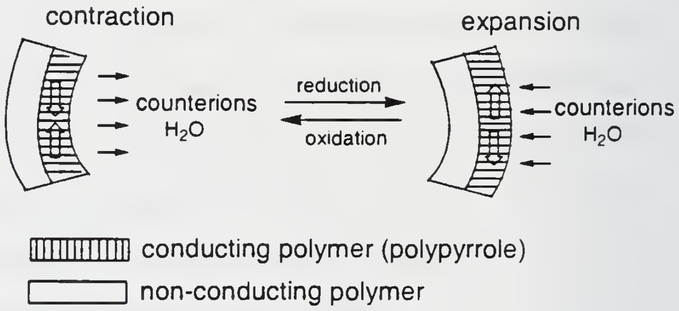

Figure 7. Movement of conducting/nonconducting polymer bilayers.

Multilayer Hydrogel Actuator with Linear Motion

There are two major problems with previously developed artificial muscles based on bulk materials. First, bending rather than contraction was achieved. Second, the actuators usually achieved a change in volume by absorbing or extruding some fluid such as an aqueous solution. The associated fluid reservoir greatly limited the practical application of these materials. A multilayer hydrogel-based actuator recently developed by Calvert and his coworker resolved these issues by generating linear motion, rather than bending, while retaining the water within the actuator during contraction and expansion.[21]

It is well known that polyacrylic acid (PAA) gel swells significantly when moved from acid to base, while polyacrylamide (AAM) gel does not. So, when the stacked layers of PAA and PAAM gels were exposed to basic solution, a strong bending motion was expected. However, the stacks responded to a change from acid to base by swelling with little bending. It was suggested that a weaker PAAM-water interaction allowed this gel to absorb an excess of water and swell with minimal energetic expense when it experiences biaxial tension as the attached PAA swells strongly. This system can be thought of as a bilayer of a stiff material (PAA gel) attached to soft and elastic material (PAAM gel). When the stiff material undergoes a strong expansion or contraction, the soft material is simply deformed without being able to bend the stiff part.

An extension of these results involved an electrically-driven muscle-like actuator constructed from stacked layers of cross-linked polyacrylamide gel over layers of cross-linked polyacrylic acid gel. It was proposed that this system would respond to an external electrical field with an internal water transfer and a contraction or expansion instead of bending. Partially-swollen gel-stacks were placed between two electrodes. When a potential was applied with the PAA side positive, the gels contracted laterally with increased thickness (Figure 8, a to d). When the current was reversed, the gels expanded and thickness decreased. Then the sample was subjected to alternatively positive and negative currents for 10 cycles. The contracting and expanding process was reproducible, except in the first few cycles where ion redistribution occurred in the gels.

The action of this device stemmed from coupling polyacrylic acid gel with polyacrylamide. The ionized PAA has a high affinity for water, while PAAM has a much lower water affinity and its contraction/expansion behavior is relatively insensitive to pH. When a potential was applied with the PAA side positive, a pH gradient arising from electrolysis of water was established within the gel stack with PAA side more acidic. PAA layers subsequently shrank, causing PAAM to shrink laterally. Meanwhile, water was extruded from PAA layers into PAAM layers causing PAAM to expand in thickness (Figure 8).

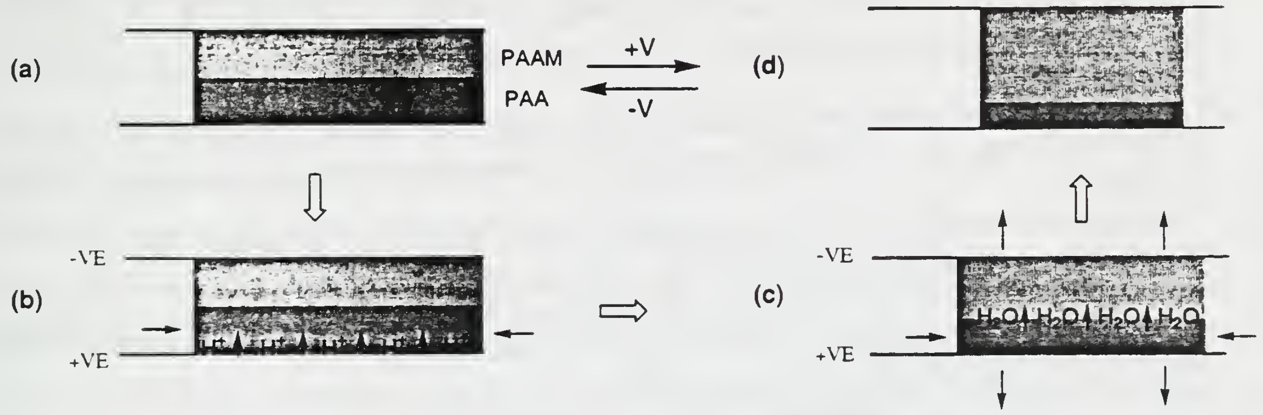

Figure 8. Schematic illustration of contractive behavior of PAA/PAAM gels.

One additional prerequisite for this system was that the PAAM must have a lower elastic modulus than that of the PAA, so that the PAAM deforms with the PAA as the PAA expands or contracts. This allows for expansion and contraction without bending.

CONCLUSION

Scientific research aimed at reproducing or mimicking the essential properties and functions of natural muscles with synthetic materials has been conducted with both molecular devices and bulk materials. At the molecular level, a multi-component molecular assembly was developed, which could undergo a contraction motion reminiscent of the behavior of the myosin-actin complex in muscles. On the other hand, diversified systems with macroscopic muscle-like properties have been developed using polymeric as well as other types of materials. The applications of these artificial muscles are promising in such areas as microelectronics, intelligent, and biomedical materials.

REFERENCES

(1) Voet, D.; Voet, J. *Biochemitry, 2nd Ed.*, John Wiley & Sons Inc., **1995**.

(2) Rayment, I.; Holden, H. M.; Whittaker, M.; Yohn, C. B.; Lorenz, M.; Holmes, K. C.; Milligan, R. A. *Science* **1993**, *261*, 58.

(3) Dibbie, I.; Linari, M.; Piazzesi, G.; Reconditi, M.; Koubassova, N.; Ferenczi, M. A.; Lombardi, V.; Irving, M. *Nature* **1998**, *396*, 383.

(4) (a) Boyer, P. D. *Angew. Chem. Int. Ed.* **1998**, *37*, 2296. (b) Walker, J. E. *Angew. Chem. Int. Ed.* **1998**, *37*, 2308. (c) Allison, W. S. *Acc. Chem. Res.*, **1998**, *31*, 819.

(5) Balzani, V.; Credi, A.; Raymo, F. M.; Stoddart, J. F. *Angew. Chem. Int. Ed.* **2000**, *39*, 3349.

(6) Shinkai, S.; Ishihara, M.; Ueda, K.; Manabe, O. *J. Chem. Soc., Chem. Commun.* **1984**, 727.

(7) Zelikovich, L.; Libman, J.; Shanzer, A. *Nature* **1995**, *374*, 790.

(8) (a) Balzani, V.; Gómez-López, M.; Stoddart, J. F. *Acc. Chem. Res.* **1998**, *31*, 405. (b) Sauvage, J.-P. *Acc. Chem. Res.* **1998**, *31*, 611, and references therein.

(9) Bissel, R. A.; Córdova, E.; Kaifer, A. E.; Stoddart, J. F. *Nature* **1994**, *369*, 133.

(10) Collin, J.-P.; Gaviña, P.; Sauvage, J.-P. *New J. Chem.* **1997**, *21*, 525.

(11) Lane, A. S.; Leigh, D. A.; Murphy, A. *J. Am. Chem. Soc.* **1997**, *119*, 11092.

(12) (a) Ashton, P. R.; Baxter, I.; Cantrill, S. J.; Fyfe, M. C. T.; Glink, P. T.; Stoddart, J. F.; White, A. J. P.; Williams, D. J. *Angew. Chem. Int. Ed.* **1998**, *37,* 1294. (b) Ashton, P. R.; Parsons, I. W.; Raymo, F. M.; Stoddart, J. F.; White, A. J. P.; Williams, D. J.; Wolf, R. *Angew. Chem. Int. Ed.* **1998**, *37,* 1913.

(13) (a) Jiménez, M. C.; Dietrich-Buchecker, C.; Sauvage, J.-P. *Angew. Chem. Int. Ed.* **2000,** *39*, 1295. (b) Jiménez, M. C.; Dietrich-Buchecker, C.; Sauvage, J.-P. *Angew. Chem. Int. Ed.* **2000,** *39*, 3284.

(14) Yamaguchi, N.; Nagvekar, D. S.; Gibson, H. W. *Angew. Chem. Int. Ed.* **1998**, *37*, 2361.

(15) Marsella, M. J.; Reid, R. J. *Macromolecules* **1999,** *32*, 5982.

(16) (a) Kuhn, W.; Hargitay, B.; Katchalsky, A.; Eisengerg, H. *Nature* **1950**, *165*, 514. (b) Steingerb, I. Z.; Oplatka, A.; Katchalsky, A. *Nature (London)* **1966**, *210*, 568.

(17) Osada, Y.; Okuzaki, H.; Hori, H. *Nature*, **1992**, *355*, 242.

(18) Smela, E.; Inganas, O.; Lundstrom, I. *Science* **1995**, *268*, 1375.

(19) Baughman, R. H. et al. *Science* **1999**, *284*, 1340.

(20) (a) Otero, T. F.; Grande, H.; Rodríguez, J. *J. Phys. Org. Chem.* **1996**, *9*, 381. (b) Otero, T. F.; Sansiñena, J. M. *Adv. Mater.* **1998**, *10*, 491.

(21) Liu, Z.; Calvert, P. *Adv. Mater.* **2000,** *12*, 288.

NICKEL-CATALYZED SEQUENTIAL CARBON-CARBON BOND FORMATIONS

Reported by Shinji Fujimori November 13, 2000

INTRODUCTION

A one-pot process which sequentially creates multiple carbon-carbon bonds is an important topic in modern synthesis. This type of transformation is often called a tandem, cascade or domino reaction.[1] In this type of reaction, multiple bond-forming (or breaking) events take place without isolation of intermediates, addition of reagents or changes in conditions during the course of reaction.[1a] Thus, a high degree of molecular complexity can be achieved from simple starting materials in a single procedural operation. With the assistance of transition metal catalysts, this type of multiple bond forming reactions can be very powerful and general transformations in organic synthesis (Scheme 1). During the past decade, transition metal-catalyzed multiple bond forming reactions have been extensively studied using various transition metals, however it was not until recently when nickel catalysts were used in this type of reaction.[2]

SCHEME 1

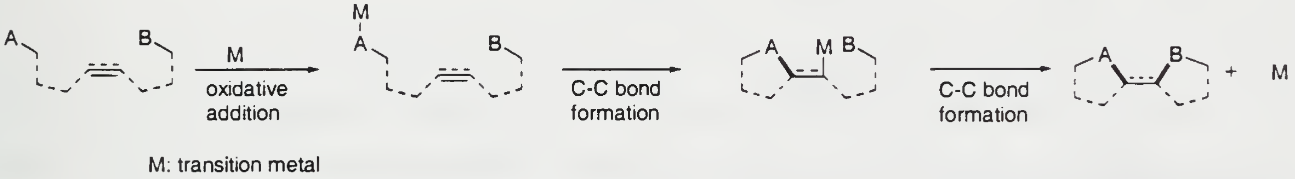

NICKEL-CATALYZED MULTIPLE C-C BOND FORMATIONS

Nickel catalysts are widely used in many important industrial processes.[3] However, nickel-catalyzed reactions have not gained much attention from synthetic chemists despite the fact that numerous nickel-catalyzed carbon-carbon bond forming reactions exist. In the sane group 10 metals, palladium has been far more extensively used in organic synthesis. Recently, more organic chemists have turned their focus on nickel-catalyzed reactions as an alternative to palladium-catalyzed reactions. Nickel catalysts are inexpensive, air stable in the Ni(II) or Ni(0) oxidation states salts and compatible with hard nucleophiles; therefore, nickel-catalyzed processes may possibly complement or substitute the existing palladium-catalyzed reactions.[2] Recent studies on Ni-catalyzed reactions lead to discovery of various multiple carbon-carbon bond forming reactions.

Copyright © 2000 by Shinji Fujimori

Carbonylation Approach

One of the early synthetically useful nickel-catalyzed multiple component coupling reactions was developed by Chiusoli (Scheme 4).[4] In the presence of the Ni(0) catalyst, allylchloride (**1**), carbon monoxide and acetylene undergoes a carbonylative allylation of the alkyne to yield the $\alpha,\beta,\delta,\varepsilon$-unsaturated ester **7** as the sole product. The proposed mechanism for the reaction was as follows.[4,5] The coordination of **1** to Ni(0) yields a π-allylnickel species **2**. Acetylene coordinates to **2** followed by the insertion of acetylene yielding an alkenyl nickel intermediate **4**. Carbonylation of **4** affords the acylnickel intermediate **5**, and reductive elimination of **5** gives the 2,5-hexadienyl chloride **6**. The acyl chloride **6** is esterified by methanol to give the observed unsaturated ester **7**. It was remarkable that the reaction yielded a sole product in the presence of multiple insertable reagents.

SCHEME 2

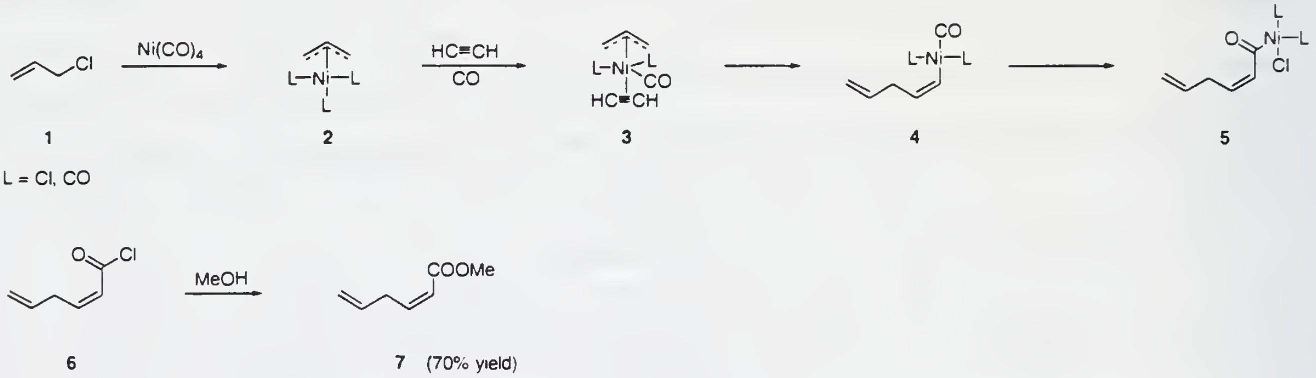

Transmetallation Approach – Intermolecular Three Component Coupling

More recently, Sato and coworkers were able to design a stereoselective nickel-catalyzed three component coupling reaction.[6] The reaction employs methyl vinyl ketone (**8**), various terminal alkynes **9** and alkynylstannanes **12** in the presence of Ni(0) catalyst generated *in situ*. The stereodefined enynes **11** were obtained with low to modest yield but with excellent isomeric purity (Scheme 3).

SCHEME 3

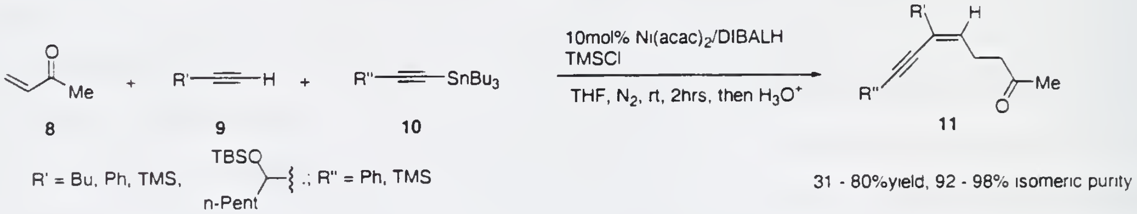

It was initially proposed that the π-allylnickel species **12** is involved in the reaction mechanism (Scheme 4).[6] The active Ni(0) catalytic species first coordinates to enone **8**. This initially formed Ni-enone complex and chlorotrimethylsilane (TMSCl) affords the π-allylnickel intermediate **12**. The coordiantion of alkyne to **12** is followed by alkyne insertion to yield the alkenylnickel **14**. Transmetallation of **14** with alkynylstannane affords the alkenylalkynylnickel **15**, and subsequent reductive elimination gives the observed product **11**.

SCHEME 4

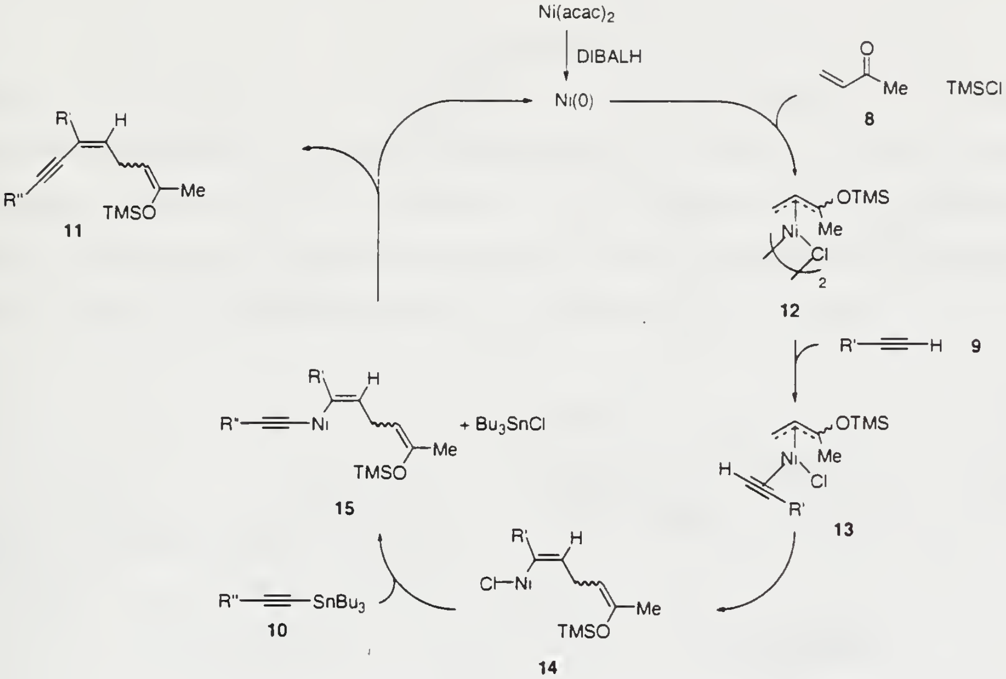

The existence of the π-allylnickel intermediate **12** was supported by Mackenzie's observation (Scheme 5a).[7] In the presence of a stoichiometric amount of Ni(0) species, the reaction of acrolein with TMSCl forms the π-allylnickel species **16** as a dimeric species. The dimer **16** was isolated as a stable solid and was well characterized using NMR spectroscopy and X-ray crystallography.

SCHEME 5

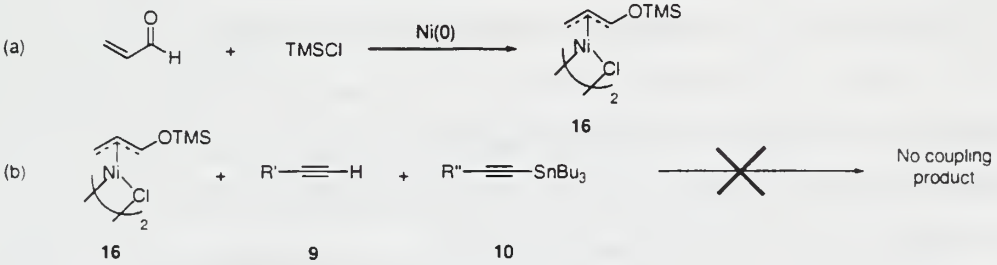

However, in later mechanistic studies, it was found that independently prepared π-allylnickel species **16** did not undergo further alkyne insertion under the conditions used for the coupling (Scheme 5b).[8] Thus, the possibility of a π-allylnickel **12** as an intermediate prior to the alkyne insertion step was eliminated, and an alternative mechanism was proposed (Scheme 6). The *in situ* generated Ni(0) species coordinates to both enone **8** and alkyne **9**, and the nickel complex **17** undergoes an oxidative cyclization to produce the nickellacycle intermediate **18**. The nickellacycle intermediate can be either the η^1- (**18**) or η^3-bound (**19**) forms. The TMSCl acts as an electrophile in the following reaction with the nickellacycle to give the TMS enol ether **14** which is the same intermediate shown in Scheme 4. Subsequent transmetallation with the alkynylstannane **9** followed by reductive elimination affords the observed product **11**.

SCHEME 6

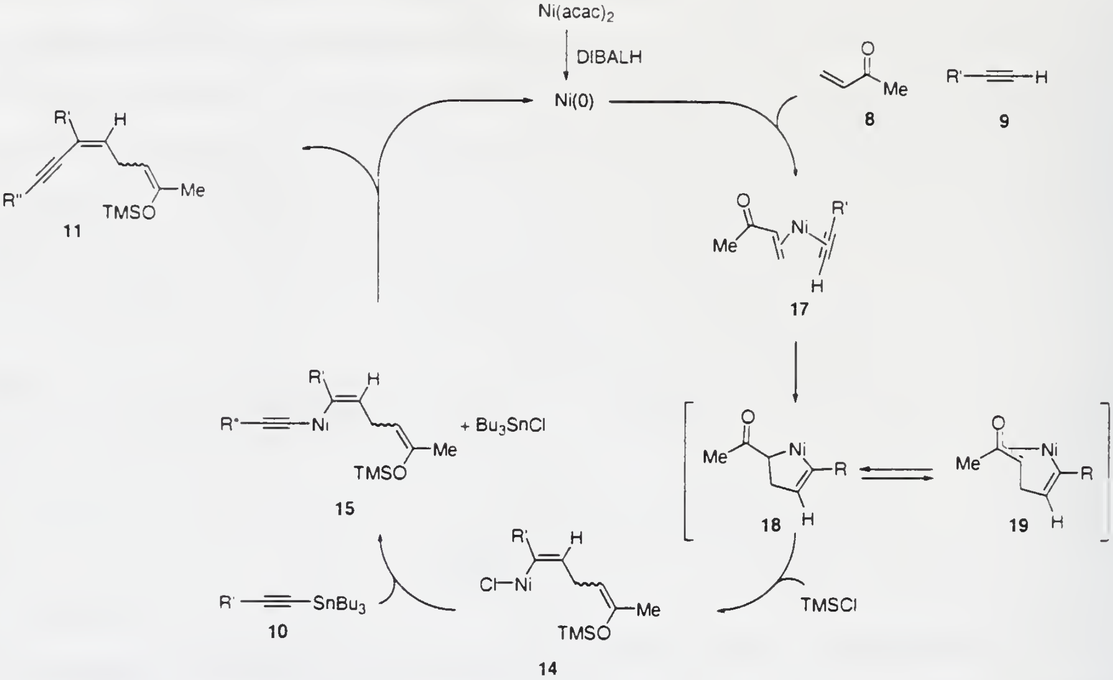

In addition to enones, other electrophiles such as allylchloride (**1**) also undergoes a similar coupling reaction with 3-hexyne (**20**) and tributylphenylethynylstannane (**21**) (Scheme 7).[9] The reaction yielded the enyne **22** with almost complete stereocontrol in the olefin geometry where the allyl group and alkynyl group are in a *cis* relationship to each other and the allyl group is connected to the terminal carbon of the alkyne. The reaction is likely to go through a similar mechanism as Chiusoli's carbonylative allylation (Scheme 2). The formation of the π-allylnickel chloride **2** from Ni(0) and allyl chloride followed by alkyne insertion yields the alkenylnickel intermediate similar to **4**. The next steps include: transmetallation with the stannane **21** and reductive elimination of the resulting alkenyl alkynyl nickel intermediate.

SCHEME 7

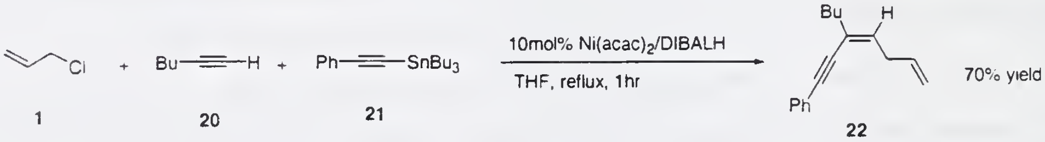

Intramolecular Cyclization/Transmetallation Sequence

Inspired by the reports on intermolecular three component coupling from Sato and Ikeda, Montgomery and coworkers developed a similar nickel-catalyzed sequential carbon-carbon bond forming system.[10] It was proposed that if two of the three component were tethered, the three component reaction can create a cyclic product via intramolecular cyclization following the similar mechanism shown in Scheme 6. This proposal was realized by employing **23**, a tethered enone and an alkyne with an alkyl chain, in the coupling conditions. Dialkylzinc generated *in situ* was used as an alkylating agent (Scheme 8). The reaction of **23** with dialkylzinc in the presence of a Ni(0) catalyst afforded a stereodefined alkylidenecyclopentane **24**. When dibutylzinc was employed as an alkylating agent, 8% ~ 11% of the reductive cyclization product **25** was also obtained.

SCHEME 8

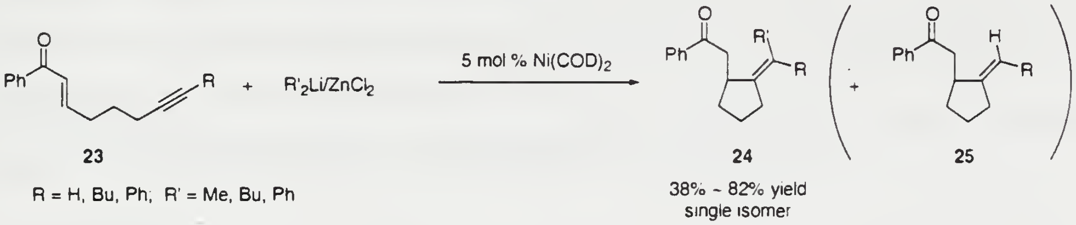

Montgomery and coworkers proposed a catalytic cycle similar to Scheme 6 (Scheme 9).[11, 12] The enone and alkyne in **23** coordinate to the Ni(0) catalyst and undergoes an enyne-type cyclization to yield the nickelacyclopentene intermediate **27**. In the presence of dialkylzinc, the nickelacycle **27** can be opened via transmetallation to afford the alkenylnickel intermediate **29**. The subsequent reductive elimination yields the observed product **24**. The minor product **25** may be derived from the β-hydride elimination from the alkenylnickel **28**.

When the nickel catalyst was pretreated with four equivalent of triphenylphosphine prior to the coupling reaction, only the reductive coupling product **25** was obtained in 92% yield (Scheme 8, R' = Bu). This observation can be explained by the σ-donating effect of triphenylphosphine which promotes the β-hydride elimination path from the alkenylnickel **28** to the hydridonickel **29**.

Scheme 9

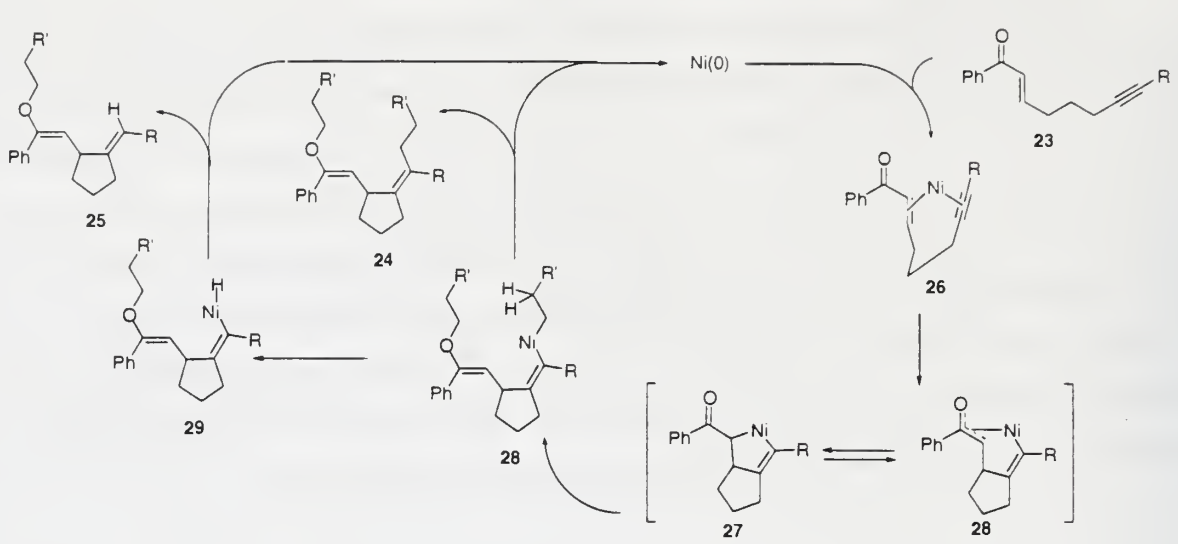

Mori and coworkers designed a similar type of nickel-catalyzed multicomponent coupling reaction using the tethered diene-aldehyde **30** and organometallic reagents in the presence of a Ni(0) catalyst (Scheme 10).[13] The reaction was initially carried-out under a stoichiometric amount of a Ni(0) reagent and yielded the substituted cyclohexanol **31** using various organometallic reagents (R = Me).

Scheme 10

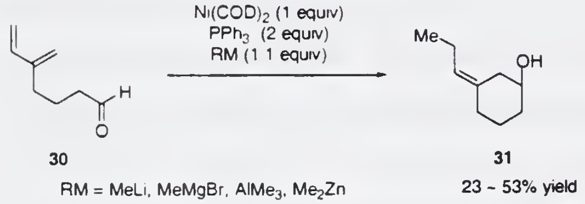

Scheme 11

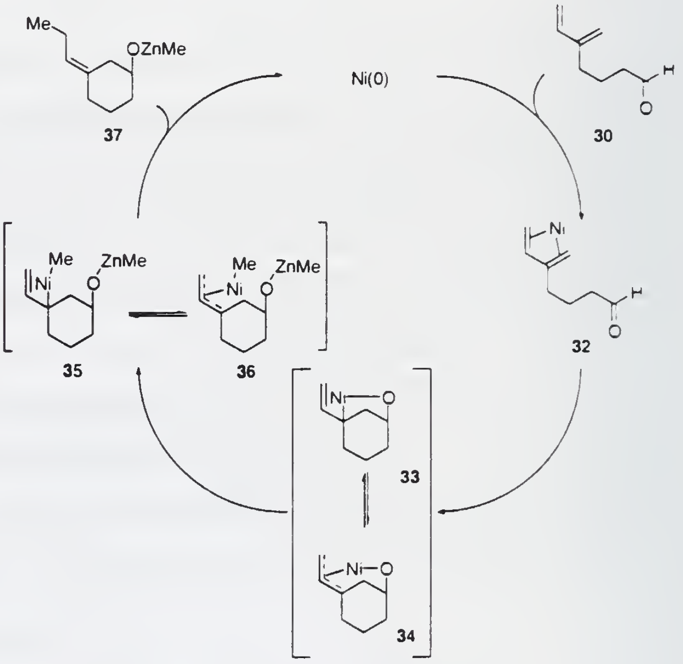

The proposed mechanism includes (Scheme 11): (1) coordination of the diene of **30** to Ni, (2) intramolecular oxidative cyclization of the activated diene-Ni(0) complex **32** to form the oxanickellacycle intermediate **33**, (3) transmetallation of the nickellacycle **33** with dimethylzinc to give the alkylmethylnickel **35** which is in equilibrium with the η^3-allylnickel species **36**, (4) reductive elimination and followed by hydrolysis of **37** to yield the observed product **31**. The reaction can be catalytic in Ni(0). When 30 mol % of $Ni(COD)_2$ was used, the cyclohexanol **31** was formed with 57% yield though the reaction time was increased to 68 hours. More recently, a mechanistically similar type of multicomponent coupling was developped by Tamaru and coworkers using diene and aldehyde in a fully intermoelecular manner.[14]

APPLICATIONS TO ORGANIC SYNTHESIS

The scope of Ni-catalyzed multiple component coupling methodologies have expanded further in the past few years, and many variants of the reactions decribed above have appeared in the literature.[15] These reactions have been applied to the field of organic synthesis to achieve an efficient construction of complex molecules (Scheme 12). Montogomery and coworkers accomplished the stereodivergent synthesis of kainic acid derivatives and the total synthesis of allopumiliotoxins.[16, 17] For the construction of the indolizidine core of (-)-Elaeokanine C, Mori and coworkers used a method similar the diene-aldehyde cyclization.[18]

SCHEME 12

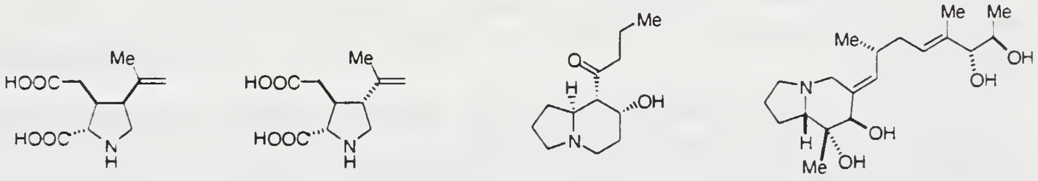

(-)-α-kainic acid (+)-α-kalloainic acid (-)-Elaeokanine C (+)-Allopumiliotoxin-339A

CONCLUSION

The nickel-catalyzed multiple component coupling reactions enabled multiple carbon-carbon bond formations under mild conditions in a regio- and stereoselective manner. Leading works by Ikeda and Montgomery have shown generality of the reaction by employing various coupling partners and alkylating reagents and allowed accesses to various types of complex structures from simple starting materials.[15] The stereoselective variant of the reactions described above have appeared in a recent literature and expanded the scope of these reactions.[19] The proposed reaction mechanisms involved formation of nickellacycle and/or π-allylnickel intermediates with the existence of such species having been supported by solid precedents and by mechanistic studies of these reactions. A few attempts of using these reactions in syntheses have been made and offered the effeicient synthesis of complex carbon skeleton.

REFERENCES

1. Various definitions for these terms were found. See: (a) Tietze, L. F. *Chem. Rev.* **1996**, 96, 115. (b) de Meijere, A; Brase, S. *J. Organometallic Chem.* **1999**, 576, 88. (c) Grigg, R.;Sridrahan, V. *J. Organometallic Chem.* **1999**, 576, 65. (d) Denmark, S. E.; Thorarensen, A. *Chem. Rev.* **1996**, 96, 137.
2. Houpis, I. N.; Lee, J. *Tetrahedron.* **2000**, 56, 817.
3. Jolly, P. W. ″ Organonickel Compounds in Organic Synthesis" in *Comprehensive Organometallic Chemistry.* Wilkinson, G.; Stone, F. G. A.; Abel, E. W. eds.; Pergamon Press: London, 1982; vol. 8, chepter 57.
4. (a) Chiusoli, G. P. *Acc. Chem. Res.* **1973**, 6, 422. (b) Llebaria, A.; Motero, J. M. *J. Organometallic Chem.* **1993**, 451, 1.
5. (a) Semmelhack, M. F. *Org. React.* **1972**, 19, 115. (b) Billington, D. C. *Chem. Soc.Rev.* **1985**, 93.
6. Ikeda, S.; Sato, Y. *J. Am. Chem. Soc.* **1994**, 116, 5975.
7. Grisso, B. A.; Johnson, J. R.; Mackenzie, P. B. *J. Am. Chem. Soc.* **1992**, 114, 5160.
8. Ikeda, S.; Kondo, K.; Sato, Y. *J. Org. Chem.* **1996**, 61, 8248.
9. Ikeda, S.; Cui, D.; Sato, Y. *J. Org. Chem.* **1994**, 59, 6878.
10. (a) Montgomery, J.; Savchenko, A. V. *J. Am. Chem. Soc.* **1996**, 118, 2099. (b) Montgomery, J.; Seo, J.; Chui, H. M. P. *Tetrahedron Lett.* **1996**, 37, 6839.
11. Montgomery, J; Seo, J. *Tetrahedron* **1998**, 54, 1131.
12. Montogomery, J.; Oblinger, E.; Savchenko, A. V. *J. Am. Chem. Soc.* **1997**, 119, 4911.
13. (a) Sato, Y.; Takanashi, T.; Mori, M. *Organometallics* **1999**, 18, 4891. (b) Sato, Y.; Takimoto, M.; Mori, M. *J. Am. Chem. Soc.* **2000**, 122, 1624.
14. Kimura, M.; Matsuo, S.; Shibata, K.; Tamaru, Y. *Angew. Chem. Int. Ed.* **1999**, 38, 3386.
15. For accounts: (a) Ikeda, S. *Acc. Chem. Res.* **2000**, 33, 511. (b) Montgomery, J. *Acc. Chem. Res.* **2000**, 33, 467.
16. (a) Chevliakov, M. V.; Motgomery, J. *J. Am. Chem. Soc.* **1999**, 11139. (b) Chevliakov, M. V.; Motgomery, J. *Angew. Chem. Int. Ed.*. **1998**, 3144.
17. (a) Tang, X.; Montgomery, J. *J. Am. Chem. Soc.* **2000**, 122, 6950. (b) Tang, X.; Montgomery, J. *J. Am. Chem. Soc.* **1999**, 121, 6098.
18. (a) Sato, Y.; Saito, N.; Mori, M. *Tetrahedron* **1998**, 54, 1153. (b) Sato, Y.; Saito, N.; Mori. M. *Tetrahedron Let.* **1997**, 38, 3931.
19. (a) Cui, D.; Yamamoto, H.; Ikeda, S.; Hatano, K.; Sato, Y. *J. Org. Chem.* **1998**, 63, 2782. (b) Ikeda, S.; Cui, D.; Sato, Y. *J. Am. Chem. Soc.***1999**, 121, 4712.

CONTROLLED RELEASE OF NITRIC OXIDE: THE DIAZENIUMDIOLATE GROUP

Reported by Margaret L. Collins November 16, 2000

INTRODUCTION

In the past fifteen years, the biological importance of nitric oxide (NO) has been revealed. Nitric oxide is an important second messenger that is involved in a number of bioregulatory processes such as prevention of thrombus via inhibition of platelet aggregation,[1] treatment of hypertension via vascular relaxation[1], prevention of cell damage via cytoprotection,[2] and inhibition of tumor cell growth via cytotoxicity.[3] In general, the pathway by which nitric oxide induces biological activity involves the activation of the enzyme soluble guanylate cyclase (sGC) through reaction of NO with the heme prosthetic group of sGC. The activated sGC catalyzes the synthesis of cyclic guanosine monophosphate (cGMP), which goes on to induce biological activity.[4] The mechanism by which NO induces cytoprotective and cytotoxic effects is still under investigation. Given the pervasive effects of NO on these systems and others, there is a necessity for controlled administration of nitric oxide.

DIAZENIUMDIOLATE

An appropriate source of nitric oxide for study and treatment of these bioregulatory processes would need to be able to release a controlled amount NO under physiological conditions over a certain period of time, not produce toxic products upon release, and have the potential to target specific tissues. A class of compounds known as diazeniumdiolates (**1**) were not only found to fit this criteria, but their ease of preparation and numerous structural analogues has warranted attention.

Figure 1. Structure of diazeniumdiolate.

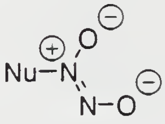

1

Nu= Nucleophile

The synthesis of diazeniumdiolate compounds involves the reaction of the appropriate nucleophile with nitric oxide gas under pressure to produce the product diazeniumdiolate. The typical nucleophile is an amine; however, enamines,[5] phenolates[6] and the sulfite ion[7] have also been used. Scheme 1 provides two mechanistic pathways by which this reaction may take place.[8] Path **A** involves radical combination of two molecules of nitric oxide to form the nitric oxide dimer (**2**). Addition of the nucleophile, **Nu**, to **2**, produces the conjugate base of *N*-hydroxyl-*N*-nitrosoamine (**4**). Structure **4** undergoes rearrangement to form the conjugate base of hydroxydiazenium *N*-oxide (**5** also known as

Copyright © Margaret L. Collins

diazeniumdiolate). Path **B** involves addition of **Nu** to electrophilic NO to give the intermediate radical anion **3**. Addition of a second molecule of NO affords structure **4** which would undergo subsequent rearrangement. Drago and coworkers performed a kinetic study that provided data in support of Path **B** where the initial addition of NO is the rate-limiting step.[8]

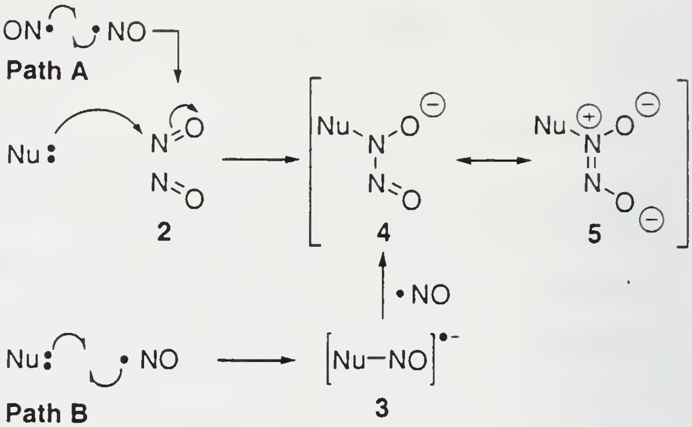

Scheme 1. Proposed mechanisms for the synthesis of diazeniumdiolate.

An important aspect in understanding the NO donor ability of diazeniumdiolates is to know its structure. Early X-ray crystal studies of the solid protonated diazeniumdiolate group revealed that the structure was either *N*-hydroxyl-*N*-nitrosoamine (**6**) or hydroxydiazenium *N*-oxide (**7**).[9] Analysis of the bond lengths in the X-ray crystal structure where R = 4-methylcyclohexyl and computational analysis of the stabilities of **6** and **7** provided strong evidence for structure **7**.[9,10]

Figure 2. Potential structures of protonated diazeniumdiolate.

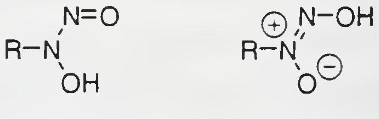

6 **7**

NITRIC OXIDE RELEASE

The most important aspect in the utility of diazeniumdiolate compounds as nitric oxide donors is the capacity to control NO release. Ideally, the NO donor would only release nitric oxide at the desired physiological pH 7.4. Diazeniumdiolate compounds have been observed to be stable at alkaline pH while NO release is observed at or below the physiological pH 7.4, thus providing an element of control over NO release. Two other controlling factors are the period of time over which NO is released and the extent of the release. The desired half-life ($t_{1/2}$) of a compound is application dependent. For example, it is advantageous to have a short half-life resulting in a quick release for treatment of hypertension, while a long-term delivery is desired for the inhibition of platelet aggregation in the prevention of thrombus. The extent of release (E_{NO}) is important in determining if the compound would be an efficient source of NO. The E_{NO} is the moles of NO released per mole of starting material consumed. In general, it is more desirable to have complete NO release ($E_{NO} = 2$). Values less than two may be the result of decomposition byproducts such as N_2O. Research has revealed that the chemical structure of the nucleophilic substrate offers control of the half-life and E_{NO}.

Nitric Oxide Release in Aqueous Solution

It is important to know how nitric oxide is released in aqueous solution in order to better understand the NO release studies that have been performed using various nucleophiles. The likely mechanism involves acid catalysis as shown in Scheme 2.[9] In solution, protonation of **1** would afford the corresponding intermediates **8** or **9**. The tautomerization of N-hydroxyl-N-nitrosoamine (**8**) to hydroxydiazenium N-oxide (**9**) occurs due to the greater thermodynamic stability of **9**. Under acidic conditions, protonation and extrusion of the free nucleophile results in the formation of protonated nitric oxide dimer **10**. Proton transfer from **10** to the aqueous solvent affords the nitric oxide dimer (**2**), which readily decomposes to two molecules of NO. Support for this mechanism arises from the observations that: 1) the half-life of NO release is increased with an increase in acidity, 2) free amine is one of the products when Nu is an amine, 3) alkylation of the terminal oxygen results in no nitric oxide release.

Scheme 2. Proposed mechanism of nitric oxide release.

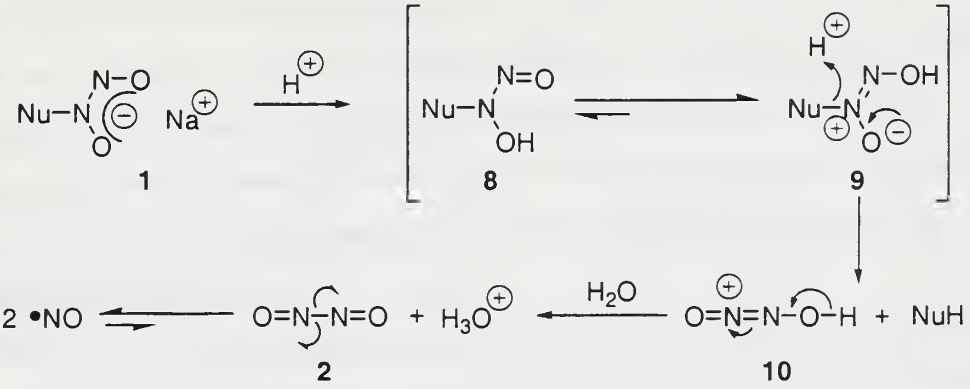

One significant study comparing the nitric oxide releasing properties of different substrates was performed in 1991 by Keefer and coworkers.[11] They determined that the release of NO is a first-order process. The study focused on the half-lives and extent of NO release for diazeniumdiolates of structure **1** with five different nucleophilic substrates. A summary of the data collected is given in Table 1.

Table 1. Half-life and extent of NO release for various diazeniumdiolates.

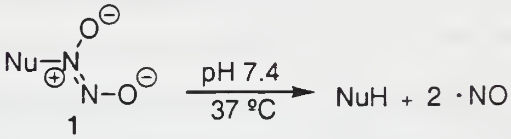

compound	Nu	$t_{1/2}$ (min)	E_{NO}
1a	Et_2N	2.1	1.5
1b	i-PrHN	2.3	0.73
1c	$H_2N(H_2C)_3H_2N^+(H_2C)_4$ N $H_2N(H_2C)_3$	39	1.9
1d	O^-	2.3	0.54
1e	^-O_3S	6.8	0.001

Keefer and coworkers were interested in the vasodilator effects (ability to dilate blood vessels) of these compounds. Vasodilation via NO is most effective when NO is delivered fully and quickly. Thus a potent compound for vasodilation would have a short half-life and an E_{NO} of two. Although the diethylamine derivative **1a** and isopropylamine derivative **1b** have similar half-lives, the extent of release during that time differs by a factor of two. That means that compound **1a** is about twice as potent as **1b**. Detrimental to using **1a** as a drug is its decomposition in the presence of oxygen leading to the formation of the carcinogen *N*-nitrosodiethylamine.[12] Although the spermine derivitave **1c** has a greater E_{NO}, it is a less potent vasodilator than **1a** and **1b** due to its significantly longer half-life. A benefit to this derivative is when **1c** breaks down it releases free spermine which is known to have biological activity including hypotensive activity. Compounds **1a-1c** could serve as suitable sources of NO as well as potential vasodilators. The last two compounds, oxyhyponitrite (**1d** Angeli's salt) and N-nitrosohydroxylamine-N sulfonate (**1e**), were found to be much less potent vasodilators than **1a**-**1c** due to the low extent of NO released. Other investigations of **1d**,[13] reveal that the major decomposition products are nitrous oxide and nitrite under physiological conditions. Nitric oxide is mostly produced at pH ≤ 3, conditions which would be too extreme for most applications. Similarly, compound **1e** decomposes almost exclusively to nitrous oxide[7] demonstrating that diazeniumdiolates with sulfite ion nucleophiles make poor NO donors. Keefer and coworkers found that the potency of a compound was directly proportional to the extent of NO released.

In the interest of exploring the control over the half-life of diazeniumdiolates through alteration of the substrate, Hrabie and coworkers performed a study that focused on zwitterionic nitrogen-based intramolecular salts of the general form **11**.[14] One variation focused on the affect of alkyl chain length on the half-life of the compound (Table 2). The data indicates that as the chain is lengthened, the half-life of the compound decreases. One possible explanation is that when intramolecular hydrogen bonding occurs, the diazeniumdiolate group would be less susceptible to NO release by protonation. This would lead to a longer half-life for the compound. Looking at Table 2, one can see that as the chain is lengthened, hydrogen bonding would have less of an effect, leading to the observed shorter half-life.

Table 2. Half-life of zwitterionic diamines.

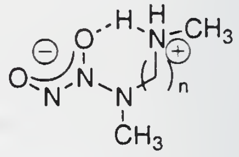

11

compound	n	$t_{1/2}$ (min)
12	2	36.1
13	3	10.1
14	4	1.3
15	6	2.7

The resulting stabilization of the diazeniumdiolate compounds by hydrogen bonding prompted Hrabie and coworkers to look at substrates containing additional amines. The hypothesis was that incorporation of a primary amine would further stabilize the compound resulting in a longer half-life (**16**). Based on compound **17** in Table 3, this was true. As seen with the diamines, the lengthening of the alkyl chain resulted in a decrease of the half-life likely for the same reason. Adding more amines beyond triamines resulted in complex mixtures of products due to the presence of too many reactive sites.

Table 3. Half-life of zwitterionic triamines.

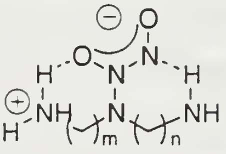

16

compound	m	n	$t_{1/2}$ (min)
17	2	2	3400
18	3	3	284
19	3	4	165

In the interest of converting natural products, drugs, and other useful complex substrates into NO donors, Saavedra and coworkers proposed piperazine as a plausible linker to the diazeniumdiolate functional group.[15] Piperazine would make a good linker since it has two secondary amines that could be functionalized and its use as an anthelminitic (treatment for parasites) means it would not have undesirable pharmacological consequences. Scheme 3 shows the synthesis of select piperazine derived diazeniumdiolates with the distal piperazine nitrogen protected as a carbamate. Removal of this protecting group would provide a handle for addition to another molecule. Saavedra and coworkers noted the NO releasing abilities of piperazine derived diazeniumdiolates (**21** Table 4). The nearly complete release of NO and the reasonably short half-lives indicates that compounds of type **21** would make good NO donors. For biological studies the dansyl derivative **21c** is of particular interest due to its fluorescence. A fluorescent group on the diazeniumdiolate would aid in the identification of the site of NO release.

Scheme 3. Piperazine derived diazeniumdiolate synthesis and NO release data.

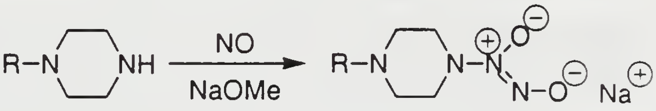

20 **21**

compound	R=	$t_{1/2}$ (min)	E_{NO}
21a	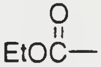 $\mathrm{EtOC(=O)}$—	2.8	1.92
21b	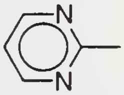	1.9	1.96
21c	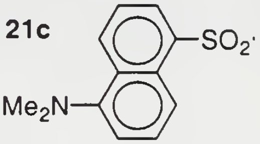	5.6	1.43

Piperazine has recently been utilized as a linker between the polysaccharide heparin and diazeniumdiolate.[16] Heparin has been widely used as an anticoagulant due to its inhibition of the coagulation cascade that converts fibrinogen to fibrin. Keefer and coworkers hypothesized that the combination of this anticoagulant activity of heparin with the cGMP-dependent inhibition of platelet aggregation of nitric oxide would produce a molecule with dual antithrombotic activity. The significant reduction of coagulation and platelet aggregation in platelet-rich human plasma treated with diazeniumdiolated heparin provided evidence for the potential use of this compound to treat thrombus. The interest in cardiovascular treatment has also led to the use of more complex substrates like proline,[17] proteins,[18] and polymers[19,20] that could aid in localized treatment by being incorporated into biological tools such as vascular grafts.

Enzymatic Release of Nitric Oxide

The compounds described so far are good for in vitro biological studies, but could pose a risk when administered in vivo. In order to prevent damage to other NO sensitive parts of the body, there is a need for targeted delivery of NO. To date, the best solution has been to functionalize the terminal oxygen of the diazeniumdiolate group. In doing so, the compound is stable under physiological conditions until acted upon by an enzyme. The goal is to design functional groups for the terminal oxygen that would only be removed by enzymes present in the targeted tissue.

Scheme 4. Synthesis and proposed enzymatic NO release of O^2- vinyl diazeniumdiolate.

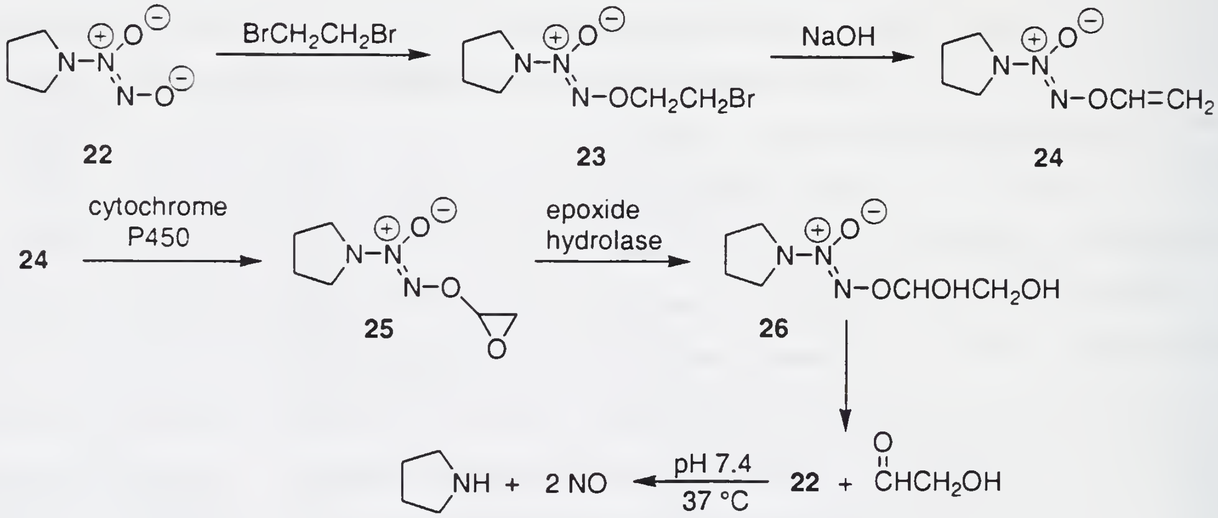

Keefer and coworkers have looked at three possibilities, one of which could prevent liver damage[2] and two which have potential in preventing leukemia cell growth.[3] With the knowledge that hepatic cytcochrome P450 is capable of epoxidizing vinyl ethers, the researchers proposed the prodrug **24**, the synthesis of which is shown in Scheme 3. The proposed mechanism for the enzyme-induced release of NO from the vinyl ether derivative **24** involves epoxidation by cytochrome P450 followed by hydrolysis via catalysis by epoxidase hydroxylase which is prevalent in the liver (Scheme 3). These reactions would result in a hemiacetal **26** that decomposes to **22** and hydroxyacetaldehyde, which would break down further to nitric oxide and the free amine by the mechanism proposed in Scheme 2.

Subsequent biological studies showed that **24** was capable of preventing TNFα-mediated damage to liver cells by increasing the amount of cGMP.

Scheme 5. Syntheses of thioacetate esters and O2-acetoxymethylated diazeniumdiolates.

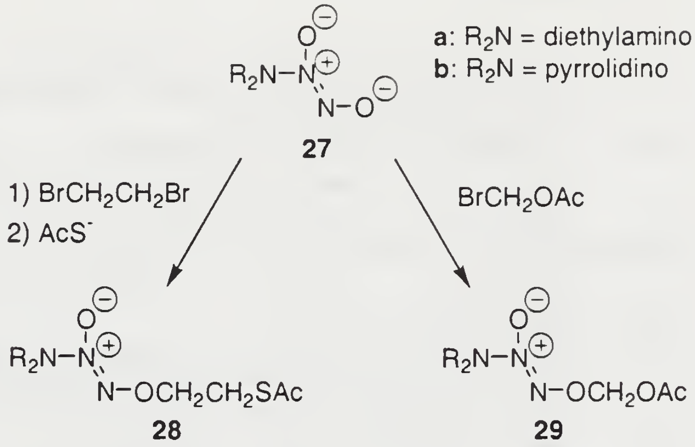

Esterase-induced release of NO that could be useful in preventing leukemia cell growth was explored by looking at thioacetate ester derivative (**28**) and O^2-acetoxymethylated derivative (**29**). These compounds were prepared by the routes shown in Scheme 4. The proposed mechanism of NO release utilizing esterase (Scheme 5) is hydrolysis of **29** resulting in the free diazeniumdiolate **28**, formaldehyde, and acetate. For the thioacetate esters **28**, the esterase would hydrolyze the thioester bond to produce acetate and the mercaptoethyl intermediate **30**. The sulfur would attack the β–carbon resulting in the free diazeniumdiolate **27** and the expulsion of thiirane. From this point **37** breaks down to the free amine and NO due to the physiological environment. Biological studies have shown that prodrugs **28** and **29** both have the ability to inhibit leukemia cell growth with **29** being the more potent of the two.

Scheme 6. Proposed mechanisms for esterase-induced release.

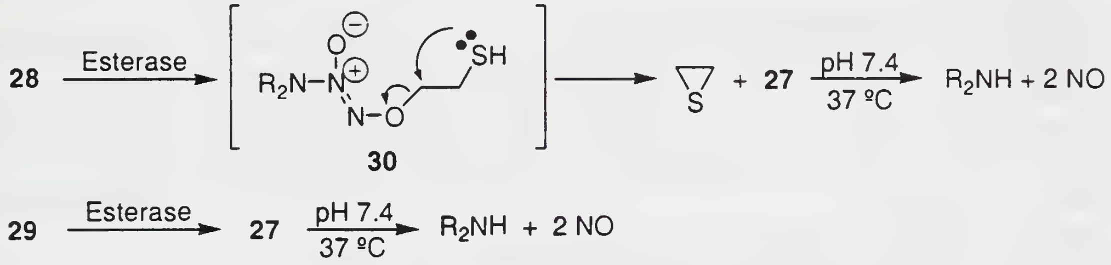

CONCLUSION

The biological importance of nitric oxide has resulted in a search for controllable sources of NO. That ability to control the release of NO can be utilized in the study and treatment of various nitric oxide sensitive bioregulatory processes. The diazeniumdiolate group not only has the ability to release nitric oxide, but using assorted nucleophilic substrates offers control of a wide range of half-lives and extents of NO release. Furthermore, through functionalization of the terminal oxygen of the diazeniumdiolate group, enzyme-induced target specific NO release is possible. Future research includes the exploration of applications for known diazeniumdiolate compounds and the quest for more *O*-functionalized diazeniumdiolate prodrug candidates.

REFERENCES

(1) Kerwin, J. F.; Lancaster, J. R.; Feldman, P. L. *J. Med. Chem.* **1995**, *38*, 4343-4362.

(2) Saavedra, J. E.; Billiar, T. R.; Williams, D. L.; Kim, Y.; Watkins, S. C.; Keefer, L. K. *J. Med. Chem.* **1997**, *40*, 1947-1954.

(3) Saavedra, J. E.; Shami, P. J.; Wang, L. Y.; Davies K. M.; Booth, M. N.; Citro, M. L.; Keefer, L. *J. Med. Chem* **2000**, *43*, 261-269.

(4) Knowles, R. G.; Moncada, S. *Trends Biol. Sci.* **1992**, *17*, 399-402.

(5) Hrabie, J. A.; Arnold, E. V.; Citro, M. L.; George, C.; Keefer, L. K. *J. Org. Chem.* **2000**, *65*, 5745-5751.

(6) Bohle, D. S.; Imonigie, J. A. *J. Org. Chem.* **2000**, *65*, 5685-5692.

(7) Bhat, J. I.; Clegg, W.; Maskill, H.; Elsegood, M. R. J.; Menneer, I. D.; Miatt, P. C. *J. Chem. Soc., Perkin Trans. 2* **2000**, 1435-1446.

(8) Drago, R. S.; Ragsdale, R. O.; Eyman, D. P. *J. Am. Chem. Soc.* **1961**, *83*, 4337-4339.

(9) Taylor, D. K.; Bytheway, I.; Barton, D. H. R.; Bayse, C. A.; Hall, M. B. *J. Org. Chem.* **1995**, *60*, 435-444 and citations therein.

(10) Hickmann, E.; Hädicke, E.; Reuther, W.; *Tetrahedron Lett.* **1979**, *26*, 2457-2460.

(11) Maragos, C. M.; Morley, D.; Wink, D. A.; Dunams, T. M.; Saavedra, J. E.; Hoffman, A.; Bove, A. A.; Isaac, L.; Hrabie, J. A.; Keefer, L. K. *J. Med. Chem.* **1991**, *34*, 3242-3247.

(12) Ragsdale, R. O.; Karstetter, B. R.; Drago, R. S. *Inorg. Chem.* **1965**, *4*, 420-422.

(13) Hughes, M. N.; Wimbledon, P. E. *J. Chem. Soc., Dalton Trans.* **1976**, 703-707.

(14) Hrabie, J. A.; Klose, J. R.; Wink, D. A.; Keefer, L. K. *J. Org. Chem.* **1993**, *58*, 1472-1476.

(15) Saavedra, J. E.; Booth, M. N.; Hrabie, J. A.; Davies, K. M.; Keefer, L. K. *J. Org. Chem.* **1999**. *64*, 5124-5131.

(16) Saavedra, J. E.; Mooradian, D. L.; Mowery, K. A.; Schoenfisch, M. H.; Citro, M. L.; Davies, K. M.; Meyerhoff, M. E.; Keefer, L. K. *Bioorg. Med. Chem. Lett.* **2000**, *10*, 751-753.

(17) Saavedra, J. E.; Southan, G. J.; Davies, K. M.; Lundell, A.; Markou, C.; Hanson, S. R.; Adrie, C.; Hurford, W. E.; Zapol, W. M.; Keefer, L. K. *J. Med. Chem.* **1996**, *39*, 4361-4365.

(18) Hrabie, J. A.; Saavedra, J. E.; Roller, P. P.; Southan, G. J.; Keefer, L. K. *Bioconjugate Chem.* **1999**, *10*, 838-842.

(19) Pulfer, S. K.; Ott, D.; Smith, D. J. *J. Biomed. Mater. Res.* **1997**, *37*, 182-189.

(20) Smith, D. J.; Chakravarthy, D.; Pulfer, S.; Simmons, M. L.; Hrabie, J. A.; Citro, M. L.; Saavedra, J. E.; Davies, K. M.; Hutsell, T. C.; Mooradian, D. L.; Hanson, S. R.; Keefer, L. K. *J. Med. Chem.* **1996**, *39*, 1148-1156.

VIRTUAL COMBINATORIAL LIBRARIES AND THEIR APPLICATIONS

Reported by Keunchan Oh November 20, 2000

INTRODUCTION

The specific interactions between host and guest molecules that lead to more stable complexes are essential to biological processes. Thus the mimicking of these interactions in abiotic (supra)molecular systems is claimed to offer a new concept in synthesis.

Conventional combinatorial libraries (CL) are used extensively in searching for and generating new drugs, materials and reaction catalysts. Such libraries are based on the irreversible covalent syntheses from building blocks ($a_1, \ldots, a_m$) and high throughput screening of the resulting libraries ($A_1, \ldots, A_n$) with target molecules (T) (Figure 1). While the use of CL has proven helpful, this approach is still highly limited by the rate of component synthesis and sequential screening.

Virtual combinatorial libraries (VCL)[1-4] bypass the necessity of individual component synthesis using the reversible interactions between building blocks ($a_1, \ldots, a_m$). The distribution depends on the thermodynamic stability of each component ($A_1, \ldots, A_n$). In the presence of target molecules, this dynamic nature of the library will shift the overall composition towards enriching itself in the component ($A_i \cdot T$) which have highest affinity for target molecules. It is claimed to be a type of

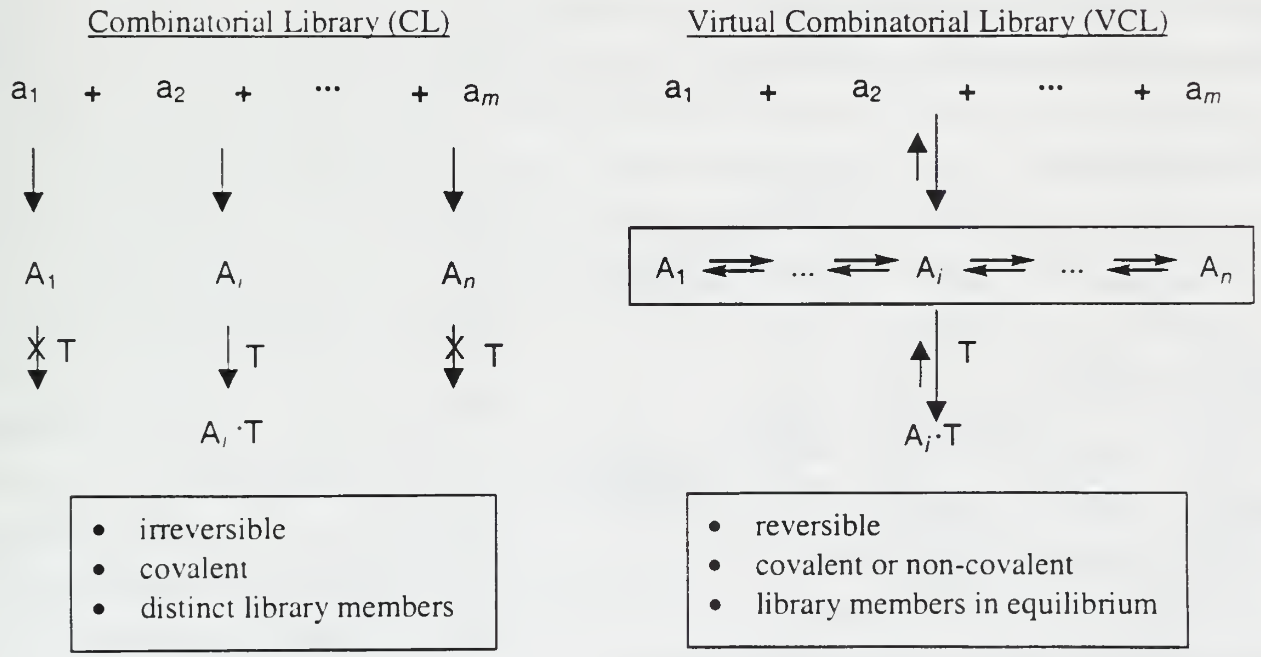
Combinatorial Library (CL)
Virtual Combinatorial Library (VCL)
a_1 + a_2 + ··· + a_m
a_1 + a_2 + ··· + a_m
A_1
A_i
A_n
T
T
T
$A_i \cdot T$
A_1 ... A_i ... A_n
T
$A_i \cdot T$
irreversible
covalent
distinct library members
reversible
covalent or non-covalent
library members in equilibrium

Figure 1. Comparative Basic Features of Conventional and Virtual Combinatorial Library[1, 3]

Copyright © 2000 Keunchan Oh

(supra)molecular Darwinism[1, 2] or chemical evolution[5] in which dynamic mixture of components evolves to fit target molecules. It can be moderately referred to as templated [6,7] or targeted [8] equilibrium shifting.

A selection of potentially reversible events[1], then, is important to the design of VCL. Possible reactions include reversible bond formation such as imine formation, transacylation, and disulfide bond formation, reversible interactions such as metal coordination and hydrogen bonding, and reversible intramolecular processes like *cis-trans* isomerization, tautomerization, and internal rotation (Figure 2).

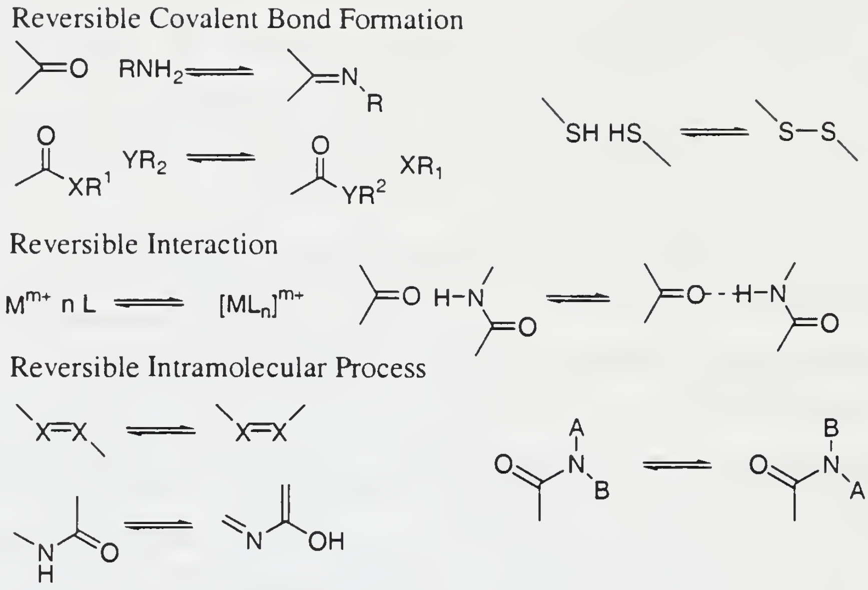

Figure 2. Examples of Reversible Chemistry That Could Form the Basis of VCL.

The templated shifting of VCLs can be achieved by two main methods (Figure 3).[1,6] One is a casting process where substrates, generated reversibly from a set of building blocks, are selected by specific interactions with a complementary target receptor. The other method is a molding process where a receptor, generated reversibly from a set of building blocks, is chosen by specific interactions with a complementary target substrate. The purpose of this review is to see if reversible

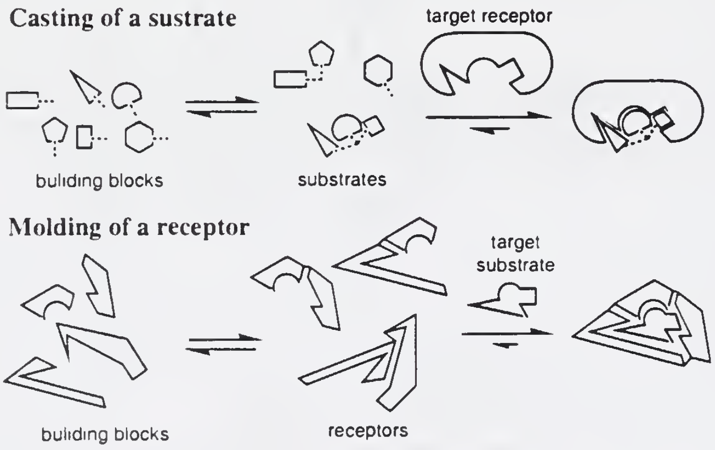

FIGURE 3. CASTING AND MOLDING

reaction can de done in a combinatorial fashion, and to explore the possibility that VCL is complementary to CL.

REVERSIBLE COVALENT BOND FORMATION

Sanders et al. have used transamination[4,9,10] and transesterification[6,7,11] to generate a VCL of macrocycles, where each major macrocycle could interconvert to its linear analogue, which was also a member of the VCL. A VCL of pseudo-peptide hydrazides can be generated under acidic conditions from AB type monomer **1** which has a protected aldehyde at one end and a hydrazide at the other (Scheme 1). HPLC analysis of the library shows that major products are the dimer **2**, trimer **3**, tetramer **4**, pentamer **5**, and higher macrocyles. The linear members of the library have free hydrazide functional group which are protonated under acidic conditions. When the strong affinity of [18]-crown-[6] for ammonium, primary alkyl ammonium,[12] and hydrazinium[13] is exploited in this VCL, the equilibrium is shifted, favoring linear compound **6** which is undetectable in the absence of [18]-crown-6. The molecular recognition by non-covalent interactions between [18]-crown-[6] and protonated hydrazide is used to shift the VCL of cyclic pseudo-peptidic hydrazides to a linear analogue. Although the authors claimed this is an example of amplification, it seems like a simple templating of equilibrium mixtures.

Scheme 1. The Formation of Pseudopeptide Macrocycles

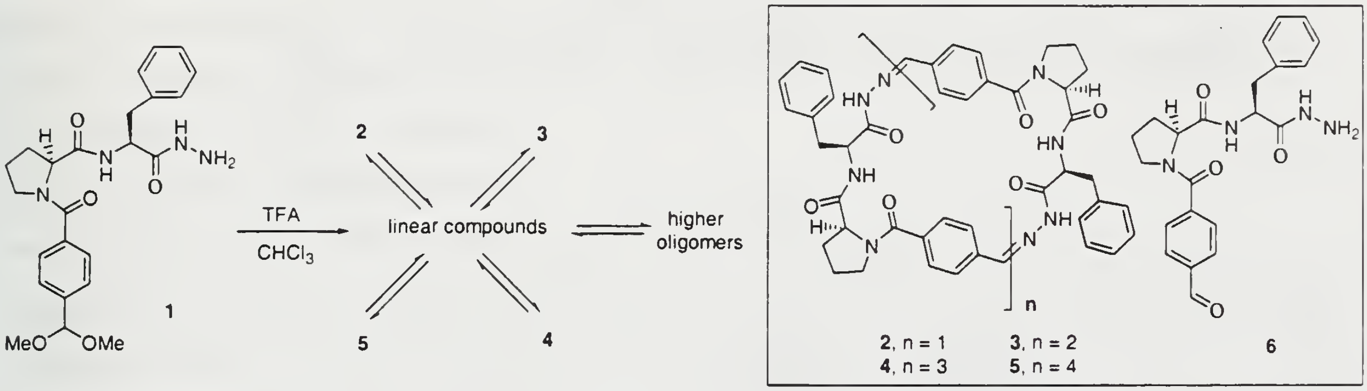

Chart 1.

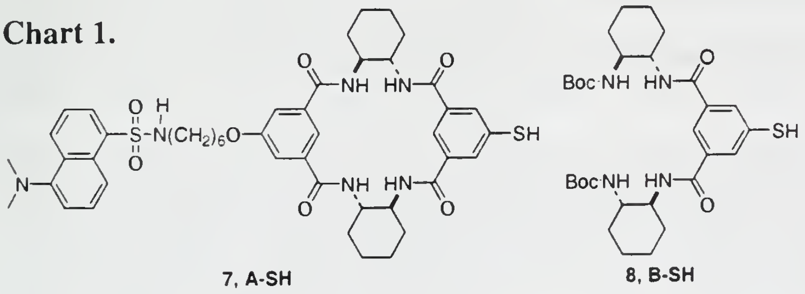

Still et al.[5] have used disulfide bond formation/exchange to generate a VCL of tripeptide receptors. Dansyl-labled mercaptan **7**, **A-SH** is oxidized with I_2 to disulfide **A-SS-A** (Chart 1). **A-SS-A** shows selective binding for polystyrene-supported tripeptide sequence, Ac(D)Pro(L)Val(D)Val-PS. The disproportionation of unsymmetrical **A-SS-Ph** to **A-SS-A** and **Ph-SS-Ph** shows a 100-fold increase in equilibrium constant in the presence of Ac(D)Pro(L)Val(D)Val-PS. This amplification is a molding process where effective receptors can be enriched in response to the tripeptide substrate. A similar amplification is observed in the disproportionation of **A-SS-B**.

REVERSIBLE NONCOVALENT INTERACTIONS

Rebek et al.[14] have reported a VCL of self-assembled tetrameric capsules (Chart 2). Homo-molecular capsules form when the subunit has appropriate curvature, self-complementary hydrogen bond donors and acceptors and only in the presence of a guest of suitable size and shape. Sulfamide glycouril compound **9** assembles into a tetrameric capsule, **14**, using hydrogen bonds between cyclic sulfamide donors and glycouril acceptors in the presence of a variety of guest molecules.[15] Substituents on the central aromatic ring are designed to modify the size, shape, and chemical surface of the cavity without disrupting self-assembly. Each capsule shows different affinities for different guests because of attractive interactions (**10** and **12**) or repulsive steric interactions (**11** and **13**). The peripheral alkyl groups on the glycouril moiety are chosen and attached for unique detection of each tetrameric capsule by ESI-MS. The resulting mixture of tetrameric capsules from **9**, **10**, and guest **15**, which is small and flexible, shows a nonstatistical distribution of all five observable complexes without any favored species. The nonstatistical distribution comes from the thermodynamic bias for binding. In the presence of guest **16**, which is large and rigid, the VCL of capsules shows a significant amplification of tetrameric capsule from **9**, which represents 69% of the observable complexes. A more complex VCL resulting from mixtures of **9-13** shows a similar preference. This example shows that the receptor can be amplified that best fits the structure and electronics of the target molecule.

Chart 2.

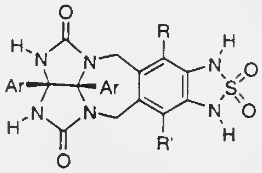

9, R=R'=H, Ar=p-C_7H_{15}Ph
10, R=R'=OH, Ar=p-C_7H_{15}Ph
11, R=R'=OMe Ar=p-$C_{12}H_{25}$Ph
12, R=H, R'=OH, Ar=p-$C_{12}H_{25}$Ph
13, R=H, R'=OMe, Ar=p-C_7H_{15}Ph

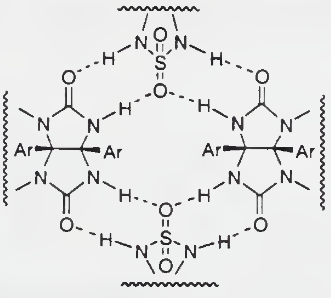

14

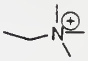

15

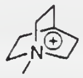

16

Reinhoudt et al.[16-18] have made a VCL from calix[4]arene dimelamine **17** and **18** and diethyl barbituric acid (**DEB**), **19**, through 36 cooperative hydrogen bonds (Chart 3). In the absence of tripyridine **20**, the mixture of **17** and **18** gives a statistical mixture of nine-component hydrogen bond assembly, **17_3:DEB_6**, **17_2:18:DEB_6**, **17:18_2:DEB_6**, and **18_3:DEB_6** with a ratio of 1:3:3:1. It has been

Chart 3.

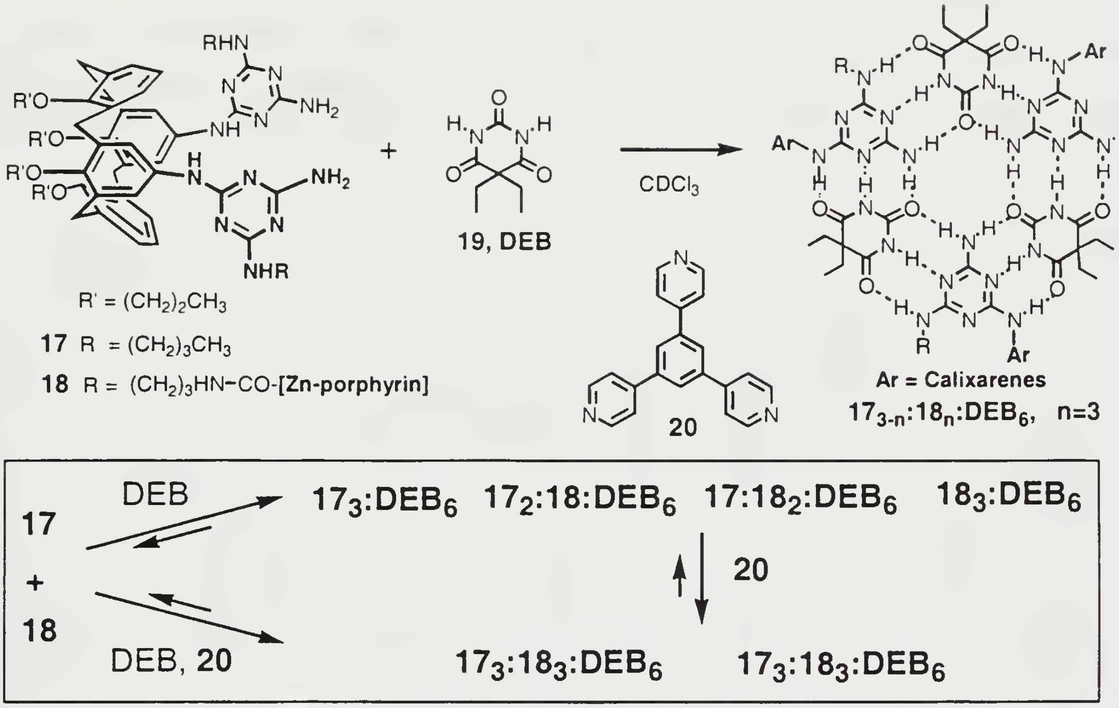

known that Zn porphyrin complex has a moderate affinity (K_a = 3000 M^{-1} in CDCl$_3$) for pyridine derivatives.[19] The cooperative binding of tripyridine to cyclic multiporphyrin arrays results in a much stronger affinity ($K_a \sim 10^{10}$ M^{-1} in CDCl$_3$).[20] Upon addition of **20**, the statistical mixture of **17$_3$:DEB$_6$**, **17$_2$:18:DEB$_6$**, **17:18$_2$:DEB$_6$**, and **18$_3$:DEB$_6$** shifts to 1:1 mixture of **17$_3$:DEB$_6$** and **18$_3$:DEB$_6$** because of the strong affinity between Zn-porphyrin moiety of **18** and tripyridine, **20**. The affinity between Zn and pyridine is used to drive the redistribution of receptor components favoring the best receptor for the tripyridine.

REVERSIBLE INTRAMOLECULAR PROCESS

Lehn et al. have developed a structural and configurational library[21, 22] using 5,5-dimethyl-1,3-cyclohexanedione **21** and 2-hydrazino-pyridine **22** (Scheme 2). Various equilibria, such as hydrazino-enone tautomerism, cis/trans isomerization, hydrolysis of the hydrazino-imine bond and transamination, contributed to the formation of the library. The library consists of hydrazino-enone, **23**, monohydrazone monoketone (**24** and **25**), and dihydrazone (**26**, **27**, and **28**). The complex mixture of tautomers and isomers lead to a new species upon addition of one equiv of dibutyl barbituric acid **29** which has complimentary hydrogen bond array with *Z/Z* isomer **27**. The exclusive formation of **30** is confirmed by the fact that a dramatically simple NMR spectrum was observed after addition of **29**, which excludes the asymmetric *E/E* isomer. NOE data shows a strong correlation between hydrazone NH and cyclohexanone proton ortho to both ketones. The crystal structure of dimeric **30** also confirmed the structure of **30**. NMR dilution and competition experiments involving the barbiturate receptor show the strong and specific association between **27** and **29** as well as reversibility of the library. This example shows that the configurational and structural isomers can generate libraries and specific interaction with guest can amplify one isomer.

Scheme 2.

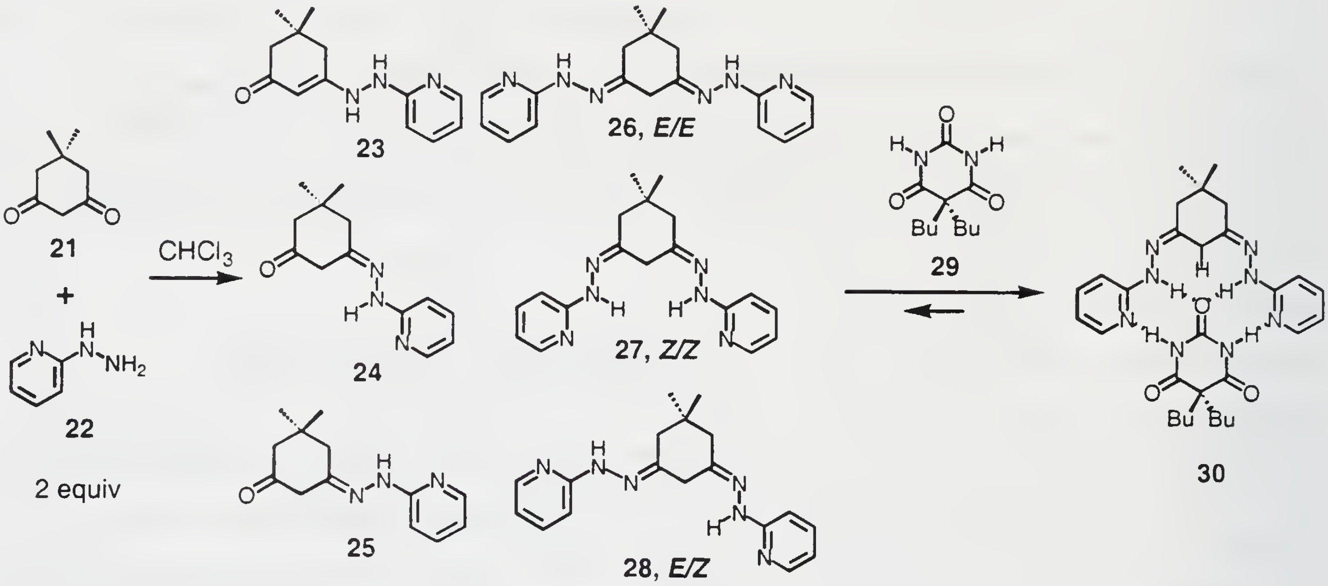

APPLICATIONS

The examples shown above are feasibility study to prove the concept of VCLs and their amplifications. The following example shows a practical aspect of VCLs and possibility of their applications.

Lehn et al.[1,2] have utilized an enzyme (Carbonic anhydrase II, CAII) as a cast to find an inhibitor from imine-based VCL. CAII is a Zn-metalloenzyme and sulfamides are a class of strong inhibitor of CAII. Sulfamide group is bound to Zn via coordination and hydrophilic site of CAII by hydrogen bonding. The reversible combination of various amines and aldehydes forms a dynamic mixture of imines (Scheme 3). The mixture of imines subsequently is reduced to corresponding amines in the absence of CAII and in the presence of CAII. The comparison of each distribution of the resulting amine mixture reveals that the constituent **31** is significantly amplified whereas the other sulfamoylbezaldehyde derived amines shows decrease in amount. It turns out that sulfamoyl benzaldehyde benzyl amine **31** has very similar structure to known strong inhibitor **32** of CAII. This VCL uses a casting process where the inhibitor is selected by specific interaction with the enzyme active site.

Scheme 2. Casting of Inhibitor by Enzyme

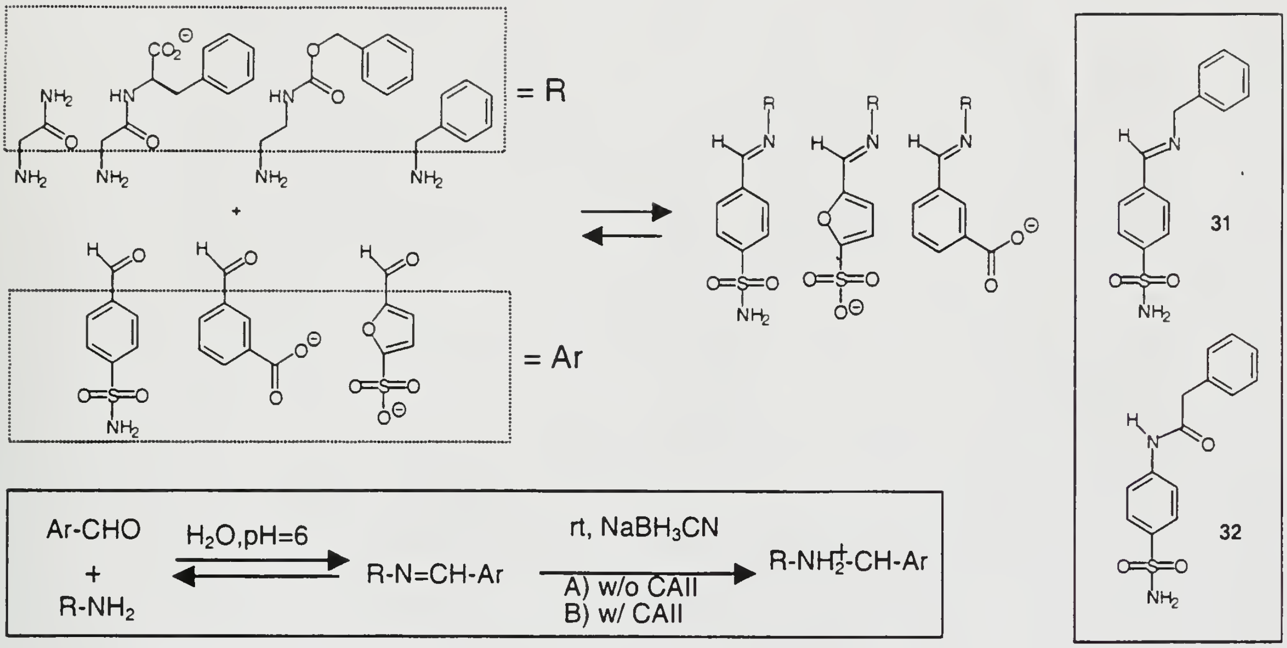

CONCLUSIONS

Various reversible bond formations, interactions, and intramolecular processes have been exploited to generate VCLs. In the presence of target, amplifications of specific components have been shown. However, VCL has several limitations.[3] A reversibilty which is used for the generation of VCL limits a selection of possible reactions. The presence of target may interfere with the reaction. A biological target, such as a protein, may not be stable under reaction conditions. The analysis of the library is difficult if the amplification is not significant. Moreover, the controversy that VCL amounts only to "new examples of an old principle" such as synthesis under thermodynamic control and templating effect has to be resolved.

VCL needs to be improved, but recent reports of a target–accelerated combinatorial synthesis of antibiotics by Nicolau et al.[23] and a target-guided combinatorial ligand assembly by Ellman et al.[24] show that VCL is complementary and compatible with CL.

REFERENCES

(1) Lehn, J. -M. *Chem. Eur. J.* **1999**, *5*, 2455-2463.

(2) Huc, I.; Lehn, J. -M. *Proc.Natl. Acd. Sci. USA* **1997**, *94*, 2106-2110.

(3) Ganesan, A. *Angew. Chem. Int. Ed.* **1998**, *37*, 2828-2831.

(4) Poulson, S.-A.; Gates, P. J.; Cousins, G. R. L.; Sanders, J. K. M. *Rapid Commun. Mass Spectrom.* **2000**, *14*, 44-48.

(5) Hioki, H.; Still, W. C. *J. Org. Chem.* **1998**, *63*, 904-905.

(6) Rowan, S. J.; Lukeman, P. S.; Reynolds, D. J.; Sanders, J. K. M; *New J. Chem.* **1998**, 1015-1018.

(7) Brady, P. A.; Sanders, J. K. M. *J. Chem. Soc., Perkin Trans. 1* **1997**, 3237-3253.

(8) Moore, J. S.; Zimmerman, N. W. *Org. Lett.* **2000**, *2*, 915-978

(9) Furlan, R. L. E.; Cousins, G. R. L; Sanders, J. K. M. *Chem. Commun.* **2000**, 1761-1762.

(10) Cousins, G. R. L.; Poulsen, S.-A.; Sanders, J. K. M. *Chem. Commun.* **1999**, 1575-1576.

(11) Brady, P. L.; Bonar-Law, R. P.; Rowan, S. J.; Suckling, J. C.; Sanders, J. K. M. *Chem. Commun.* **1996**, 319-320.

(12) Beer, P. D.; Gale, P. A.; Smith, D. K. *Supramolecular Chemistry*; Oxford University Press: New York, **1999**; p 22.

(13) Trueblood, K. N.; Knobler, C. B.; Lawrence, D. S.; Stevens, R. V. *J. Am. Chem. Soc.* **1982**, *104*, 1355-1362.

(14) Hof, F.; Nuckolls, C.; Rebek, J., Jr. *J. Am. Chem. Soc.* **2000,** *122*, 4251-4252.

(15) Martin, T.; Obst, U.; Rebek, J., Jr. *Science* **1998,** *281*, 1842-1845.

(16) Calama, M. C.; Timmerman, P.; Reinhoudt, D. N. *Angew. Chem. Int. Ed.* **2000**, *39*, 755-758.

(17) Calama, M. C.; Hulst, R.; Fokkens, R.; Nibbering, N. M. M; Timmerman, P.; Reinhoudt, D. N. *Chem. Commun.* **1998**, 1021-1022.

(18) Timmerman, P.; Reinhoudt, D. N. *Adv. Mater.* **1999**, *11*, 71-74.

(19) Anderson, H. L.; Sanders, J. K. M. *J. Chem. Soc. Chem. Commun.* **1989**, 1714-1715.

(20) Anderson, H. L.; Sanders, J. K. M. *Angew. Chem. Int. Ed.* **1990**, 29, 1400-1403.

(21) Berl, V.; Krische, M. J.; Huc, I.; Lehn, J. -M.; Schmutz, M. *Chem. Eur. J.* **2000**, 6, 1938-1946.

(22) Berl, V.; Huc, I.; Lehn, J. -M.; DeCian, A.; Fischer, J. *Eur. J. Org. Chem.* **1999,** 3089-3094.

(23) Nicolaou, K. C.; Hughes, R.; Cho, S. Y.; Winssinger, N.; Smethurst, C.; Labischinski, H.: Endermann, R. *Angew. Chem. Int. Ed.* **2000**, *39*, 3823-3828.

(24) Mali, D. J.; Choong, I. C.; Ellman, J. A. *Proc. Natl. Acd. Sci. USA* **2000**, *97*, 2419-2424.

UNIVERSITY OF ILLINOIS-URBANA
3 0112 037728703